# Signal Designs for Non-negative Channels

# SIGNAL DESIGNS FOR NON-NEGATIVE CHANNELS

BY

WEI ZHAO, B.Eng.

A THESIS

SUBMITTED TO THE DEPARTMENT OF ELECTRICAL & COMPUTER ENGINEERING

AND THE SCHOOL OF GRADUATE STUDIES

OF MCMASTER UNIVERSITY

IN PARTIAL FULFILMENT OF THE REQUIREMENTS

FOR THE DEGREE OF

MASTER OF APPLIED SCIENCE

Master of Applied Science (2017) McMaster University

(Electrical & Computer Engineering) Hamilton, Ontario, Canada

| | |
|---|---|
| TITLE: | Signal Designs for Non-negative Channels |
| AUTHOR: | Wei Zhao<br>B.Sc., (Electrical Engineering)<br>Xidian University, Xi'an, China |
| SUPERVISOR: | Dr. Jian-Kang Zhang |
| NUMBER OF PAGES: | xv, 92 |

*This thesis is dedicated to my parents and all my friends for their encouragement.*

# Abstract

In this thesis, we would like to design signals for non-negative channels in some wireless communication systems such as visible light communication (VLC) systems and massive multiple-input and multiple-output (MIMO) RF communication systems. In the first part of this thesis, we consider the design of the optimal precoding matrix for an indoor multiple-input and multiple-output visible light communication system with a zero-forcing (ZF) equalizer and a threshold detector. We assume that the channel state information (CSI) is available at both transmitters and receivers. For such a system with non-negative $q$-PAM modulation, we propose an optimal precoding matrix design for transmitted signals such that the average symbol error probability (SEP) (or the bit error rate (BER)) is minimized. On the one hand, in the low SNR regime, our theoretical analysis suggests that we need to turn off one of two transmitters, and let the other work individually. Meanwhile, the constellation size should be improved to maintain the transmission rate. On the other hand, in high SNR scenario, both transmitters should transmit concurrently. The computer simulations show that in high SNR, BER for our proposed design is better than that of currently available methods.

In the second part of this thesis, considering the non-negative constraint on the transmitted signal and the channel in VLC systems, we are interested in designing

a two-dimensional non-negative constellation with a specific unique decomposition. Compared with repetition coding (RC), spatial multiplexing (SMP) and spatial modulation (SM), space-collaborative constellation (CC) has the lowest average normalized optical power and better error performance in practical application for VLC. As for the multi-user situation, by using a recently developed concept called additively uniquely decomposable constellation group (AUDCG), a whole (sum) constellation can be uniquely decomposed into several sub constellations to serve multi users at the same time. However, not all the CC can be decomposed into AUDCG. Then, we introduce several new methods to design a 2-dimensional constellation based on the idea of CC and AUDCG, which can serve two users with different priority strategies. The simulation result shows that our constellation design has lower average symbol error probability than traditional SMP in all strategies.

# Acknowledgements

Two years' study in the McMaster University is going to the end. Here, I have experienced so much happiness and hardships with friends and colleagues, which becomes a bunch of great asset in my life.

At this special moment, I would like to show my highest respect and heartfelt thanks to my supervisor Dr. Jian-Kang Zhang, who provided me extremely careful guidance. With his help, I can get rid of hesitation while doing research step by step, and finally become so confident to explore new knowledge. Besides, I really appreciate his strict requirement, since it makes me correct many inappropriate habits which may be great obstacles in my future development. During this process, I obtained much philosophy for both study and life.

In addition, I would like to thank my friends. They gave me countless help during my life in Canada, which makes me become an experienced person in this new country. Thus, I can save a lot of time to do scientific research at school.

Finally, I wish to thank my parents for their encouragement. With their words, I am equipped with strong spiritual support in my mind to face numerous challenges.

# Notation and abbreviations

## Notations

| | |
|---|---|
| $(\cdot)^T$ | Matrix transpose |
| $(\cdot)^H$ | Matrix hermitian |
| $(\cdot)^{-1}$ | Matrix inverse |
| $\langle \cdot, \cdot \rangle$ | Inner product |
| $\lvert \cdot \rvert$ | Magnitude of a complex quantity |
| $\lVert \cdot \rVert$ | Euclidean norm of a vector or a matrix |
| $Q(\cdot)$ | Q-function |
| $\mathbb{E}[\cdot]$ | Expectation |
| $\mathrm{diag}\{\cdot\}$ | Diagonal matrix |
| $f(\cdot\lvert\cdot)$ | Conditional probability density function |
| $d_{min}(\cdot)$ | Minimum Euclidean distance between any points in a constellation |

## Abbreviations

| | |
|---|---|
| AUDCG | Additively Uniquely Decomposable Constellation Group |

| | |
|---|---|
| AWGN | Additive White Gaussian Noise |
| BER | Bit Error Rate |
| CC | space-Collaborative Constellation |
| CSI | Channel State Information |
| DC | Direct Current |
| FOV | Field-Of-View |
| LOS | Light Of Sight |
| MIMO | Multiple-Input and Multiple-Output |
| MISO | Multiple-Input and Single-Output |
| MK | Monte Carlo |
| ML | Maximum-Likelihood |
| PAM | Pulse Amplitude Modulation |
| PD | Photo-Detector |
| QAM | Quadrature Amplitude Modulation |
| RC | Repetition Coding |
| RF | Radio Frequency |
| SEP | Symbol Error Probability |
| SM | Spatial Modulation |
| SMP | Spatial Multiplexing |
| SNR | Signal to Noise Ratio |
| VLC | Visible Light Communication |
| ZF | Zero-Forcing |

# Contents

# List of Figures

# Chapter 1

# INTRODUCTION

Nowadays, with the Internet of Things growing rapidly, one of the new technologies that have great potential and can be used to exchange information is light. In recent years, visible light communication (VLC) has been explored widely and deeply, since it has many advantages, such as free license, light of sight security and health concern. VLC can be widely deployed because almost all the indoor-rooms and outside streets have illuminants. People can use light for communication without paying any fee. It is also quite easy to use VLC to transmit signals. On the one hand, transmitters send data by light source, such as light emitting diode (LED). The data can be modulated into light by changing intensities or colors. On the other hand, at receiver side, optical sensors like photodiodes demodulate the light signals and recover the data. Human eyes cannot feel the flicks if the modulation rate is fast enough, and the intensities can also be adjusted, so there is little harm to us. Today, the spectrum of traditional radio frequency (RF) becomes much crowded with the number of network devices growing sharply, and VLC would be a desirable substitute to relief spectrum (O'Brien *et al.*, 2008b), (Tiwari *et al.*, 2015). In some specific situations like airplanes, radio

frequency (RF) communication is restricted, while VLC would be an ideal option. As for the indoor situation, VLC has a higher secure property than conventional RF communication, such as WIFI, due to that the light cannot penetrate walls, which may prevent it to be accessed or even hacked from outside. Besides, international standardization organization has created standards for it, e.g. IEEE 802.15.7 (iee, 2011).

There are many similarities between traditional RF and VLC. Many ideas of modulation, demodulation, constellation, and equalizer design for RF can be used in VLC with related changes, since there is a nonnegative constraint on transmitted signals and channels. (Li *et al.*, 2012) explores a TDMA-like model to eliminate interference in VLC by tuning the LED beam-widths and beam-angles. (Elgala *et al.*, 2009) brings the OFDM to indoor broadcasting VLC channel. It recommends to use big array structures or many lamps to transmit the same signal simultaneously, which can boost the signal to noise ratio (SNR). There are many interesting usages in our daily life with VLC, which are similar but more efficient and suitable than RF. For example, in the intelligent transportation systems (Kumar *et al.*, 2012), (Yamazato *et al.*, 2014), (Yendo *et al.*, 2010), the traffic light can be a light source and also transmit the signal. It can tell the drivers real time information about road condition. The rear brake light of vehicles can be designed as a transmitter and a camera would be set at the front of a car. Then, the communication can be established between two neighbour cars on the road. The two neighbour cars can exchange the information, such as the distance between each other in order to avoid collision or the road condition ahead. To find and track in the road-to-vehicle VLC system, high-speed camera image processing would be utilized and it is very effective

even though other light sources may overlap the main source.

To improve the performance of data transmission in VLC channel, there are two channel coding techniques, repetition code (RC) and spatial modulation (SM) (Jha *et al.*, 2015). RC usually has constant SNR. But for larger room where receivers have longer distance between each other, SM has better SNR. We also need to consider the dispersive nature of indoor VLC channels, because many factors attribute to this phenomenon, such as LED in combination with its driver, or the multipath propagation channel. The dispersion caused by LEDs can be modeled by a Gaussian low-pass filter, and the multipath propagation effect can be modeled by four light sources set at different locations. To deal with them, discrete multitone transmission (DMT) is a very effective method. As for space time coding, RC and Alamouti-type space time coding scheme are proposed. In the RF communication, Alamouti code has better performance than that of RC; In VLC, both coding schemes can achieve full diversity and the performance between them are nearly the same (Jia *et al.*, 2015). For multi-user situations, code-division multiple access (CDMA) is one of the most popular channel access methods in RF communication. In the VLC, we also face the same problem that transmitting multiple messages through very few channels at the same time, and the similar technology has been created for VLC system. To make better simultaneous message broadcasting framework, (Chen *et al.*, 2015) exploits the CDMA-based VLC. With simple and low-cost VLC network devices, CDMA-based VLC can allow multiple LED transmitting distinct signals simultaneously and avoiding collisions. According to (Shoreh *et al.*, 2015), the proposed CDMA system is established on an orthogonal frequency division multiplexing (OFDM) platform. In order to get over the light-dimming problem, a new methodology called polarity

reversed optical OFDM (PRO-OFDM) has been introduced. VLC also has zero-configuration property, which means that a new user does not have to pre-configure its devices when entering the VLC network. With the robustness of this special OFDM scheme combined with the CDMA scheme, VLC system can be the desirable option to substitute the RF communication.

Here, we would like to clearly emphasize a major technical difference between RF communications and VLC, that is a nonnegative constraint on the design of transmission for VLC. It is due to this constraint that the currently available well-developed techniques for RF communications cannot be directly utilized for MIMO-VLC successfully. In spite of the fact that the nonnegative constraint can be met by carefully adding some direct current (DC) components into transmitter designs so that the currently existing advanced techniques for RF communications could be used in MIMO-VLC, the significant power loss resulting from the DC incurs the fact that these modified methods have much worse error performance than RC.

Therefore, our primary task in this thesis is to develop novel transmission design techniques for particularly dealing with this constraint for some specific applications. There are two parts in this thesis. In the first part of this thesis, we consider a $2 \times 2$ VLC system model, where channel state information is assumed to be known at both transmitters and receivers. For such a system, we propose the design of a linear non-negative map (non-negative matrix) or a linearly precoding non-negative matrix, which maps a non-negative two dimensional $q$-ary PAM constellation into another two-dimensional non-negative constellation, such that the average symbol error probability (or BER) with the ZF detector is minimized. In the second part of this thesis, we aim to design a two-dimensional non-negative sum constellation with a

specific decomposition property called an additively uniquely decomposable constellation group (AUDCG), i.e., a sum constellation which can be uniquely decomposed into several sub-constellations to serve multi users at the same time.

# Chapter 2

# Part I: Optimal Precoding Matrix Design for MIMO-VLC Systems

## 2.1 System Model

In this section, we will discuss a special MIMO-VLC system (Fath and Haas, 2013), which is equipped with $M = 2$ transmitters and $N = 2$ photo-detectors at the receiver end. For such an MIMO-VLC system model, the received signal vector is represented by

$$\mathbf{y} = \mathbf{HFs} + \mathbf{n}, \tag{2.1}$$

where $\mathbf{y} = (y_1, y_2)^T$ is an $N \times 1$ received signal vector, $\mathbf{s} = (s_1, s_2)^T$ is an $M \times 1$ transmitted symbol vector, with each symbol being chosen equally likely and independently from a unipolar $q$-level ($q = 2^P$) PAM constellation, which can be represented by $\mathcal{A} = \{kd\}_{k=0}^{M-1}$, $\mathbf{H}$ is the channel matrix and $\mathbf{F} = (\mathbf{f}_1, \mathbf{f}_2)$ is a linear space coding

matrix subject to the total transmission power constraint,

$$\mathbb{E}\left[\mathbf{1}^T\mathbf{F}\mathbf{s}\right] = P_T, \quad f_{ij} \geq 0, \tag{2.2}$$

where $\mathbf{1} = (1,1)^T$ is an $M \times 1$ column vector. The channel is an optical wireless link with light of sight (LOS) characteristics.

Figure 2.1 shows direct LOS links, where $\theta_{Tj}$ is the angle of emergence with respect to the transmitter $j$ axis and $\theta_{Ri}$ is the angle of incidence with respect to the receiver $i$ axis, and $d_{i,j}$ is the distance between the $j$-the transmitter and the $i$-th receiver. According to (Kahn and Barry, 1997), the channel gain between the $j$-th transmitter and the $i$-th receiver is given by

$$h_{ij} = \begin{cases} \frac{(K+1)J}{2\pi d_{i,j}^2}\cos^K\left(\theta_{Tj}\right)\cos\left(\theta_{Ri}\right) & 0 \leq \theta_{Ri} \leq \theta_{R\frac{1}{2}} \\ 0 & \theta_{Ri} > \theta_{R\frac{1}{2}} \end{cases}, \tag{2.3}$$

for $i = 1, \ldots, N$ and $j = 1, \ldots, M$, where $K = \frac{-\ln 2}{\ln\left(\theta_{R\frac{1}{2}}\right)}$ and the field-of-view (FOV) semiangle of the receiver $\theta_{R\frac{1}{2}}$ is assumed to be 15° (Bouchet *et al.*, 2011), (O'Brien

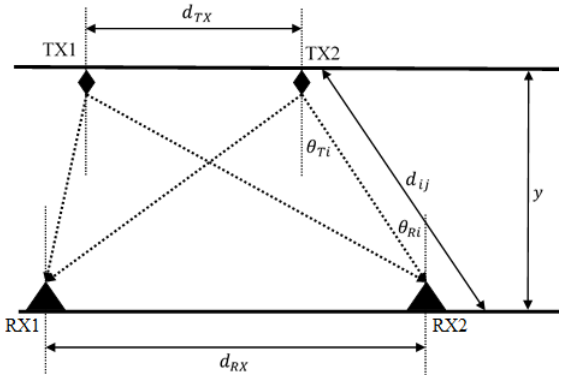


Figure 2.1: Geometric scenario for $2 \times 2$ MIMO-VLC system

*et al.*, 2008a). In this paper, $J$ is the area of receiver which is assumed to be 1 $cm^2$. The $h_{ij}$ depends on the unique position of $j$-th transmitter and $i$-the receiver. If $j$-th transmitter and $i$-the receiver are not in FOV, then $h_{ij} = 0$.

Furthermore, as for the noise vector $\mathbf{n}$ in the channel model (2.1), there are two kinds of noise at the receiver side: one is from the receiving electronics and the other is shot noise from the received DC photocurrent induced by background radiation (Karp *et al.*, 2013), (Barry, 2012). On the one hand, the exact number of the photons arriving at the receiver during a given duration is random and modelled by a Poisson distribution with a rate proportional to the input. This model reflects the physical nature of the transmitted signal consisting of many photons, and the noise component is signal-dependent. On the other hand, the signal is also corrupted with background radiation (called dark current), which is modelled by an additional constant rate added to the rate of the Poisson distribution. In addition to the above two major noise components, the received signal is also impaired by thermal noise from the receiving device. In this paper, we assume that the shot noise caused by background radiation is dominant compared with other noise (Zhu and Kahn, 2002), (Lee and Chan, 2004). By the central limit theorem, the high-intensity shot noise for the lightwave-based OWC is closely approximated as AWGN noise with zero mean and covariance $\sigma^2\mathbf{I}$ (Barry, 2012), (Zhu and Kahn, 2002), (Marcuse, 1991).

## 2.2 Precoding Matrix Design

### 2.2.1 Problem Statement and Formulation

Now we consider this special indoor MIMO-VLC system with $N = 2$ photo-detectors at the receiver side and $M = 2$ transmitters. We assume that channel state information is known at both the transmitters and the receivers. In order to estimate the transmitted signal with a simple receiver, we use a zero-forcing (ZF) equalizer. Then, our main task in this chapter is to find a linear space coding matrix $\mathbf{F}$ that minimizes the average symbol error probability ($\bar{P}_{\text{sep}}$) subject to the total transmission power constraint.

First we need to derive the formulate of the average symbol error probability $\bar{P}_{\text{sep}}$. The conditional probability density function of the received signal $y$ given $s = s_k$ is the Gaussian distribution with mean $s_k$ and variance $\sigma^2$, i.e.,

$$f\left(y|s_k\right) = \frac{1}{\sqrt{2\pi\sigma^2}} e^{-\frac{(y-s_k)^2}{2\sigma^2}}.$$

Hence, the conditional probability of making correct decision ($P_{c|s_k}$) is defined by

$$P_{c|s_k} = \int_{\Gamma_k} f(y|s) dy,$$

where $\Gamma_k$ is the correct decision region for detecting $s_k$. In order to evaluate this integral, we consider the following three cases:

(a) For the left edge point, the conditional probability of making correct decision

on $s = s_0 = 0$ is

$$P_{c|s_0} = \int_{\Gamma_0} f(y|s_0) = \int_{-\infty}^{\frac{d}{2}} \frac{1}{\sqrt{2\pi\sigma^2}} e^{-\frac{(y)^2}{2\sigma^2}} dy = 1 - Q\left(\frac{d}{2\sigma}\right).$$

(b) For the right point, the conditional probability of making correct decision on $s = s_{q-1} = q - 1$ is

$$P_{c|s_{q-1}} = \int_{\Gamma_{q-1}} f(y|s_{q-1}) = \int_{(q-1)d-\frac{d}{2}}^{\infty} \frac{1}{\sqrt{2\pi\sigma^2}} e^{-\frac{(y-(q-1)d)^2}{2\sigma^2}} dy = 1 - Q\left(\frac{d}{2\sigma}\right).$$

(c) For the $k$th inner point, the conditional probability of making correct decision on $s = s_k = k$ is

$$P_{c|s_k} = \int_{\Gamma_k} f(y|s_k) = \int_{k-\frac{d}{2}}^{k+\frac{d}{2}} \frac{1}{\sqrt{2\pi\sigma^2}} e^{-\frac{(y-kd)^2}{2\sigma^2}} dy = 1 - 2Q\left(\frac{d}{2\sigma}\right).$$

Therefore, overall average conditional probability of making correct decision is

$$\begin{aligned} P_c &= \frac{q-2}{q}\left(1 - 2Q\left(\frac{d}{2\sigma}\right)\right) + \frac{1}{q}\left(1 - Q\left(\frac{d}{2\sigma}\right)\right) + \frac{1}{q}\left(1 - Q\left(\frac{d}{2\sigma}\right)\right) \\ &= 1 - \frac{2\,(q-1)}{q} Q\left(\frac{d}{2\sigma}\right), \end{aligned}$$

and the overall average symbol error probability is

$$P_e = 1 - P_c = \frac{2\,(q-1)}{q} Q\left(\frac{d}{2\sigma}\right).$$

Let $\tilde{\mathbf{H}} = \mathbf{HF}$. Then, the model can be represented as

$$\mathbf{y} = \tilde{\mathbf{H}}\mathbf{s} + \mathbf{n}.$$

After processed by zero-forcing equalizer, the model can be written as:

$$\left(\tilde{\mathbf{H}}^T\tilde{\mathbf{H}}\right)^{-1}\tilde{\mathbf{H}}^T\mathbf{y} = \mathbf{s} + \left(\tilde{\mathbf{H}}^T\tilde{\mathbf{H}}\right)^{-1}\tilde{\mathbf{H}}^T\mathbf{n},$$

which can be also written as

$$\mathbf{z} = \mathbf{s} + \tilde{\mathbf{n}}, \tag{2.4}$$

where $\mathbf{z} = \left(\tilde{\mathbf{H}}^T\tilde{\mathbf{H}}\right)^{-1}\tilde{\mathbf{H}}^T\mathbf{y}$ and $\tilde{\mathbf{n}} = \left(\tilde{\mathbf{H}}^T\tilde{\mathbf{H}}\right)^{-1}\tilde{\mathbf{H}}^T\mathbf{n}$.

In this problem, we prefer to write (2.4) as an equation array to make it easier to compute the average $P_{\text{sep}}$:

$$\begin{cases} z_1 = s_1 + \tilde{n}_1 \\ z_2 = s_2 + \tilde{n}_2 \end{cases}.$$

Then the $P_{\text{sep}}$ for each channel is

$$P_{\text{sep1}} = \frac{2(q-1)}{q} Q\left(\frac{d}{2\sigma\sqrt{\left(\tilde{\mathbf{H}}^T\tilde{\mathbf{H}}\right)^{-1}_{11}}}\right); \tag{2.5}$$

$$P_{\text{sep2}} = \frac{2(q-1)}{q} Q\left(\frac{d}{2\sigma\sqrt{\left(\tilde{\mathbf{H}}^T\tilde{\mathbf{H}}\right)^{-1}_{22}}}\right). \tag{2.6}$$

The average symbol error probability is

$$\bar{P}_{\text{sep}}(\mathbf{F}) = \frac{1}{2}\left(P_{\text{sep1}} + P_{\text{sep2}}\right). \tag{2.7}$$

Now, we can state our goal as an optimization problem formally as follows:

**Problem 1.** *Find a nonnegative linear coding matrix* $\mathbf{F}$ *such that its corresponding*

$\bar{P}_{\text{sep}}$ *is minimized, i.e.,*

$$\mathbf{F}_{\text{opt}} = \arg\min_{\mathbf{F}} \bar{P}_{\text{sep}}(\mathbf{F}), \tag{2.8}$$

*subject to the total transmission power constraint*

$$E\left[\mathbf{1}^T\mathbf{F}\mathbf{s}\right] = 1.$$

■

The main obstacle to solve this problem is that the coding matrix $\mathbf{F}$ must be non-negative. Thus, we cannot use the methods in MIMO RF communications directly. In the next subsection we will simplify the problem by parameterizing the coding matrix.

### 2.2.2 Nonnegative Constraints and Parameterization

As mentioned above, in order to solve the problem, we need to parameterize the coding matrix $\mathbf{F}$. Let

$$\mathbf{A} = \tilde{\mathbf{H}}^T\tilde{\mathbf{H}} = \mathbf{F}^H\mathbf{H}^T\mathbf{H}\mathbf{F} = \begin{pmatrix} a_{11} & a_{12} \\ a_{21} & a_{22} \end{pmatrix},$$

and let the eigenvalue decomposition of the matrix $\mathbf{H}^T\mathbf{H}$ be $\mathbf{H}^T\mathbf{H} = \mathbf{V}\mathbf{\Lambda}\mathbf{V}^T$, where $\mathbf{\Lambda} = diag\{\lambda_1^2, \lambda_2^2\}$ with $\lambda_1 \geq \lambda_2 > 0$ are the singular values of the channel $\mathbf{H}$, and

$$\mathbf{V} = \begin{pmatrix} \cos\psi & -\sin\psi \\ \sin\psi & \cos\psi \end{pmatrix}$$

with $\psi \in \left[0, \frac{\pi}{2}\right]$. We also let $\mathbf{G} = \mathbf{V}^T\mathbf{F} = (\mathbf{g_1}, \mathbf{g_2})$. Then

$$a_{11} = \mathbf{g}_1^H \mathbf{\Lambda} \mathbf{g}_1 = (\lambda_1 g_{11})^2 + (\lambda_2 g_{21})^2 = d_1^2, \tag{2.9}$$

$$a_{22} = \mathbf{g}_2^H \mathbf{\Lambda} \mathbf{g}_2 = (\lambda_1 g_{12})^2 + (\lambda_2 g_{22})^2 = d_2^2. \tag{2.10}$$

Using polar coordinates, we can rewrite $\mathbf{G}$ as

$$\mathbf{G} = \begin{pmatrix} \frac{d_1}{\lambda_1}\cos\alpha & \frac{d_2}{\lambda_1}\cos\beta \\ \frac{d_1}{\lambda_2}\sin\alpha & \frac{d_2}{\lambda_2}\sin\beta \end{pmatrix},$$

where $\alpha, \beta \in [-\pi, \pi]$. Since $\mathbf{F} = \mathbf{VG}$, the nonnegative constraint of $\mathbf{F}$ is equivalently transfered to $\mathbf{G}$ such that

$$\begin{aligned} d_1\left(\frac{1}{\lambda_1}\cos\psi\cos\alpha - \frac{1}{\lambda_2}\sin\psi\sin\alpha\right) &\geq 0, \\ d_1\left(\frac{1}{\lambda_1}\sin\psi\cos\alpha + \frac{1}{\lambda_2}\cos\psi\sin\alpha\right) &\geq 0, \\ d_2\left(\frac{1}{\lambda_1}\cos\psi\cos\beta - \frac{1}{\lambda_2}\sin\psi\sin\beta\right) &\geq 0, \\ d_2\left(\frac{1}{\lambda_1}\sin\psi\cos\beta + \frac{1}{\lambda_2}\cos\psi\sin\beta\right) &\geq 0. \end{aligned}$$

From the four equations above, we can derive that

$$\begin{aligned} -\frac{\lambda_2}{\lambda_1}\tan\psi \leq \tan\alpha \leq \frac{\lambda_2}{\lambda_1}\cot\psi, \\ -\frac{\lambda_2}{\lambda_1}\tan\psi \leq \tan\beta \leq \frac{\lambda_2}{\lambda_1}\cot\psi. \end{aligned}$$

Let

$$\theta_L = -\arctan\left(\frac{\lambda_2}{\lambda_1}\tan\psi\right), \tag{2.11}$$

$$\theta_U = \arctan\left(\frac{\lambda_2}{\lambda_1}\cot\psi\right). \tag{2.12}$$

Then $\theta_L \in \left[-\frac{\pi}{2}, 0\right]$, $\theta_U \in \left[0, \frac{\pi}{2}\right]$, and

$$\theta_L \leq \alpha \leq \theta_U,$$

$$\theta_L \leq \beta \leq \theta_U.$$

Let

$$\frac{d_1}{d_2} = \mu \quad \mu \in [0, \infty]. \tag{2.13}$$

Then, we can simplify the power constraint as

$$\begin{aligned} P_T &= E\left[\mathbf{1}^T\mathbf{F}\mathbf{s}\right] \\ &= \mathbf{1}^T\mathbf{F}\begin{bmatrix} E_s \\ E_s \end{bmatrix} \\ &= E_s\mathbf{1}^T\mathbf{F}\mathbf{1} = 1, \end{aligned} \tag{2.14}$$

where

$$\begin{aligned} E_s &= (0 + d + 2d + \ldots + (q-1)\,d)\,/q \\ &= d \cdot \frac{q-1}{2}. \end{aligned} \tag{2.15}$$

Then, the power constraint is equal to

$$d_2 = \frac{1/E_s}{F(\alpha, \beta, \mu)},$$

where

$$\begin{aligned} F(\alpha, \beta, \mu) &= \mu \left( \frac{1}{\lambda_2} (\cos\psi - \sin\psi) \sin\alpha + \frac{1}{\lambda_2} (\cos\psi + \sin\psi) \cos\alpha \right) \\ &\quad + \frac{1}{\lambda_2} (\cos\psi - \sin\psi) \sin\beta + \frac{1}{\lambda_2} (\cos\psi + \sin\psi) \cos\beta. \end{aligned} \tag{2.16}$$

For convenience, we let $F(\alpha, \beta, \mu) = \Delta(\lambda_1, \lambda_2, \psi) f(\alpha, \beta, \mu)$, where $\Delta(\lambda_1, \lambda_2, \psi) = \sqrt{\frac{(\cos\psi + \sin\psi)^2}{\lambda_1^2} + \frac{(\cos\psi - \sin\psi)^2}{\lambda_2^2}}$ and $f(\alpha, \beta, \mu) = \mu \cos(\alpha - \theta) + \cos(\beta - \theta)$ with $\tan\theta = \frac{\lambda_1}{\lambda_2} \tan\left(\frac{\pi}{4} - \psi\right)$, $\theta \in \left[-\frac{\pi}{2}, \frac{\pi}{2}\right]$. Thus, the coding matrix can be written as

$$\mathbf{F} = d_2 \mathbf{V} \begin{pmatrix} \frac{\mu}{\lambda_1} \cos\alpha & \frac{1}{\lambda_1} \cos\beta \\ \frac{\mu}{\lambda_2} \sin\alpha & \frac{1}{\lambda_2} \sin\beta \end{pmatrix}. \tag{2.17}$$

### 2.2.3 Optimal Solutions

Let's simplify the formulation $\bar{P}_{\text{sep}}(\mathbf{F})$ in (2.7). Using (2.17) we obtain

$$\begin{aligned} \left(\tilde{\mathbf{H}}^T \tilde{\mathbf{H}}\right)^{-1} &= \left(\mathbf{F}^H \mathbf{H}^T \mathbf{H} \mathbf{F}\right)^{-1} \\ &= \frac{1}{\det \mathbf{A}} \begin{pmatrix} a_{22} & -a_{12} \\ a_{21} & a_{11} \end{pmatrix}. \end{aligned} \tag{2.18}$$

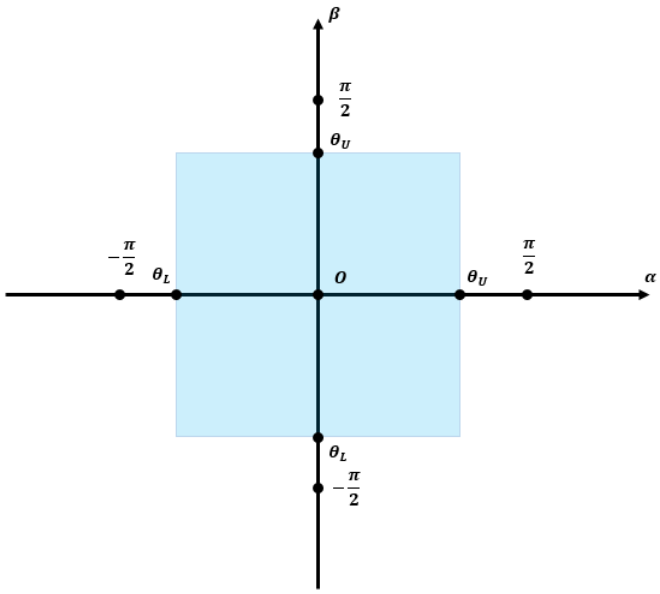


Figure 2.2: The definition domain for $\alpha$ and $\beta$

Since

$$\begin{aligned}
\det \mathbf{A} &= \det\left(\mathbf{F}^H \mathbf{H}^T \mathbf{H} \mathbf{F}\right) \\
&= (\det \mathbf{F})^2 \det\left(\mathbf{H}^T \mathbf{H}\right) \\
&= \left(d_2^2 \frac{\mu}{\lambda_1 \lambda_2} \left(\cos\alpha \sin\beta - \sin\alpha \cos\beta\right)\right)^2 \det\left(\mathbf{V} \mathbf{\Lambda} \mathbf{V}^T\right) \\
&= \left(d_2^2 \frac{\mu}{\lambda_1 \lambda_2} \sin\left(\beta - \alpha\right)\right)^2 \lambda_1^2 \lambda_2^2 \\
&= d_1^2 d_2^2 \sin^2\left(\beta - \alpha\right), \qquad (2.19)
\end{aligned}$$

we get

$$\left(\tilde{\mathbf{H}}^T \tilde{\mathbf{H}}\right)^{-1} = \frac{1}{d_1^2 d_2^2 \sin^2\left(\beta - \alpha\right)} \begin{pmatrix} a_{22} & -a_{12} \\ a_{21} & a_{11} \end{pmatrix}. \qquad (2.20)$$

According to (2.15), we have $d = \frac{2E_s}{q-1}$. Let

$$\mathrm{SNR} = \frac{1}{2\sigma^2}, \tag{2.21}$$

we obtain

$$\begin{aligned} P_{\mathrm{sep1}} &= \frac{2\,(q-1)}{q} Q\left(\frac{d}{2\sigma\sqrt{\left(\tilde{\mathbf{H}}^H\tilde{\mathbf{H}}\right)^{-1}_{11}}}\right) \\ &= \frac{2\,(q-1)}{q} Q\left(\frac{d}{2\sigma\sqrt{\frac{a_{22}}{d_1^2 d_2^2 \sin^2(\beta-\alpha)}}}\right) \\ &= \frac{2\,(q-1)}{q} Q\left(\frac{d}{2\sigma\sqrt{\frac{d_2^2}{d_1^2 d_2^2 \sin^2(\beta-\alpha)}}}\right) \\ &= \frac{2\,(q-1)}{q} Q\left(\frac{d\sqrt{\mathrm{SNR}}\,|\sin(\beta-\alpha)|}{\sqrt{2}} d_1\right). \end{aligned} \tag{2.22}$$

Similarly,

$$\begin{aligned} P_{\mathrm{sep2}} &= \frac{2\,(q-1)}{q} Q\left(\frac{d}{2\sigma\sqrt{\left(\tilde{\mathbf{H}}^H\tilde{\mathbf{H}}\right)^{-1}_{22}}}\right) \\ &= \frac{2\,(q-1)}{q} Q\left(\frac{d\sqrt{\mathrm{SNR}}\,|\sin(\beta-\alpha)|}{\sqrt{2}} d_2\right). \end{aligned} \tag{2.23}$$

Hence, the average symbol error probability is represented by

$$\begin{aligned}\bar{P}_{\text{sep}}(\mathbf{F}) &= \frac{1}{2}(P_1+P_2)\\ &= \frac{(q-1)}{q}\left(Q\left(\frac{d\sqrt{\text{SNR}}\,|\sin(\beta-\alpha)|}{\sqrt{2}}d_1\right)+Q\left(\frac{d\sqrt{\text{SNR}}\,|\sin(\beta-\alpha)|}{\sqrt{2}}d_2\right)\right).\end{aligned}$$

Now, Problem 1 can be simplified as the following problem:

**Problem 2.** *Find $\alpha, \beta, d_1$ and $d_2$ such that*

$$\begin{aligned}\min_{\alpha,\beta,d_1,d_2} \quad & \bar{P}_{\text{sep}}(\alpha,\beta,d_1,d_2)\\ s.t. \quad & \theta_L \le \alpha \le \theta_U\\ & \theta_L \le \beta \le \theta_U\end{aligned}$$

■

Some important relationships among parameters should be investigated in order to solve Problem 2. To do that, we need to establish the following lemma.

**Lemma 1.** *Let $a = \Delta\cos(\theta_U-\theta)$, $b = \Delta\cos(\theta_L-\theta)$. Then*

$$a = \frac{1}{\sqrt{\lambda_1^2\sin^2\psi+\lambda_2^2\cos^2\psi}}, \tag{2.24}$$

$$b = \frac{1}{\sqrt{\lambda_1^2\cos^2\psi+\lambda_2^2\sin^2\psi}}. \tag{2.25}$$

*We have the following three statements:*

*1) When $0 \le \psi < \frac{\pi}{4}$, we have $a > b$.*

*2) When $\psi = \frac{\pi}{4}$, we have $a = b$.*

*3) When $\frac{\pi}{4} < \psi \le \frac{\pi}{2}$, we have $a < b$.*

■

The proof of this lemma is provided in Appendix A.1. After establishing the lemma above, it is time to show our main results formally in this chapter.

**Theorem 1.** *Let the eigenvalue decomposition (ED) of* $\mathbf{H}^T\mathbf{H}$ *be* $\mathbf{H}^T\mathbf{H} = \mathbf{V}\mathbf{\Lambda}\mathbf{V}^{\mathrm{T}}$, *where* $\mathbf{\Lambda} = \mathrm{diag}\{\lambda_1^2, \lambda_2^2\}$ *with* $\lambda_1 \geq \lambda_2 > 0$ *and*

$$\mathbf{V} = \begin{pmatrix} \cos\psi & -\sin\psi \\ \sin\psi & \cos\psi \end{pmatrix}$$

*with* $\psi \in \left[0, \frac{\pi}{2}\right]$. *Let* $C_1 = \frac{\sqrt{2}\sin(\theta_U - \theta_L)}{q-1}$ *and* $C = \frac{2}{c_1^2}\ln\frac{b}{a}$. *The linear space coding matrix* $\mathbf{F}$ *is parameterized by* (2.17). *and according to the power constraint* (2.14),

$$\mathbf{1}^T\mathbf{F}\mathbf{1} = \frac{1}{E_s} = e.$$

*Let*

$$\mathbf{J} = \mathbf{H}^T\mathbf{H} = \begin{pmatrix} j_{11} & j_{12} \\ j_{21} & j_{22} \end{pmatrix}.$$

*Then, the optimal solution to the problem is:*

*Case 1: $\mathbf{H}$ is a non-invertible matrix*

*We turn off one of the transmitters and let the other work alone. Let* $q_1 = q^2$.

1. $j_{11} \geq j_{22}$, $\mathbf{F}_{opt} = \begin{pmatrix} e \\ 0 \end{pmatrix}$.

2. $j_{11} < j_{22}$, $\mathbf{F}_{opt} = \begin{pmatrix} 0 \\ e \end{pmatrix}$.

*Then,*

$$\min \bar{P}_{\text{sep}} = \frac{2\left(q_1-1\right)}{q_1} Q\left(\frac{dh\cdot\sqrt{\text{SNR}}}{\sqrt{2}}\right),$$

*and the BER is*

$$\begin{aligned}\min \bar{P}_b &= \frac{1}{q_1 \log_2 q_1} \sum_{k=1}^{\log_2 q_1} \sum_{i=0}^{\left(1-2^{-k}\right)q_1-1} \left\{(-1)^{\left\lfloor \frac{i\cdot 2^{k-1}}{q_1}\right\rfloor}\left(2^{k-1}-\left\lfloor \frac{i\cdot 2^{k-1}}{q_1}+\frac{1}{2}\right\rfloor\right)\right. \\ &\quad \left.\cdot 2Q\left(\frac{(2i+1)\,dh\cdot\sqrt{\text{SNR}}}{\sqrt{2}}\right)\right\},\end{aligned}$$

*where* $h = \sqrt{\left(\mathbf{H}\mathbf{F}_{opt}\right)^T\left(\mathbf{H}\mathbf{F}_{opt}\right)}$.

*Case 2: $\mathbf{H}$ is an invertible matrix.*

1. $0 \le \psi < \frac{\pi}{4}$

   (a) *In the low* SNR *situation (*$\text{SNR} \le -\text{Cb}^2$*), we turn off one of the transmitters and let the other work alone. Let* $q_1 = q^2$.

   i. $j_{11} \ge j_{22}$, $\mathbf{F}_{opt} = \begin{pmatrix} e \\ 0 \end{pmatrix}$.

   ii. $j_{11} < j_{22}$, $\mathbf{F}_{opt} = \begin{pmatrix} 0 \\ e \end{pmatrix}$.

   *Then,*

$$\min \bar{P}_{\text{sep}} = \frac{2\left(q_1-1\right)}{q_1} Q\left(\frac{dh\cdot\sqrt{\text{SNR}}}{\sqrt{2}}\right),$$

*and the BER is*

$$\min \bar{P}_b = \frac{1}{q_1 \log_2 q_1} \sum_{k=1}^{\log_2 q_1} \sum_{i=0}^{\left(1-2^{-k}\right)q_1-1} \left\{ (-1)^{\left\lfloor \frac{i \cdot 2^{k-1}}{q_1} \right\rfloor} \left( 2^{k-1} - \left\lfloor \frac{i \cdot 2^{k-1}}{q_1} + \frac{1}{2} \right\rfloor \right) \cdot 2Q\left( \frac{(2i+1)\, dh \cdot \sqrt{\mathrm{SNR}}}{\sqrt{2}} \right) \right\},$$

*where* $h = \sqrt{(\mathbf{HF}_{opt})^T (\mathbf{HF}_{opt})}$.

*(b) In the high* SNR *situation (*$\mathrm{SNR} > -\mathrm{Cb}^2$*), both transmitters can transmit concurrently. Then, we have* $\tilde{\alpha} = \theta_U$, $\tilde{\beta} = \theta_L$, $\tilde{\mu} = \frac{abC + \sqrt{\mathrm{C{\cdot}SNR(b^2 - a^2) + SNR^2}}}{\mathrm{SNR - Ca^2}}$, $\tilde{d}_2 = \frac{1/E_s}{F(\theta_U, \theta_L, \tilde{\mu})}$,

$$\mathbf{F}_{\mathrm{opt}} = \tilde{d}_2 \mathbf{V} \begin{pmatrix} \frac{\tilde{\mu}}{\lambda_1} \cos\theta_U & \frac{1}{\lambda_1} \cos\theta_L \\ \frac{\tilde{\mu}}{\lambda_2} \sin\theta_U & \frac{1}{\lambda_2} \sin\theta_L \end{pmatrix}, \tag{2.26}$$

$$\min \bar{P}_{\mathrm{sep}} = \frac{(q-1)}{q} \left( Q\left( \frac{d\tilde{\mu}\sqrt{\mathrm{SNR}}}{\sqrt{2} \cdot \sqrt{\left( \tilde{\mathbf{H}}_{opt}^T \tilde{\mathbf{H}}_{opt} \right)_{11}^{-1}}} \right) + Q\left( \frac{d\sqrt{\mathrm{SNR}}}{\sqrt{2} \cdot \sqrt{\left( \tilde{\mathbf{H}}_{opt}^T \tilde{\mathbf{H}}_{opt} \right)_{22}^{-1}}} \right) \right),$$

*and the BER is*

$$\min \bar{P}_b = \frac{1}{q \log_2 q} \sum_{k=1}^{\log_2 q} \sum_{i=0}^{\left(1-2^{-k}\right)q-1} \left\{ (-1)^{\left\lfloor \frac{i \cdot 2^{k-1}}{q} \right\rfloor} \left( 2^{k-1} - \left\lfloor \frac{i \cdot 2^{k-1}}{q} + \frac{1}{2} \right\rfloor \right) \cdot \left( Q\left( \frac{(2i+1)\, d\tilde{\mu}\sqrt{\mathrm{SNR}}}{\sqrt{2} \cdot \sqrt{\left( \tilde{\mathbf{H}}_{opt}^T \tilde{\mathbf{H}}_{opt} \right)_{11}^{-1}}} \right) + Q\left( \frac{(2i+1)\, d\sqrt{\mathrm{SNR}}}{\sqrt{2} \cdot \sqrt{\left( \tilde{\mathbf{H}}_{opt}^T \tilde{\mathbf{H}}_{opt} \right)_{22}^{-1}}} \right) \right) \right\},$$

*where* $\tilde{\mathbf{H}}_{opt} = \mathbf{H}\mathbf{F}_{opt}$.

2. $\psi = \frac{\pi}{4}$

*The* SNR *does not affect the final solution, both transmitters can transmit concurrently. Then, we have* $\tilde{\alpha} = \theta_U$, $\tilde{\beta} = \theta_L$, $\tilde{\mu} = 1$, $\tilde{d}_2 = \frac{2}{(a+b)d(q-1)}$,

$$\mathbf{F}_{\text{opt}} = \frac{2}{(a+b)\,d\,(q-1)}\mathbf{V}\begin{pmatrix} \frac{1}{\lambda_1}\cos\theta_U & \frac{1}{\lambda_1}\cos\theta_L \\ \frac{\tilde{1}}{\lambda_2}\sin\theta_U & \frac{1}{\lambda_2}\sin\theta_L \end{pmatrix},$$

$$\min \bar{P}_{\text{sep}} = \frac{2\,(q-1)}{q} Q\left(\frac{d\sqrt{\text{SNR}}}{\sqrt{2}\cdot\sqrt{\left(\tilde{\mathbf{H}}_{opt}^T\tilde{\mathbf{H}}_{opt}\right)^{-1}_{11}}}\right),$$

*and the BER is*

$$\begin{aligned}\min \bar{P}_b \;=\; & \frac{1}{q\log_2 q}\sum_{k=1}^{\log_2 q}\sum_{i=0}^{\left(1-2^{-k}\right)q-1}\left\{(-1)^{\left\lfloor\frac{i\cdot 2^{k-1}}{q}\right\rfloor}\left(2^{k-1}-\left\lfloor\frac{i\cdot 2^{k-1}}{q}+\frac{1}{2}\right\rfloor\right)\right. \\ & \left.\cdot 2Q\left(\frac{(2i+1)\,d\sqrt{\text{SNR}}}{\sqrt{2}\cdot\sqrt{\left(\tilde{\mathbf{H}}_{opt}^T\tilde{\mathbf{H}}_{opt}\right)^{-1}_{11}}}\right)\right\},\end{aligned}$$

*where* $\tilde{\mathbf{H}}_{opt} = \mathbf{H}\mathbf{F}_{opt}$.

3. $\frac{\pi}{4} < \psi \leq \frac{\pi}{2}$

(a) *In the low* SNR *situation (*$\text{SNR} \leq \text{Ca}^2$*), we turn off one of the transmitters and let the other work alone. Let* $q_1 = q^2$.

i. $j_{11} \geq j_{22}$, $\mathbf{F}_{opt} = \begin{pmatrix} e \\ 0 \end{pmatrix}$.

*ii.* $j_{11} < j_{22}$, $\mathbf{F}_{opt} = \begin{pmatrix} 0 \\ e \end{pmatrix}$.

*Then,*

$$\min \bar{P}_{\text{sep}} = \frac{2\,(q_1 - 1)}{q_1} Q\left(\frac{dh \cdot \sqrt{\text{SNR}}}{\sqrt{2}}\right),$$

*and the BER is*

$$\begin{aligned} \min \bar{P}_b &= \frac{1}{q_1 \log_2 q_1} \sum_{k=1}^{\log_2 q_1} \sum_{i=0}^{\left(1-2^{-k}\right)q_1 - 1} \left\{ (-1)^{\left\lfloor \frac{i \cdot 2^{k-1}}{q_1} \right\rfloor} \left( 2^{k-1} - \left\lfloor \frac{i \cdot 2^{k-1}}{q_1} + \frac{1}{2} \right\rfloor \right) \right. \\ &\quad \left. \cdot 2Q\left(\frac{(2i+1)\,dh \cdot \sqrt{\text{SNR}}}{\sqrt{2}}\right) \right\}, \end{aligned}$$

*where* $h = \sqrt{(\mathbf{H}\mathbf{F}_{opt})^T (\mathbf{H}\mathbf{F}_{opt})}$.

*(b) In the high* SNR *situation (*$\text{SNR} > \text{Ca}^2$*), both transmitters can transmit concurrently. Then, we have* $\tilde{\alpha} = \theta_U$, $\tilde{\beta} = \theta_L$, $\tilde{\mu} = \frac{abC + \sqrt{\text{C}\cdot\text{SNR}(\text{b}^2 - \text{a}^2) + \text{SNR}^2}}{\text{SNR} - \text{Ca}^2}$, $\tilde{d}_2 = \frac{1/E_s}{F(\theta_U, \theta_L, \tilde{\mu})}$,

$$\mathbf{F}_{\text{opt}} = \tilde{d}_2 \mathbf{V} \begin{pmatrix} \frac{\tilde{\mu}}{\lambda_1} \cos\theta_U & \frac{1}{\lambda_1} \cos\theta_L \\ \frac{\tilde{\mu}}{\lambda_2} \sin\theta_U & \frac{1}{\lambda_2} \sin\theta_L \end{pmatrix},$$

$$\min \bar{P}_{\text{sep}} = \frac{(q-1)}{q} \left( Q\left( \frac{d\tilde{\mu}\sqrt{\text{SNR}}}{\sqrt{2} \cdot \sqrt{\left(\tilde{\mathbf{H}}_{opt}^T \tilde{\mathbf{H}}_{opt}\right)^{-1}_{11}}} \right) + Q\left( \frac{d\sqrt{\text{SNR}}}{\sqrt{2} \cdot \sqrt{\left(\tilde{\mathbf{H}}_{opt}^T \tilde{\mathbf{H}}_{opt}\right)^{-1}_{22}}} \right) \right),$$

*and the BER is*

$$\min \bar{P}_b = \frac{1}{q\log_2 q}\sum_{k=1}^{\log_2 q}\sum_{i=0}^{\left(1-2^{-k}\right)q-1}\left\{(-1)^{\left\lfloor\frac{i\cdot 2^{k-1}}{q}\right\rfloor}\left(2^{k-1}-\left\lfloor\frac{i\cdot 2^{k-1}}{q}+\frac{1}{2}\right\rfloor\right)\right.$$
$$\left.\cdot\left(Q\left(\frac{(2i+1)\,d\tilde{\mu}\sqrt{\mathrm{SNR}}}{\sqrt{2}\cdot\sqrt{\left(\tilde{\mathbf{H}}_{opt}^T\tilde{\mathbf{H}}_{opt}\right)_{11}^{-1}}}\right)+Q\left(\frac{(2i+1)\,d\sqrt{\mathrm{SNR}}}{\sqrt{2}\cdot\sqrt{\left(\tilde{\mathbf{H}}_{opt}^T\tilde{\mathbf{H}}_{opt}\right)_{22}^{-1}}}\right)\right)\right\},$$

*where* $\tilde{\mathbf{H}}_{opt}=\mathbf{H}\mathbf{F}_{opt}$.

■

The proof of Theorem 1 is provided in Appendix A.2. We would like to make some comments about Theorem 1 as follows:

1. In the very high SNR with the invertible $\mathbf{H}$ situation, we obtain the following results:
$$\tilde{\mu}=\lim_{\mathrm{SNR}\to\infty}\frac{abC+\sqrt{\mathrm{C}\left(b^2-a^2\right)+\mathrm{SNR}^2}}{\mathrm{SNR}-\mathrm{Ca}^2}=1.$$
Thus, the optimal $\tilde{\mu}$ approaches one, which means that both subchannels for ZF are the same.

2. In the high SNR regime, the optimal precoding matrix $\mathbf{F}_{opt}$ is a $2\times 2$ off-diagonal matrix.

3. The peak-to-average power ratio (PAPR) is 2 for both original signal constellation and pre-coded constellation. So, it does not change after using the optimal pre-coding matrix.

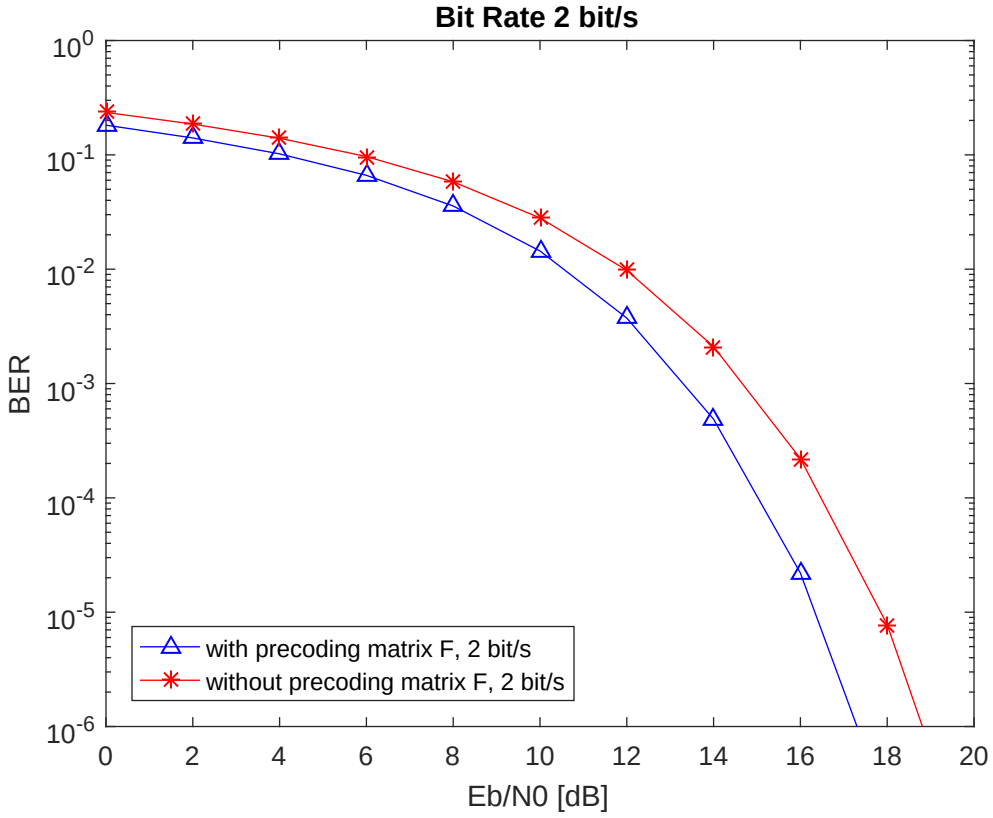


Figure 2.3: The comparison of bit error rate (BER) performance between with and without precoding matrix **F**. Each transmitter sends a 2-PAM constellation and the total bit rate is 2 bit/s.

## 2.3 Simulation Results

### 2.3.1 Bit Error Rate Simulation

In this section, we examine the average bit error rate (BER) performance of linear space code with or without our optimal precoding matrix in a room which size is 4.0m×4.0m×1.8m. We assume that $\theta_{R\frac{1}{2}} = 15°$, $J = 1cm^2$ and $N = M = 2$. The locations of the two transmitters are LED_TX1(2.0m, 1.8m, 1.8m) and LED_TX2(2.0m, 2.2m, 1.8m). The locations of the two receiver PDs are ($x_i$m, $y_i$m, 0m). We choose

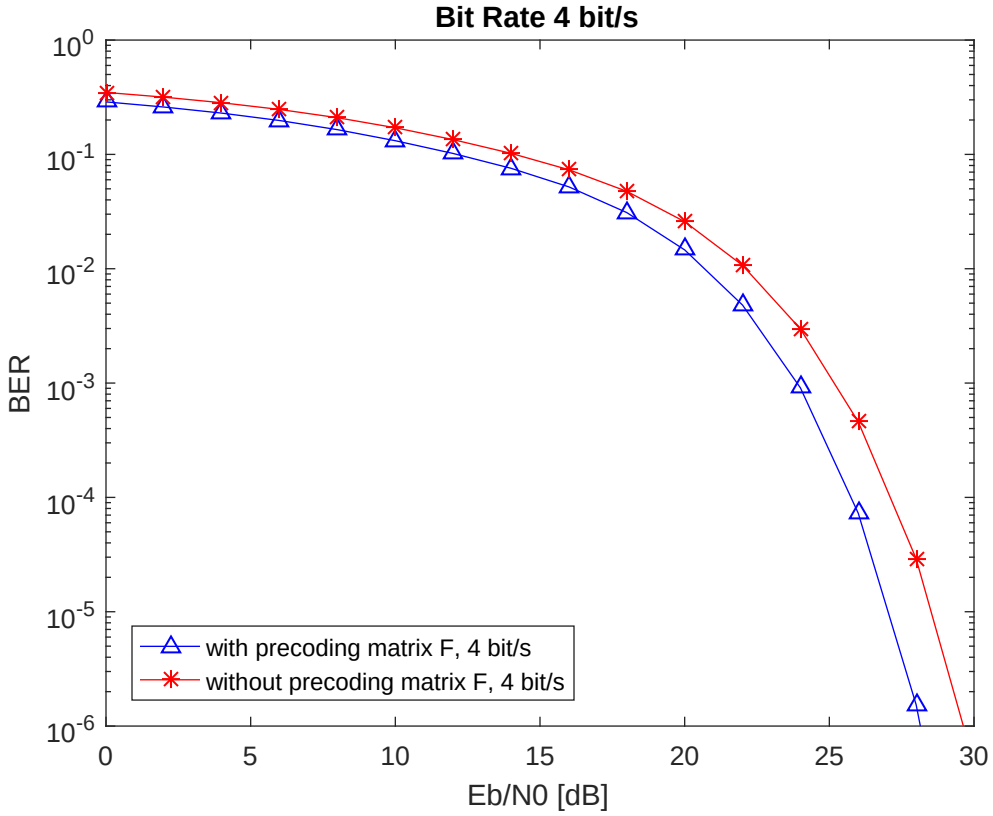


Figure 2.4: The comparison of bit error rate (BER) performance between with and without precoding matrix **F**. Each transmitter sends a 4-PAM constellation and the total bit rate is 4 bit/s.

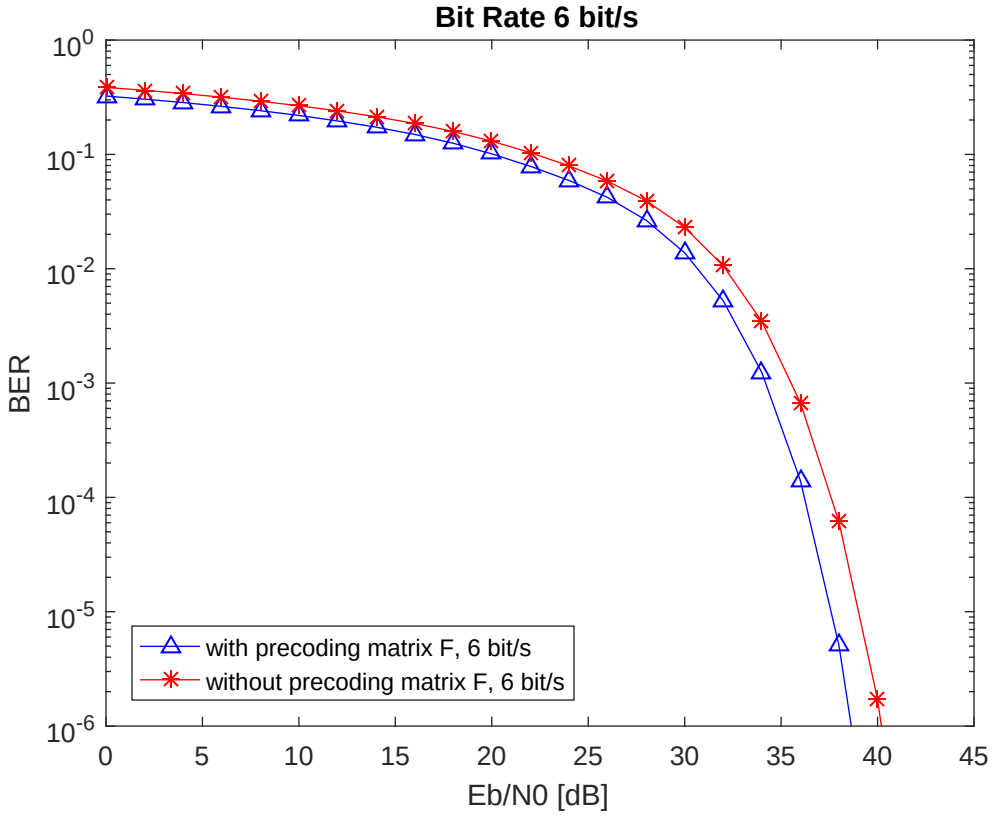


Figure 2.5: The comparison of bit error rate (BER) performance between with and without precoding matrix **F**. Each transmitter sends a 8-PAM constellation and the total bit rate is 6 bit/s.

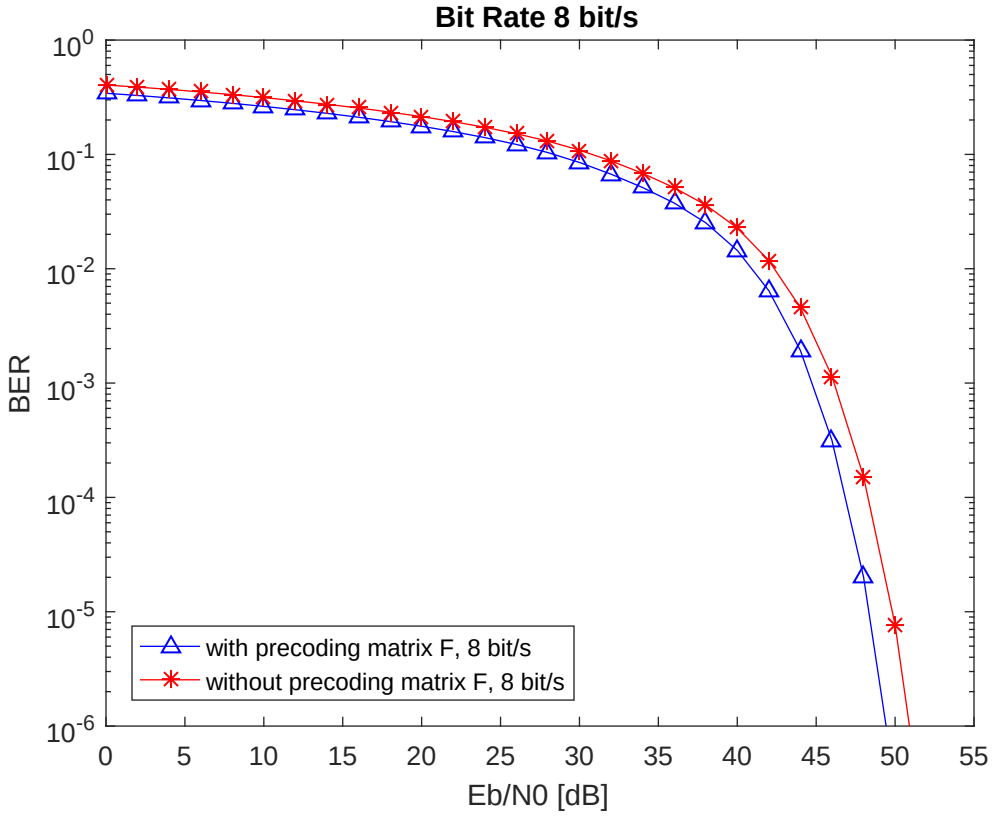


Figure 2.6: The comparison of bit error rate (BER) performance between with and without precoding matrix **F**. Each transmitter sends a 16-PAM constellation and the total bit rate is 8 bit/s.

$x_i$ and $y_i$ uniformly inside interval (0, 4). We abandon those situations which both receiver PDs are not in FOV. The channel coefficients are computed by (2.3) and each coefficient will be normalized by maximum channel coefficient, and the SNR defined as $\frac{1}{2\sigma^2}$. The receivers are ZF detectors in order to make all comparisons fair. We randomly choose 500 pairs of receiver PDs in the room and compute the average BER. Figures 2.3, 2.4, 2.5, 2.6 show the average BER of 500 pairs of receiver PDs with bit rate 2, 4, 6, 8 bit/s, respectively. Here we can observe that the linear space code with our optimized coding matrix has the best performance in both low SNR and high SNR conditions. Here, it should be mentioned that in the low SNR scenario, according to our theorem, we need to turn off one of the transmitters and let the other work alone. In order to guarantee the same transmission rate, the constellation size should be improved from $q$-PAM to $q^2$-PAM.

### 2.3.2 Received Constellation Points

Here, we draw the constellation points for received signals with or without optimal precoding matrix $\mathbf{F}$. For discussion simplicity, we choose an invertible channel matrix $\mathbf{H}$. After normalization, it is given by

$$\mathbf{H} = \begin{bmatrix} 0.8634 & 0.6062 \\ 0.3409 & 1.0000 \end{bmatrix}.$$

Each transmitter sends a 2-, 4-, 8-, 16-PAM constellation, and two $q$-PAM constellations can constitute a $q^2$-QAM constellation. We put the channel in a high SNR situation in which both transmitters can transmit concurrently. Figures 2.7, 2.8, 2.9, 2.10 show the comparison of different received constellations at the bit rate 2, 4, 8,

16 bit/s , respectively. For each figure group, in the top row, the left graph shows the original signal constellation, the right graph shows the precoded signal constellation. In the bottom row, the left graph shows the received constellation with $\mathbf{F}$, and the right graph without $\mathbf{F}$. As we can see, the precoding matrix $\mathbf{F}$ changes the distance between neighbour points both in abscissas and ordinates. In (2.4), after processed by zero-forcing equalizer, the noise is changed to $\tilde{\mathbf{n}} = \begin{bmatrix} \tilde{n}_1 \\ \\ \tilde{n}_2 \end{bmatrix}$. The optimal precoding $\mathbf{F}$ affects to detect the larger one of $\tilde{n}_1$ and $\tilde{n}_2$, broadens the distance of neighbour points in that dimension and hence, reduces the distance in the other dimension. As a result, the average $\bar{P}_{\text{sep}}$ will be reduced.

### 2.3.3 Comparison with ZF Power Appending Method

In Yu *et al.* (2013), they provide another method to design precoding matrix which, for simplicity, is called ZF power appending method. It uses the traditional idea from RF communications and adds a specific power to the transmitted signals to make the resulting signals always non-negative due to the constraint in VLC. Now, let's compare BER between this method and our method in the same system model with the same transmission power and the same transmission bit rate.

Figures 2.11, 2.12, 2.13, 2.14 show the comparison of bit error rate (BER) performance between the two precoding matrix design methods. Each transmitter sends a 2-, 4-, 8-, 16-PAM constellation, the total bit rate is 2, 4, 6, 8 bit/s, respectively. As we can see, our precoding matrix always has lower BER in both low SNR scenario and high SNR scenario.

Figures 2.15, 2.16, 2.17 show the comparison of the transmitted signal constellations and received signal constellations between our optimal precoding matrix and

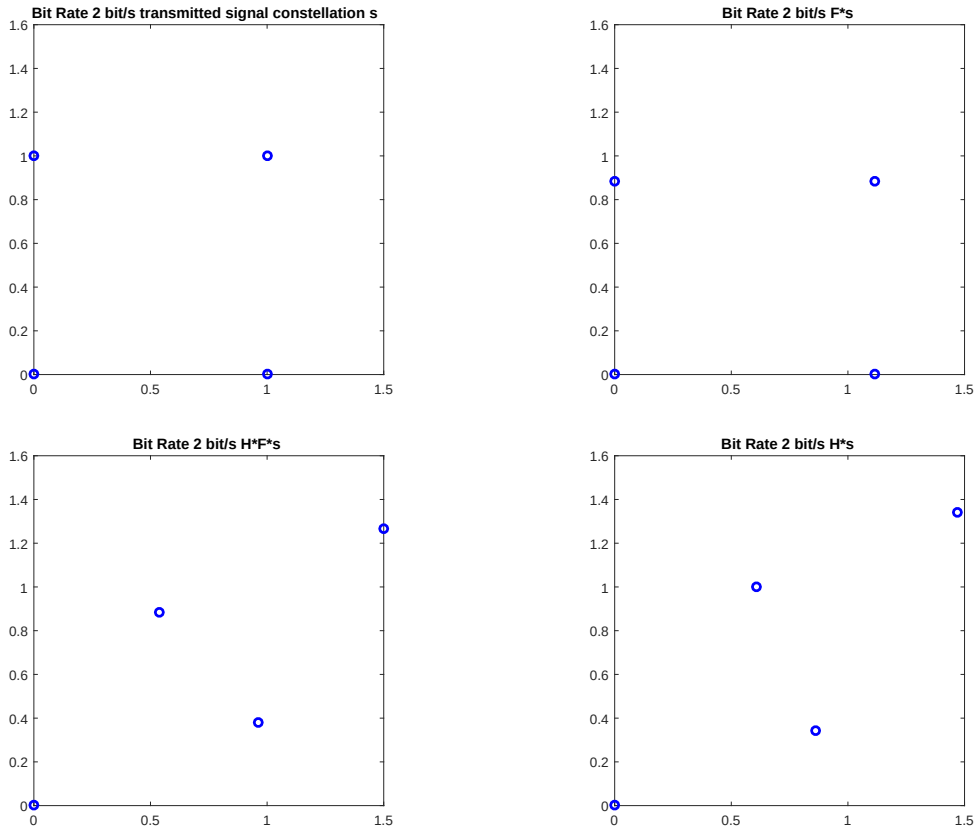


Figure 2.7: Top row: original signal constellation (top left figure), precoded signal constellation (top right figure). Bottom row: compare received signal constellations between with (**HFs**) and without (**Hs**) precoding matrix. Each transmitter sends a 2-PAM constellation, and the total bit rate is 2bit/s.

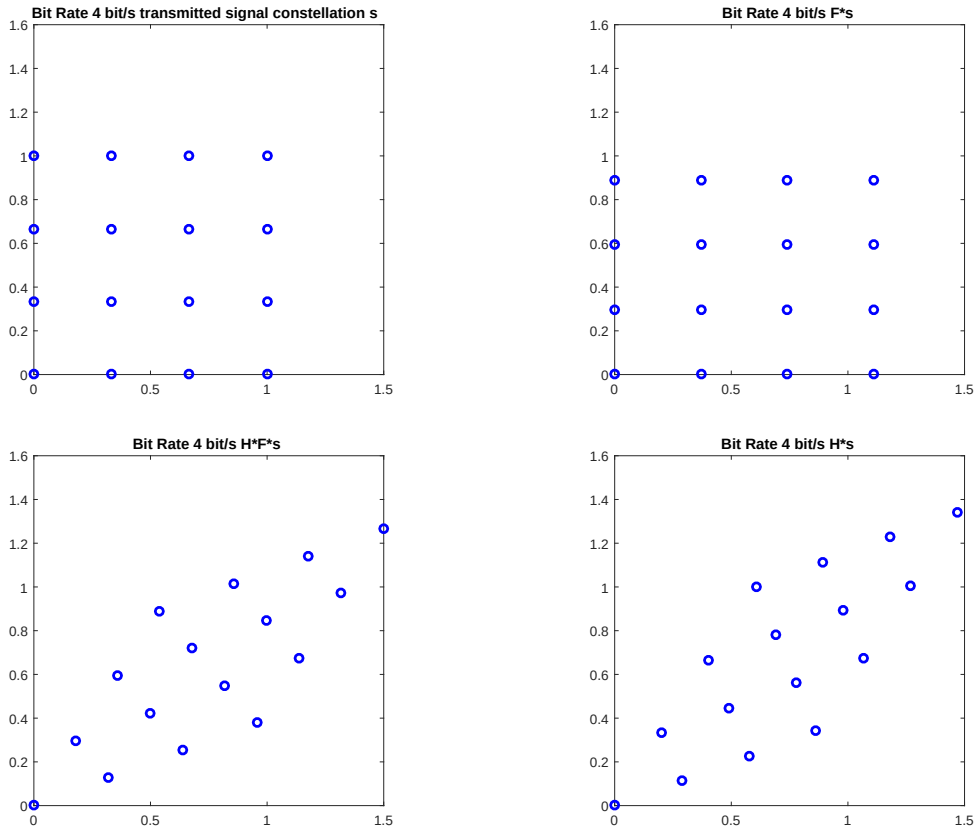


Figure 2.8: Top row: original signal constellation (top left figure), precoded signal constellation (top right figure). Bottom row: compare received signal constellations between with (**HFs**) and without (**Hs**) precoding matrix. Each transmitter sends a 4-PAM constellation, and the total bit rate is 4bit/s.

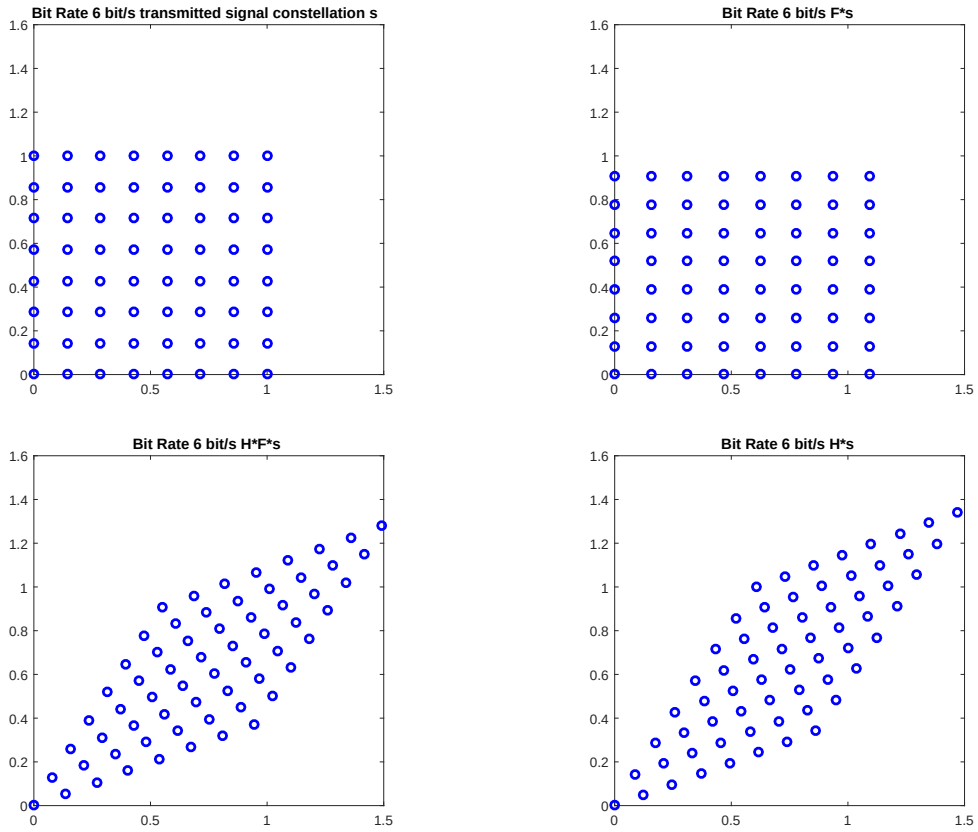


Figure 2.9: Top row: original signal constellation (top left figure), precoded signal constellation (top right figure). Bottom row: compare received signal constellations between with (**HFs**) and without (**Hs**) precoding matrix. Each transmitter sends a 8-PAM constellation, and the total bit rate is 6bit/s.

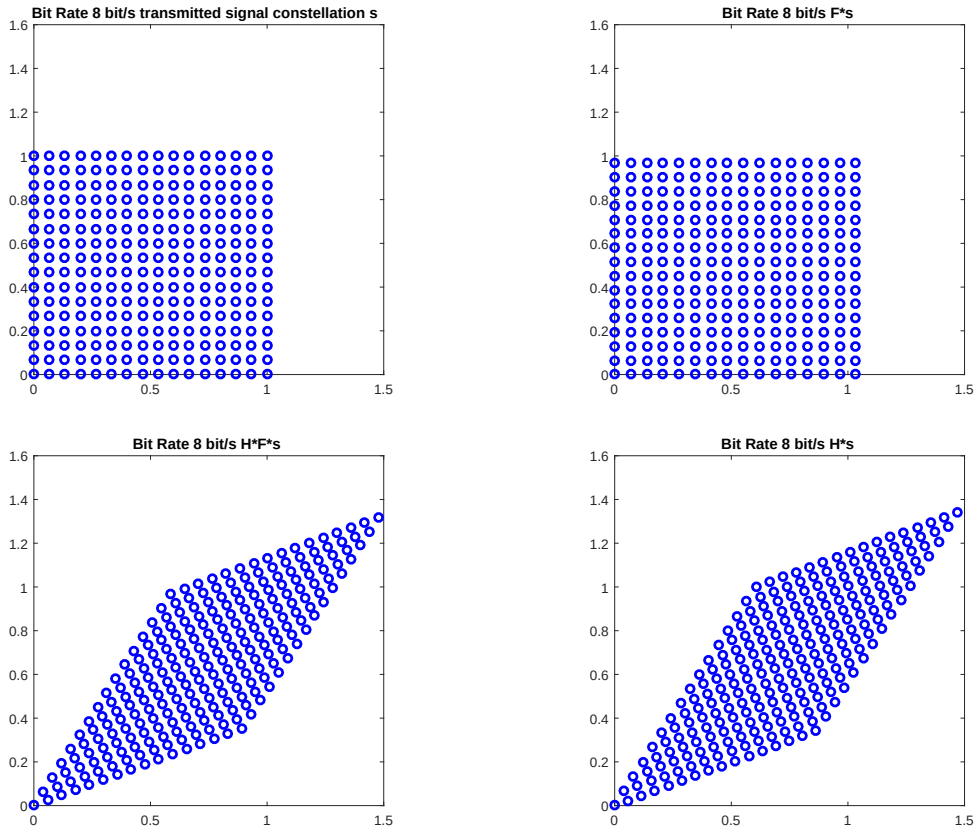


Figure 2.10: Top row: original signal constellation (top left figure), precoded signal constellation (top right figure). Bottom row: compare received signal constellations between with (**HFs**) and without (**Hs**) precoding matrix. Each transmitter sends a 16-PAM constellation, and the total bit rate is 8bit/s.

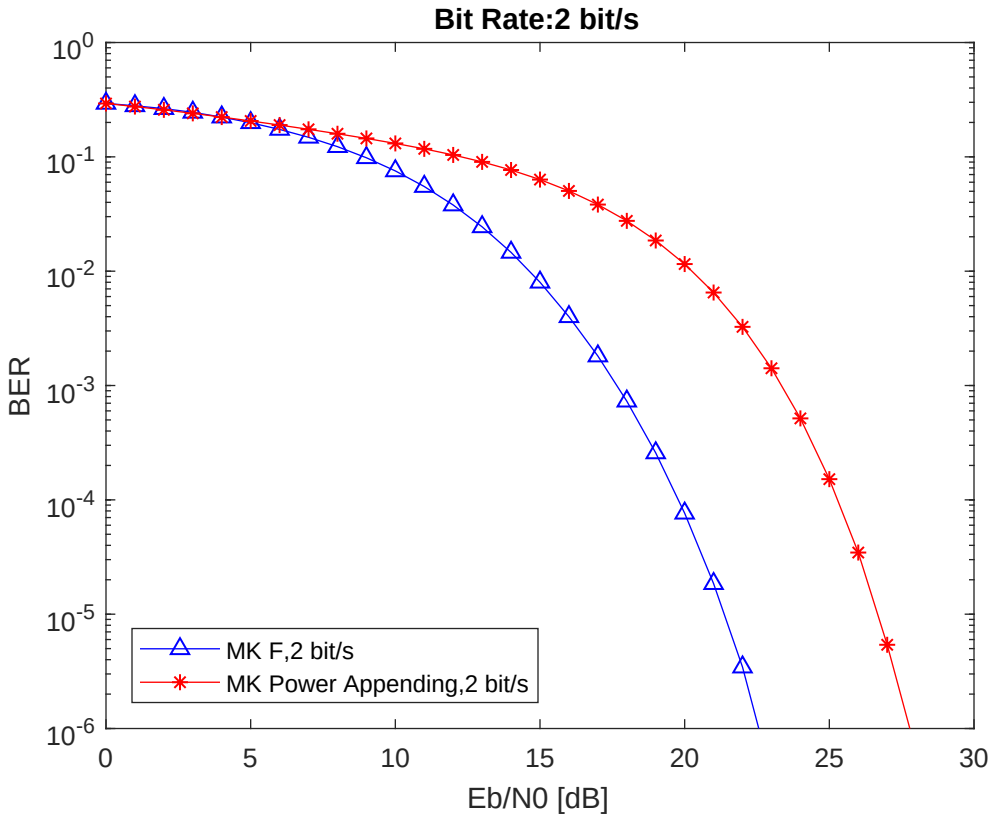


Figure 2.11: The comparison of bit error rate (BER) performance between two precoding matrix design methods. Each transmitter sends a 2-PAM constellation, and the total bit rate is 2 bit/s.

the ZF power appending method. The two figures in the left column show the transmitted signal and received signal constellations with our optimal precoding matrix. The right two figure show the constellations with the ZF power appending method. We can see that by using the ZF power appending method, the distance between signal points in the constellation is much smaller than that with optimal precoding matrix. Thus, it will lead to larger error probability under the same SNR. Hence, our optimal precoding matrix performs better than the ZF power appending method.

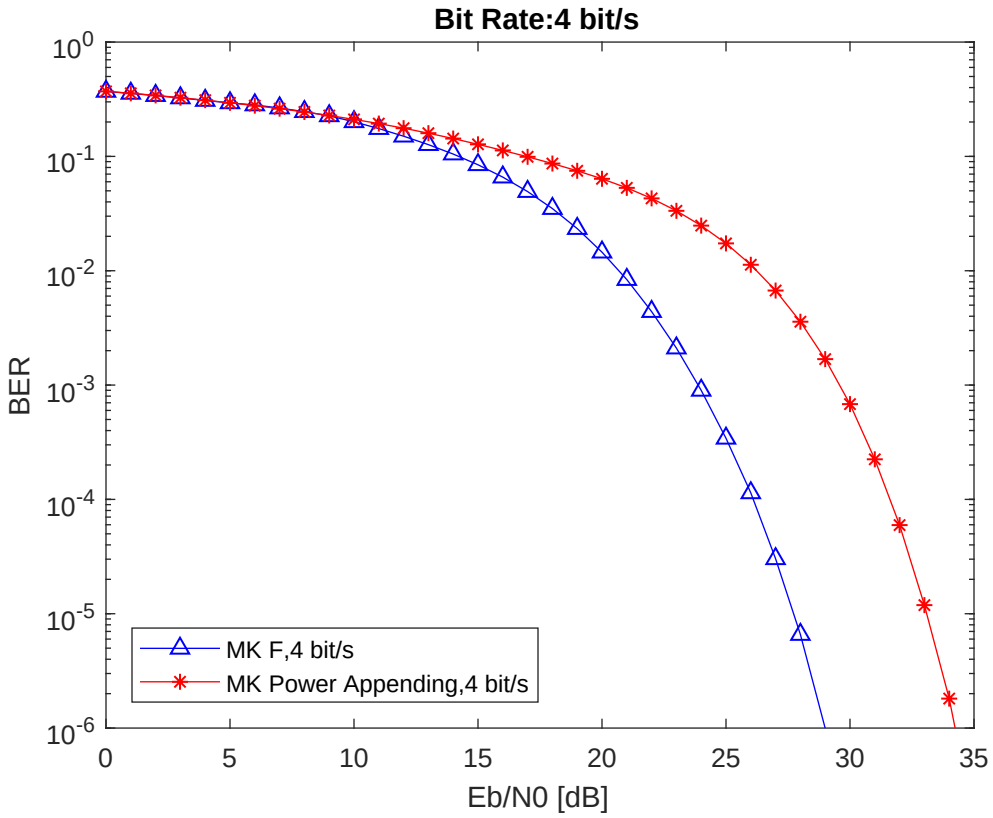


Figure 2.12: The comparison of bit error rate (BER) performance between two precoding matrix design methods. Each transmitter sends a 4-PAM constellation, and the total bit rate is 4 bit/s.

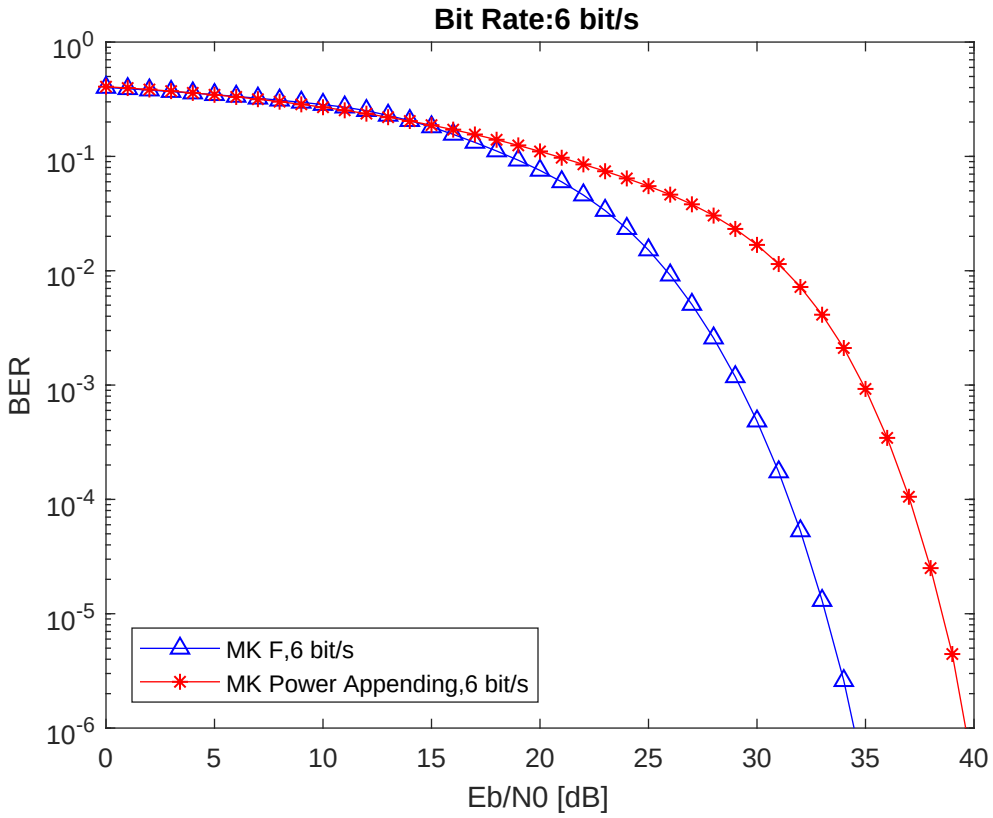


Figure 2.13: The comparison of bit error rate (BER) performance between two precoding matrix design methods. Each transmitter sends a 8-PAM constellation, and the total bit rate is 6 bit/s.

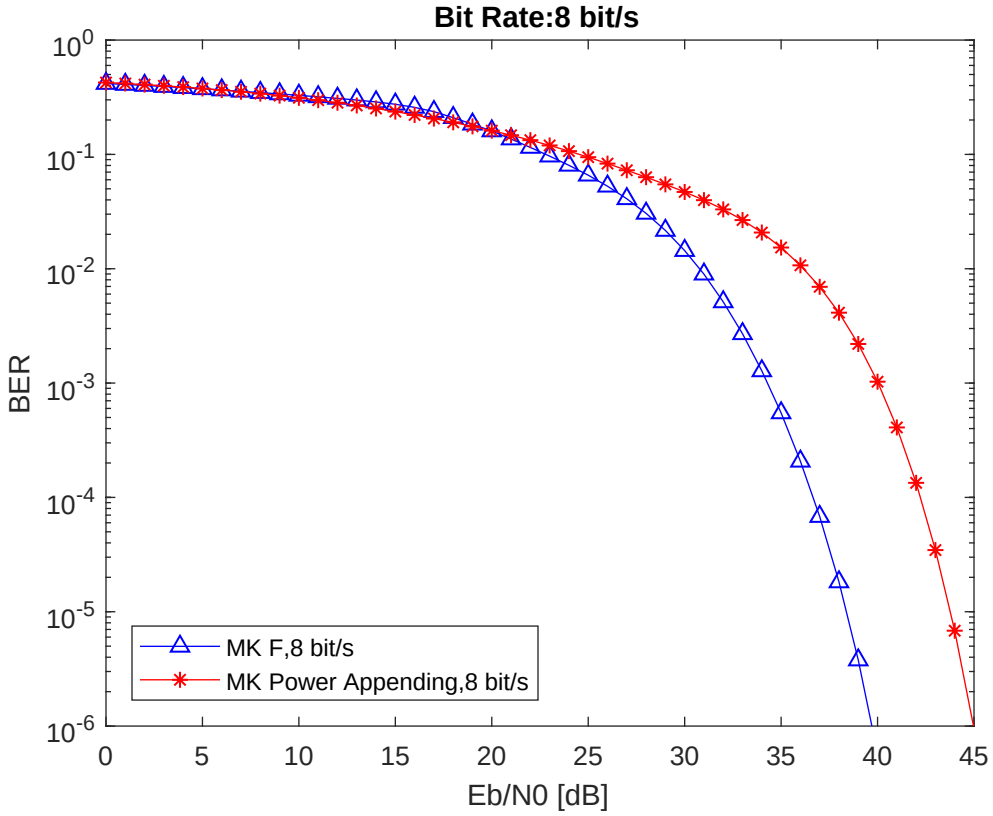


Figure 2.14: The comparison of bit error rate (BER) performance between two precoding matrix design methods. Each transmitter sends a 16-PAM constellation, and the total bit rate is 8 bit/s.

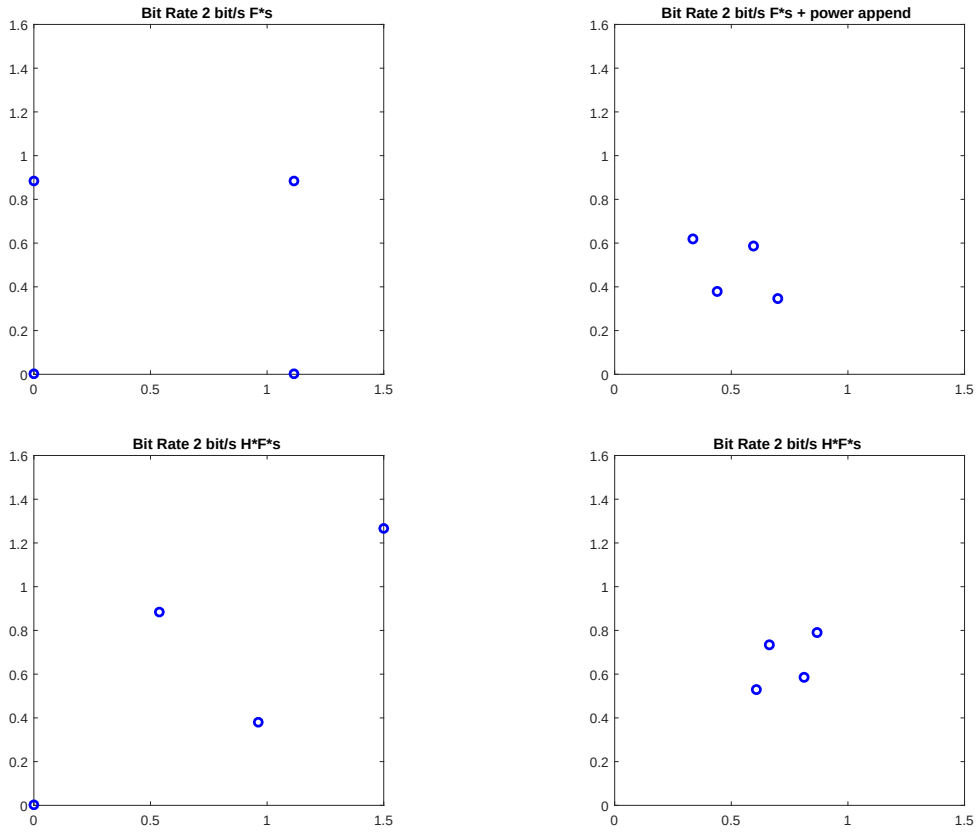


Figure 2.15: The comparison of transmitted signal constellation and received signal constellation between using our optimal precoding matrix (left column) and power appending method (right column). The Top two figures show the transmitted signals before sending out and the bottom two figures show the signals at receiver side. Each transmitter sends a 2-PAM constellation, and the total bit rate is 2 bit/s.

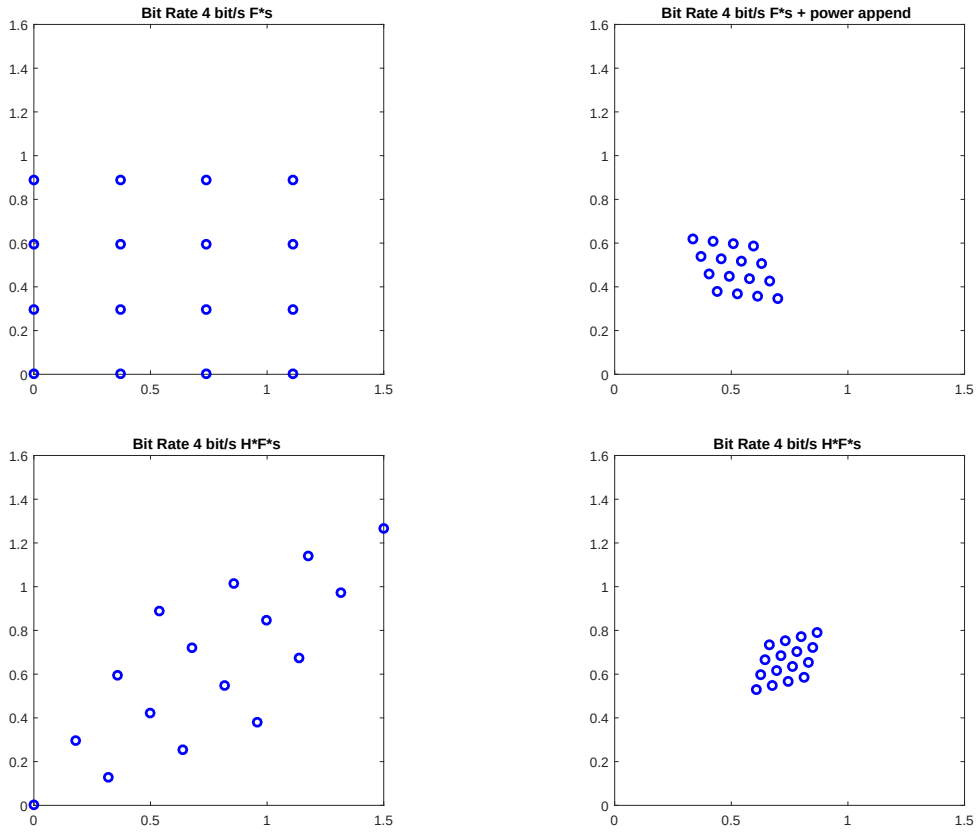


Figure 2.16: The comparison of transmitted signal constellation and received signal constellation between using our optimal precoding matrix (left column) and power appending method (right column). The Top two figures show the transmitted signals before sending out and the bottom two figures show the signals at receiver side. Each transmitter sends a 4-PAM constellation, and the total bit rate is 4 bit/s.

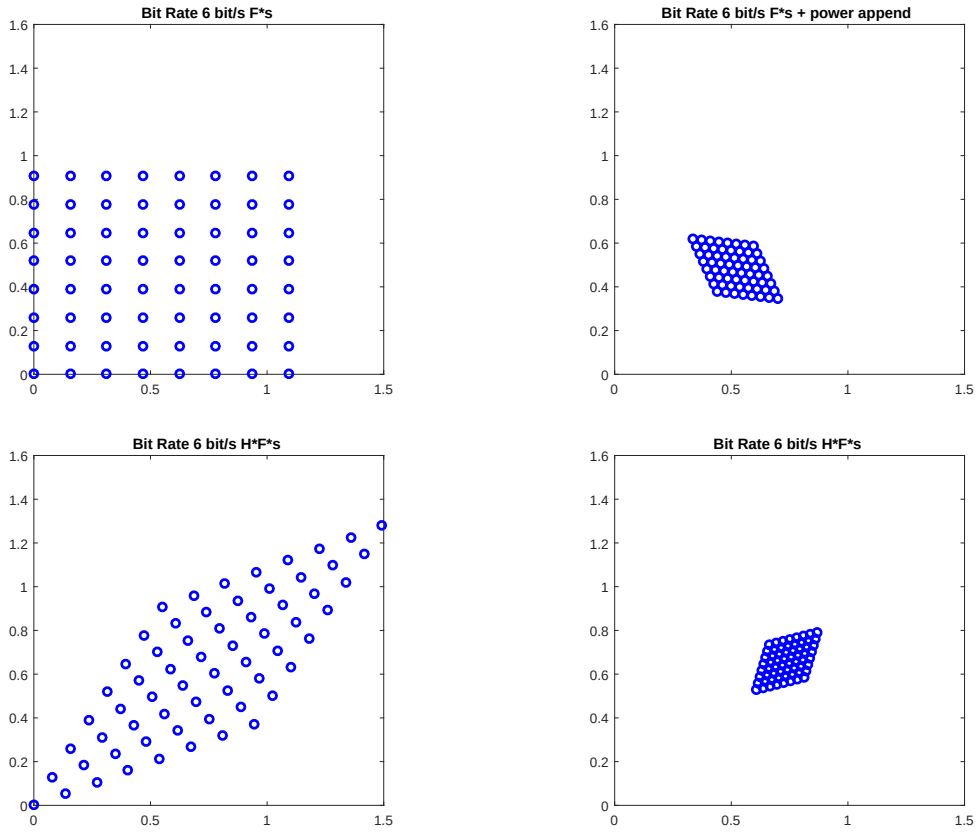


Figure 2.17: The comparison of transmitted signal constellation and received signal constellation between using our optimal precoding matrix (left column) and power appending method (right column). The Top two figures show the transmitted signals before sending out and the bottom two figures show the signals at receiver side. Each transmitter sends a 8-PAM constellation, and the total bit rate is 6 bit/s.

## 2.4 Conclusion

In this chapter, we have introduced the design of optimal precoding matrix **F** for the indoor MIMO-VLC system with the zero-forcing equalizer. The channel state information is available at both the transmitters and the receivers. We cannot use the technology for MIMO RF communications directly, since there is a nonnegative constraint on the precoding matrix and signal constellation in the visible light communication system. Thus, we develop a new method to generate the precoding matrix for this special situation. Theorem 1 shows that the design of the optimal precoding matrix should be considered separately. In the specific situations in which the channel matrix **H** is not invertible or SNR is low with the invertible **H**, one of the transmitters should be closed and the precoding matrix **F** becomes a vector. In the high SNR, both transmitters can transmit concurrently. Through computer simulations, we have shown that our optimal precoding matrix performs much better in BER than currently available methods.

# Chapter 3

# Part II: AUDCG Constellation Design for Multi-User MISO-VLC System

## 3.1 System Model

In this chapter, we consider a multi-user MISO-VLC system model with $M = 2$ antennas at transmitter end and $N = 1$ photo-detector at the receiver end for each user. The number of users is 2. For such a system, at a specific time slot $t$, the received signal $y_t$ for each user can be written as

$$y_t = \sum_{m=1}^{M} h_m x_{tm} + n_t,$$

for $t = 1, 2, \cdots$, $x_{tm}$ is the symbol emitted by the $m$-th transmitter and $n_t$ is the white Gaussian noise with zero mean and variance $\sigma^2$. $h_m$ is the channel coefficient

between the $m$-th transmitter and the receiver, which can be represented by

$$h_m = \begin{cases} \frac{(K+1)J}{2\pi d_m^2}\cos^{\mathrm{K}}(\theta_{Tm})\cos(\theta_{Rm}) & 0 \le \theta_{Rm} \le \theta_{R\frac{1}{2}} \\ 0 & \theta_{Rm} > \theta_{R\frac{1}{2}} \end{cases},$$

where $\theta_{Tm}$ is the angle of emergence with respect to the transmitter $m$ axis and $\theta_{Rm}$ is the angle of incidence with respect to the receiver axis, $d_m$ is the distance between the $m$-th transmitter and the receiver, $K = \frac{-\ln 2}{\ln\left(\theta_{R\frac{1}{2}}\right)}$, $\theta_{R\frac{1}{2}} = 15°$. In this chapter, $J$ is assumed to be $1cm^2$. The $h_m$ depends on unique position of $m$-th transmitter and the receiver. If the $m$-th transmitter and the receiver are not in FOV, then $h_m = 0$. Here, we use repetition transmission in spatial dimensions. Let $S \subseteq \mathbb{Z}_+^T$ be a $T$-dimensional constellation that we will design, where $\mathbb{Z}_+^T$ means the set of all the $T \times 1$ nonnegative integer vectors. The transmission procedures are shown as follows: First, we choose a $T \times 1$ signal vector $\mathbf{s} = [s_1, \ldots, s_T]^T$ from $S$ randomly, independently and equally. Second, at the $t$-th time slot, all the $M$ transmitters transmit the same symbol $s_t$. For example, $x_{t1} = x_{t2} = \ldots = x_{tM} = s_t$. After all the T signals have been sent, the corresponding received signals can form a $T \times 1$ vector $\mathbf{u} = [u_1, u_2, \ldots, u_T]^T$:

$$\mathbf{u} = \alpha\mathbf{x} + \mathbf{n},$$

where $\alpha = \sum_{m=1}^{M} h_m$ and $\mathbf{n} = [n_1, n_2, \ldots, n_T]^T$ is the noise vector with zero mean and covariance $\sigma^2\mathbf{I}_{T\times T}$.

If we let $u_{nt}$ be the symbol received by $n$-th user at the time slot $t$, $h_{nm}$ be the channel coefficient between the $m$-th transmitter and $n$-th user. Then, the received signal vector for each user with $T = 2$ can be written as follows:

for User 1:

$$\begin{pmatrix} u_{11} \\ u_{12} \end{pmatrix} = \begin{bmatrix} h_{11}+h_{12} & 0 \\ 0 & h_{11}+h_{12} \end{bmatrix} \begin{pmatrix} s_1 \\ s_2 \end{pmatrix} + \begin{pmatrix} n_{11} \\ n_{12} \end{pmatrix},$$

and for User 2:

$$\begin{pmatrix} u_{21} \\ u_{22} \end{pmatrix} = \begin{bmatrix} h_{21}+h_{22} & 0 \\ 0 & h_{21}+h_{22} \end{bmatrix} \begin{pmatrix} s_1 \\ s_2 \end{pmatrix} + \begin{pmatrix} n_{21} \\ n_{22} \end{pmatrix}.$$

## 3.2 Additively Uniquely Decomposable Constellation Group Design

### 3.2.1 Problem Statement and Formulation

Now we consider this specific MU-MISO-VLC system with $M = 2$ transmitters and $N = 1$ photo-detector at receiver side for each user. The amount of user is 2. We assume that the channel state information (CSI) is known at both the transmission side and the receiver side. In order to estimate the received signal, maximum-likelihood (ML) detector will be used. Then, our main task in this chapter is to design a sum constellation $\mathcal{G}$ which can be decomposed into the sum of two sub-constellations, $\chi_1$ and $\chi_2$. These two sub-constellations must be able to constitute an additively uniquely decomposable constellation group (AUDCG). At the same time, we should consider to reduce the average optical energy of the sum constellation, $P(\mathcal{G}) = \frac{1}{|\mathcal{G}|} \sum_{g \in \mathcal{G}} \mathcal{G}$, subject to a fixed minimum Euclidean distance.

During the transmission, the two transmitter LEDs repeatedly transmit the same

Table 3.1: The Average Normalized Optical Power of Codeword for SMP and CC with Different Bit Rate

| Bit Rate | SMP | CC |
|---|---|---|
| 2 bits/s | 1 | 1 |
| 3 bits/s | 2 | 1.75 |
| 4 bits/s | 3 | 2.8125 |
| 5 bits/s | 5 | 4.375 |
| 6 bits/s | 7 | 6.5625 |
| 7 bits/s | 11 | 9.6875 |
| 8 bits/s | 15 | 14.0938 |
| 9 bits/s | 23 | 20.34375 |

symbol from sum constellation $\mathcal{G}$ at the same time. Once two users receive the sum symbol, they decompose the symbols in their own sub-constellation. Then, we can state our main task as follows:

**Problem 3.** *Design a sum constellation* $\mathcal{G}$ *with* $|\mathcal{G}| = L$, $d_{min}(\mathcal{G}) = 1$ *and* $\mathcal{G} = \chi_1 \uplus \chi_2$, *i.e., for any given* $g \in \mathcal{G}$, *we can find a unique pair of* $x_1 \in \chi_1$ *and* $x_2 \in \chi_2$ *such that* $g = x_1 + x_2$, *where* $d_{min}(\mathcal{G}) = \min_{s \neq s' \in \mathcal{G}} |s - s'|$. ■

### 3.2.2 Problem Analysis

Since there is a nonnegative constraint on the channel and the transmitted signal, the constellation points must be in the first quadrant or on the non-negative coordinate axis. In order to reduce $P(\mathcal{G})$, for any constellation point $s_i(x_i, y_i)$, we need to make $x_i + y_i$ as small as possible, subject to $d_{min}(\mathcal{G}) = 1$. Let's look at the two constellations in Fig 3.1. The top graph is the spatial multiplexing (SMP) constellation, the bottom graph is the space-collaborative constellation (CC). Table 3.1 shows the average normalized optical power of codeword for SMP and CC with different bit rate.

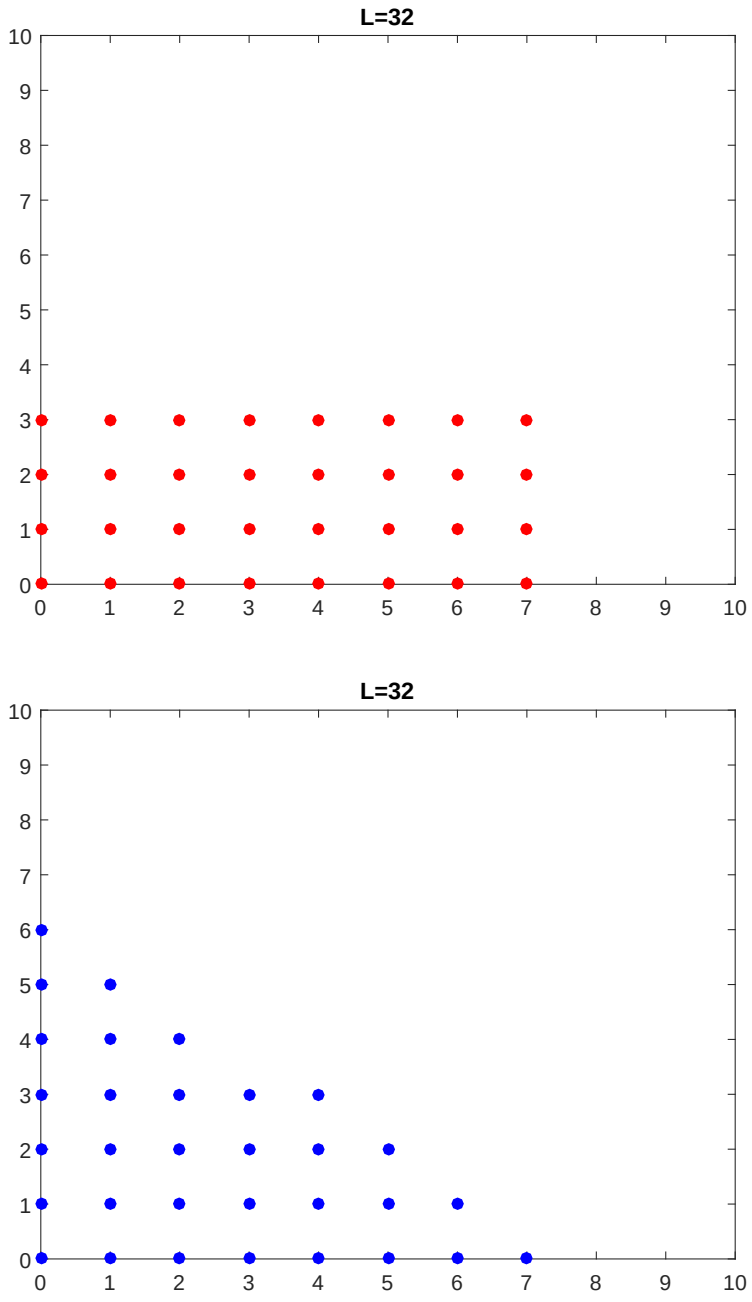


Figure 3.1: Constellations comparison: the top graph denotes SM, and the bottom graph denotes CC.

It is noticeable that with the same bit rate, the space-collaborative constellation has lower average normalized optical power. According to (Zhu *et al.*, 2015), the collaborative constellation $\tilde{\Omega}$ is defined as follows:

$$\tilde{\Omega} = \bigcup_{j=0}^{\lambda} \tilde{\Omega}_j,$$

where $\lambda = \lfloor \frac{\sqrt{8L+1}-3}{2} \rfloor$; $\tilde{\Omega}_j = \left\{ (x,y)^T | x+y=j, 0 \leq x,y \in \mathbb{Z} \right\}$ for $0 \leq j \leq \lambda - 1$; $\tilde{\Omega}_\lambda$ consists of all the solutions of $x + y = \lambda$.

However, not all the constellations can be decomposed into two sub-constellations that can form an AUDCG. Thus, we have to refine the CC.

**Definition 1.** *For any constellation point* $\mathbf{s} \in \left\{ (x,y)^T | 0 \leq x,y \in \mathbb{Z} \right\}$*, if* $\mathbf{1}^T\mathbf{s} = \lambda$*, then,* $\lambda$ *is called an energy level and* $\mathbf{s}$ *is said to be in the energy level* $\lambda$*. If an energy level* $\beta$ *has* $\beta + 1$ *integer points, then it is called full. If an energy level* $\beta$ *has 0 point, it is called empty. Otherwise, we call it not full.* ■

Let us consider the following example:

**Example 1.** *In Fig 3.1, the CC has 32 points, energy levels from 0 to 6 are full and energy level 7 is not full. This constellation cannot be uniquely decomposed into any two sub-constellations. However, we can move the positions of points in the outmost energy level to achieve our goal. Then, the results are shown in Fig 3.2. As we can see, the average normalized optical power of the sum constellation is not changed, but it can be decomposed into the sum of two sub-constellations, showed in Fig 3.3 with these two sub-constellations forming an AUDCG.*

It is not hard to compute the bit rate of them. The bit rate of sum constellation is 5 bit/s. And the bit rate of two sub-constellations are 1 bit/s and 4 bit/s, respectively.

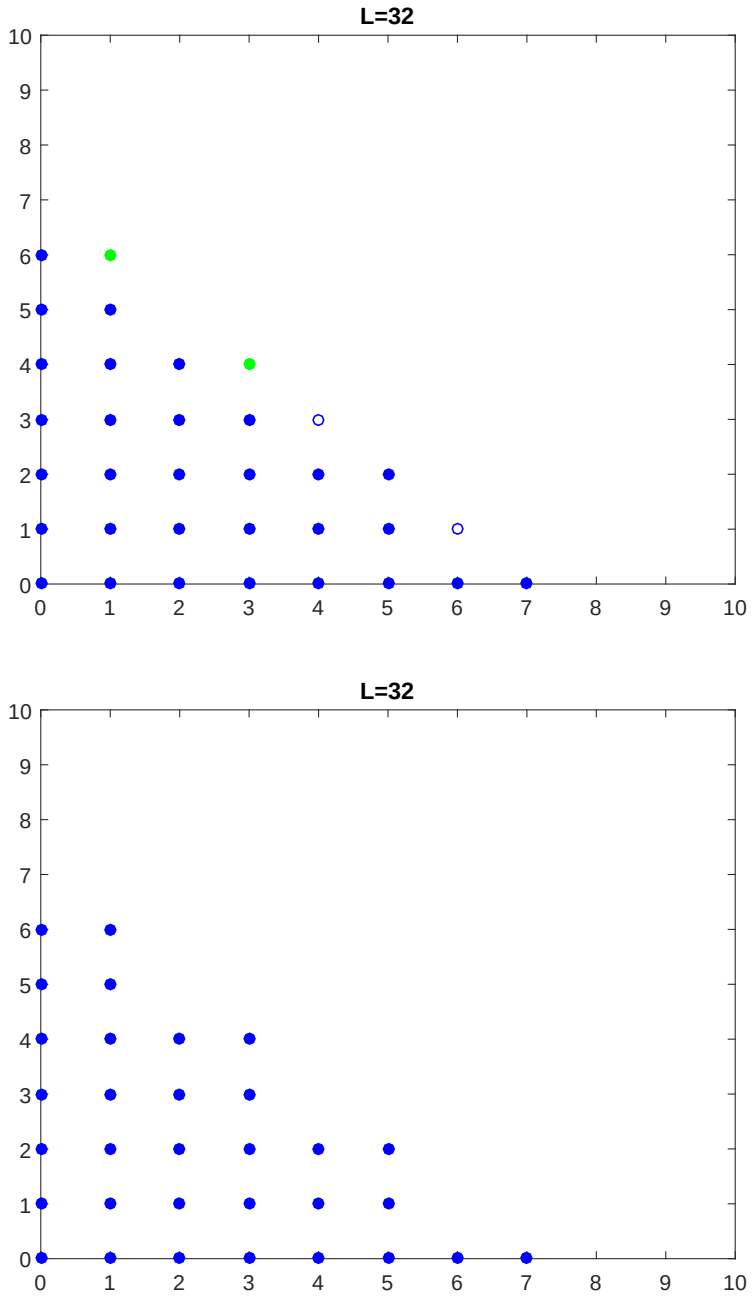


Figure 3.2: Figure for Example 1. The top graph denotes the process of points move, two blue circles are the original positions of two points in CC, and green points are new positions. The bottom graph denotes the constellation after move.

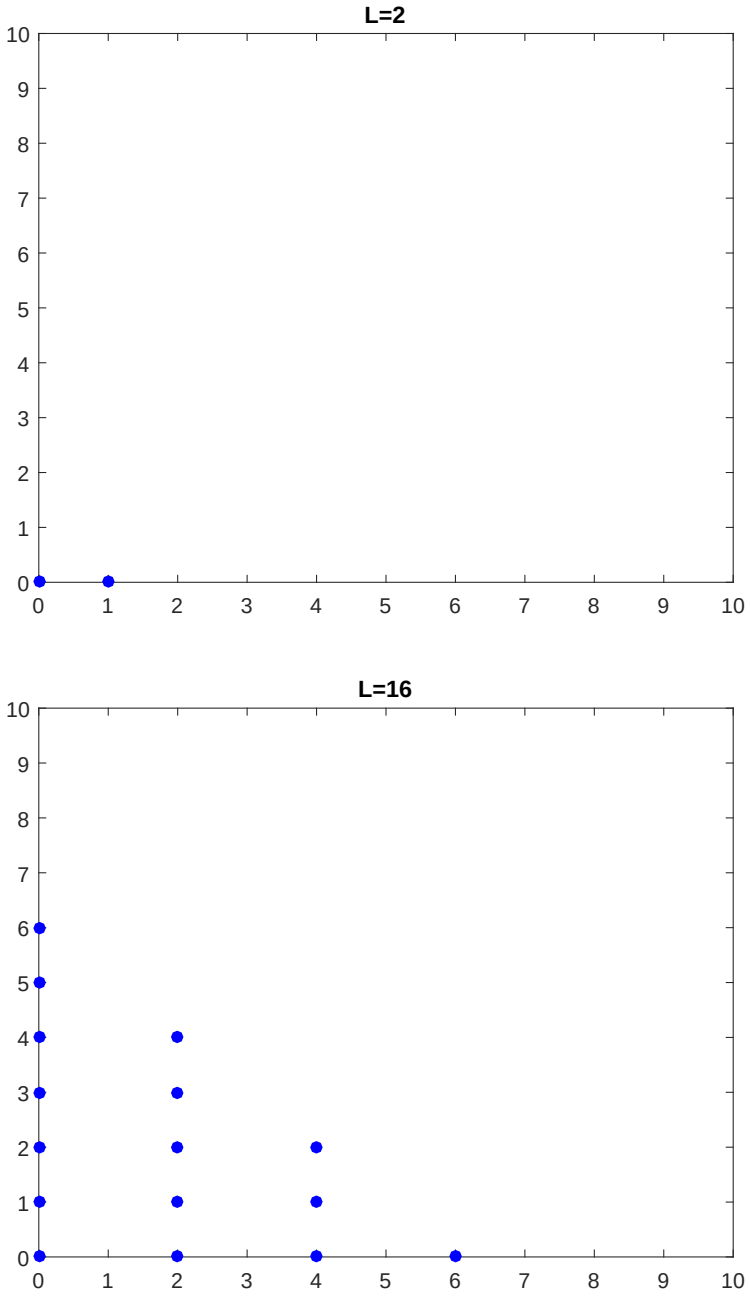


Figure 3.3: Figure for Example 1. The top graph denotes the sub-constellation $\chi_1$, and the bottom graph denotes the sub-constellation $\chi_2$.

**Method 1.** *For any constellation with $2^R$ points, R is an odd number, we can create a sum constellation that can be decomposed into two sub-constellations by changing the positions of the points in the largest energy level of CC. After the change, the abscissa value of each point in the largest energy level should have 2-unit difference with its nearest points in the same energy level.* ■

This method can always guarantee that $P(\mathcal{G})$ does not change after refinement. If the bit rate of the sum constellation is R bit/s, then, the resulting two sub-constellations have the bit rate is 1 bit/s and (R-1) bit/s, respectively. However, this method has some limitations, e.g. it only applies to the sum constellation with $2^R$ (R is odd) points. Then in some practical applications, the difference of bit rates between two users could be very large with R becoming larger. Hence, we need to make the difference of bit rates between two users as small as possible. For example, if bit rate of $\mathcal{G}$ is 8 bit/s, then, bit rates of $\chi_1$ and $\chi_2$ are both 4 bit/s. And if the bit rate of $\mathcal{G}$ is 7 bit/s, then, the bit rates of $\chi_1$ and $\chi_2$ are 3 bit/s and 4 bit/s, respectively.

The main idea of the method shown before is to design a sum constellation first, and then, refine it so that it can be decomposed uniquely. It is not very hard to execute this method when the size of the constellation is relatively small. However, when the size of $\mathcal{G}$ becomes larger or we want to make the bit rate of sub-constellations nearly the same, the method does not work. In the following, we will find a more general method to solve this problem. Let us consider the following example.

**Example 2.** *Now, we change the way from designing the sum constellation to designing sub-constellations first. Our goal is to design a sum constellation $\mathcal{G}$ with 32 points (5 bit/s), and two sub-constellations $\chi_1$ and $\chi_2$ with 4 points (2 bit/s) and 8 points*

*(3 bit/s), respectively. Fig 3.4 shows the two sub-constellations. We define length and width of a constellation as the number of points in the abscissa and the ordinate.* $\chi_1$ *is just a small-size SMP with its length and width being as close as possible and* $\chi_2$ *is another form of CC. The abscissa interval between neighbour points with same ordinate in* $\chi_2$ *is equal to the length of* $\chi_1$*, and the ordinate interval between neighbour points with same abscissa in* $\chi_2$ *is equal to the width of* $\chi_1$*. Now we produce the sum constellation* $\mathcal{G}$*. The construction of* $\mathcal{G}$ *is to move the whole points in* $\chi_1$ *to all the point positions in* $\chi_2$*.*

It is more general than method 1 and we can design sub-constellations with close bit rate. Compared with the refined CC in Fig 3.2, we move some points from its energy level to higher one. This will lead $P(\mathcal{G})$ to becoming larger.

**Method 2.** *In order to create a sum constellation* $\mathcal{G}$ *(*$2^R$ *points) which can be uniquely decomposed to two sub-constellations* $\chi_1$ *and* $\chi_2$ *with the closest bit rate, we can design sub-constellations first:* $\chi_1$ *has* $2^{\lfloor \frac{R}{2} \rfloor}$ *points, which is SMP with its length and width value closest to each other, and* $\chi_2$ *has* $2^{\lfloor \frac{R+1}{2} \rfloor}$ *points, which is CC and the abscissa interval between neighbor points with same ordinate in* $\chi_2$ *is equal to the length of* $\chi_1$*; the ordinate interval between neighbour points with same abscissa in* $\chi_2$ *is equal to the width of* $\chi_1$*. Finally, we can get the sum constellation* $\mathcal{G}$*.* ■

With method 1, in order to keep $P(\mathcal{G})$ constant, we can only solve the problem of the sum constellation with $2^R$ (R is odd) points. Now we consider the situation when R is even by using Method 2, and we also need to make $P(\mathcal{G})$ as low as possible at the same time. Let's see the example below.

**Example 3.** *Our goal is to design a sum constellation with 16 points. In order to make* $P(\mathcal{G})$ *as low as possible,* $\chi_1$ *has just 2 points* $\{(0,0),(0,1)\}$*, and* $\chi_2$ *has*

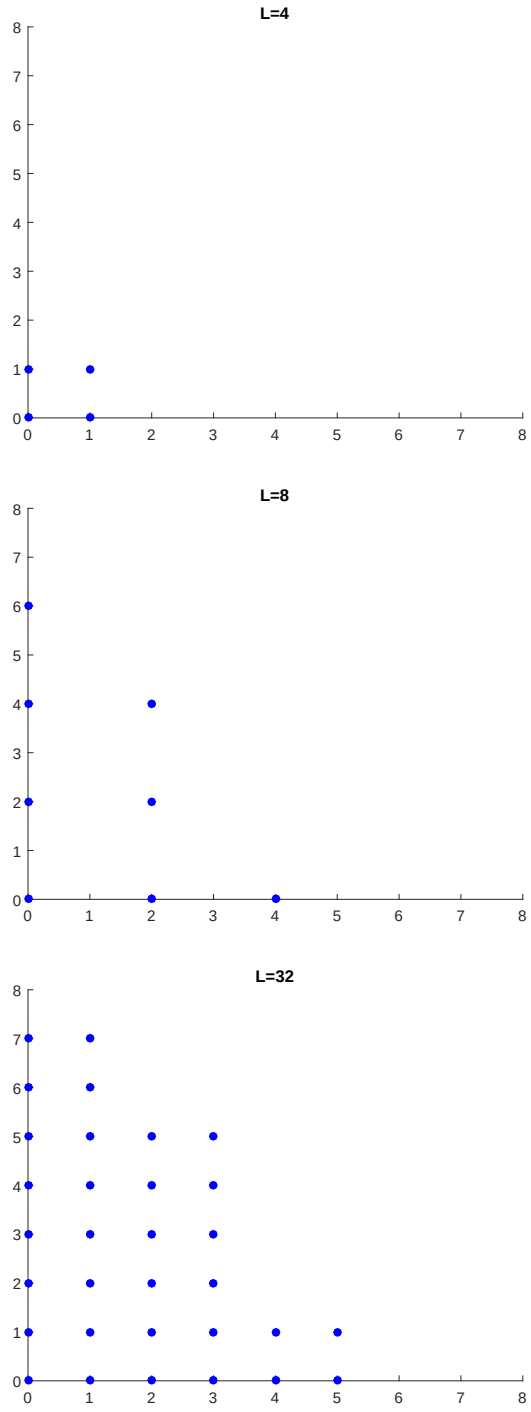


Figure 3.4: Figure for Example 2. The top graph denotes the sub-constellation $\chi_1$, the middle graph denotes the sub-constellation $\chi_2$, and the bottom one denotes the sum constellation $\mathcal{G}$.

Table 3.2: The Average Normalized Optical Power of Codeword for SMP, CC and refined CC with Different Bit Rate

| Bit Rate | SMP | CC | refined CC (Strategy 1) | refined CC (Strategy 2) |
|---|---|---|---|---|
| 2 bits/s | 1 | 1 | 1 | 1 |
| 3 bits/s | 2 | 1.75 | 1.75 | 1.75 |
| 4 bits/s | 3 | 2.8125 | 2.875 | 3 |
| 5 bits/s | 5 | 4.375 | 4.375 | 4.5 |
| 6 bits/s | 7 | 6.5625 | 6.59375 | 6.75 |
| 7 bits/s | 11 | 9.6875 | 9.6875 | 9.75 |
| 8 bits/s | 15 | 14.0938 | 14.109375 | 14.25 |
| 9 bits/s | 23 | 20.34375 | 20.34375 | 20.5 |

*8 points arranged in a form of CC. The abscissa interval between neighbor points with same ordinate in $\chi_2$ is 2, and the ordinate interval between neighbour points with same abscissa in $\chi_2$ is 1. Fig 3.5 shows the two sub-constellations and the sum constellation.*

**Method 3.** *In order to design a sum constellation with $2^R$(R is even) points whose $P(\mathcal{G})$ is as low as possible, we need to design sub-constellation first, $\chi_1$ has 2 points $\{(0,0),(0,1)\}$, $\chi_2$ and has $2^{R-1}$ points arranged in a form of CC. In addition, the abscissa interval between neighbor points with same ordinate in $\chi_2$ is 2, and the ordinate interval between neighbor points with same abscissa in $\chi_2$ is 1. Finally, we can get the sum constellation $\mathcal{G}$.* ■

Let's compute $P(\mathcal{G})$ of our refined CC with two different priority: (1)low average optical energy of the sum constellation (Strategy 1); (2)closest bit rate for 2 users (Strategy 2). Then we compare them with SMP and CC, showed in Table 3.2. As we can see, our refined CC still performs better than SMP and a little bit worse than CC. With three methods above, our design can meet the following two different priority requirements in applications:

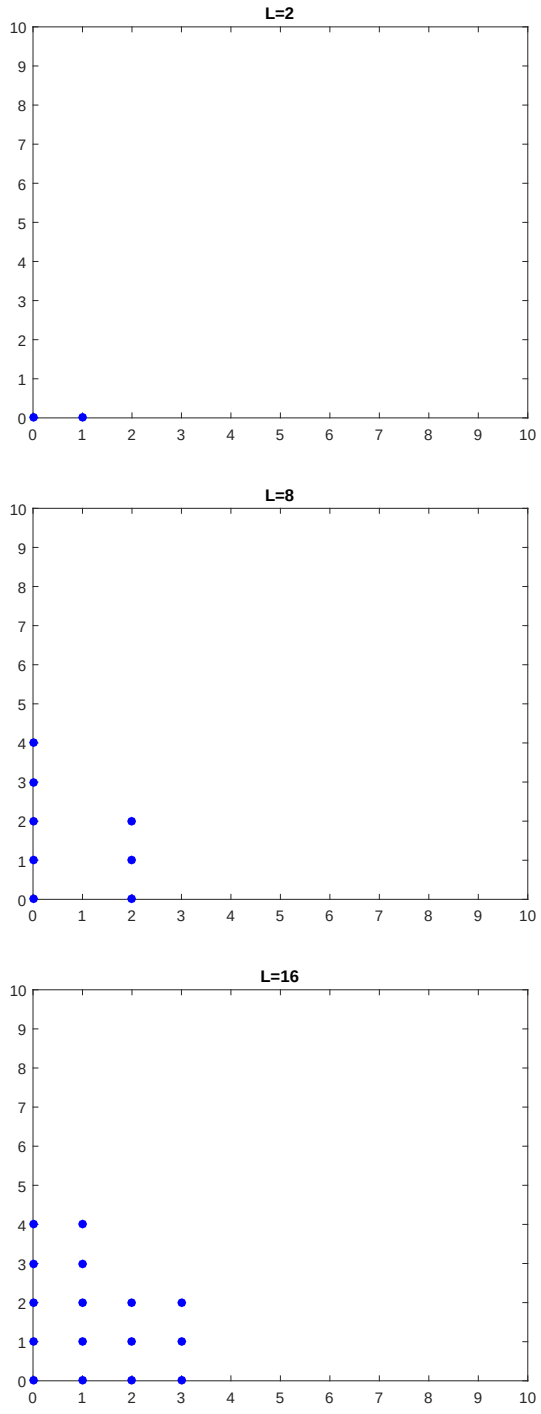


Figure 3.5: Figure for Example 3. The top graph denotes the $\chi_1$, the middle graph denotes the sub-constellation $\chi_2$, and the bottom one denotes the sum constellation $\mathcal{G}$.

(a) Strategy 1: Low average optical energy of the sum constellation with large bit rate difference between two users.

(b) Strategy 2: The same or nearly same bit rate for two users with high average optical energy of the sum constellation.

### 3.2.3 Solution

In this section, we give the solution of constellation design for the two strategies mentioned above.

Assuming the sum constellation has $2^R (R \geq 0)$ points.

1. Strategy 1: Low average optical energy of the sum constellation with large bit rate difference between two users.

   sub-constellation $\chi_1$: 2 points

   $$\chi_1 = \{(0,0),(1,0)\} \tag{3.1}$$

   $P(\chi_1) = \frac{1}{2}$.

   sub-constellation $\chi_2$: $2^{R-1}$ points

   There are two parts of $\chi_2$:

   $$\chi_2 = b_1 + b_2 \tag{3.2}$$

   Let $r_1 = \left\lfloor 2^{\frac{R-1}{2}} \right\rfloor$, $r_2 = \left\lfloor \sqrt{2^{R-1} + \frac{1}{4}} - \frac{1}{2} \right\rfloor$.

(a) $r_1^2 \geq r_2 (r_2+1)$

$$\begin{aligned} b_1 &= \{(x,y) \,|x = 2i; y = 0,1,\ldots,2(r_1-1-i); i = 0,1,\ldots,r_1-1\} \\ b_2 &= \left\{(x,y) \,|x = 2i; y = 2(r_1-i)-1; i = 0,1,\ldots,2^{R-1}-r_1^2-1\right\} \end{aligned}$$

$P(\chi_2) = \frac{1}{2^{R-1}}\left[(2r_1-1)2^{R-1} - \frac{2}{3}r_1^3 - \frac{1}{2}r_1^2 + \frac{1}{6}r_1\right]$.

Sum constellation $\mathcal{G}$: $2^R$ points.

$$\begin{aligned} \mathcal{G} &= \mathcal{G}_1 + \mathcal{G}_2 \\ &= \{(x,y) \,|x = 2i+j; y = 0,1,\ldots,2(r_1-1-i); i = 0,1,\ldots,r_1-1; j = 0,1\} \\ &+ \left\{(x,y) \,|x = 2i+j; y = 2(r_1-i)-1; i = 0,1,\ldots,2^{R-1}-r_1^2-1; j = 0,1\right\} \end{aligned} \tag{3.3}$$

$P(\mathcal{G}) = (4r_1-1)2^{R-1} - \frac{4}{3}r_1^3 - r_1^2 + \frac{1}{3}r_1$.

(b) $r_1^2 < r_2 (r_2+1)$

$$\begin{aligned} b_1 &= \{(x,y) \,|x = 2i; y = 0,1,\ldots,2(r_2-i)-1; i = 0,1,\ldots,r_2-1\} \\ b_2 &= \left\{(x,y) \,|x = 2i; y = 2(r_2-i); i = 0,1,\ldots,2^{R-1}-r_2(r_2+1)-1\right\} \end{aligned}$$

$P(\chi_2) = \frac{1}{2^{R-1}}\left[2r_2 \cdot 2^{R-1} - \frac{2}{3}r_2^3 - \frac{3}{2}r_2^2 - \frac{5}{6}r_2\right]$.

Sum constellation $\mathcal{G}$: $2^R$ points

$$\begin{aligned} \mathcal{G} &= \mathcal{G}_1 + \mathcal{G}_2 \\ &= \{(x,y) \,|x = 2i+j; y = 0,1,\ldots,2(r_2-i)-1; i = 0,1,\ldots,r_2-1; j = 0,1\} \\ &\quad + \left\{(x,y) \,|x = 2i+j; y = 2(r_2-i); i = 0,1,\ldots,2^{R-1}-r_2(r_2+1)-1; j = 0,1\right\} \end{aligned}$$

$$P(\mathcal{G}) = \frac{1}{2^R}\left[(4r_2+1)\,2^{R-1} - \frac{4}{3}r_2^3 - 3r_2^2 - \frac{5}{3}r_2\right].$$

2. Strategy 2: The same or nearly same bit rate between two users with high average optical energy of the sum constellation.

   Let $n_1 = \left\lfloor \frac{R}{2} \right\rfloor$, $n_2 = \left\lfloor \frac{R+1}{2} \right\rfloor$. Then $2^R = 2^{n_1} \times 2^{n_2}$.

   Then, the sub-constellation $\chi_1$ has $2^{n_1}$ points, and the sub-constellation $\chi_2$ has $2^{n_2}$ points.

   (a) $n_1$ is an even number

$$\chi_1 = \left\{(x,y)\,|x = 0,1,\ldots,2^{\frac{n_1}{2}}-1; y = 0,1,\ldots,2^{\frac{n_1}{2}}-1\right\}$$

   $P(\chi_1) = \frac{1}{2^{n_1}}\left[2^{\frac{3n_1}{2}} - 2^{n_1}\right]$.

   There are two parts of $\chi_2$

$$\chi_2 = b_1 + b_2$$

   Let $r = \left\lfloor \sqrt{2^{n_2+1} + \frac{1}{4}} - \frac{1}{2} \right\rfloor$.

$$\begin{aligned} b_1 &= \left\{(x,y)\,|x = i2^{\frac{n_1}{2}}; y = 0, 2^{\frac{n_1}{2}}, \ldots, (r-1-i)\,2^{\frac{n_1}{2}}; i = 0,1,\ldots,r-1\right\} \\ b_2 &= \left\{(x,y)\,|x = i2^{\frac{n_1}{2}}; y = (r-i)\,2^{\frac{n_1}{2}}; i = 0,1,\ldots,2^{n_2} - \frac{r\,(r+1)}{2} - 1\right\} \end{aligned}$$

   $P(\chi_2) = \frac{1}{2^{n_2}}\left(r2^{n_2} - \frac{1}{2}r^3 + \frac{1}{2}r - 1\right)2^{\frac{n_1}{2}}$.

Sum constellation $\mathcal{G}$: $2^R$ points

$$\begin{aligned}\mathcal{G} &= \mathcal{G}_1 + \mathcal{G}_2 \\ &= \left\{ (x,y) \,|x = i + a2^{\frac{n_1}{2}}; y = j + b2^{\frac{n_1}{2}}; i,j = 0,1,\ldots,2^{\frac{n_1}{2}} - 1; a = 0,1,\ldots,r-1; \right. \\ &\quad \left. b = 0,1,\ldots,r-1-a \right\} + \left\{ (x,y) \,|x = i + a2^{\frac{n_1}{2}}; y = j + (r-a)\, 2^{\frac{n_1}{2}}; \right. \\ &\quad \left. i,j = 0,1,\ldots,2^{\frac{n_1}{2}} - 1; a = 0,1,\ldots,2^{n_2} - \frac{r\,(r+1)}{2} - 1 \right\}\end{aligned}$$

$$\begin{aligned}P\,(\mathcal{G}) &= \frac{1}{2^R}\left[2^{n_2}E_1 + 2^{n_1}E_2\right] \\ &= \frac{1}{2^R}\left[\left(2^{\frac{3n_1}{2}} - 2^{n_1}\right)2^{n_2} + \left(r2^{n_2} - \frac{1}{2}r^3 + \frac{1}{2}r - 1\right)2^{\frac{3n_1}{2}}\right].\end{aligned}$$

(b) $n_1$ is an odd number

$$\chi_1 = \left\{(x,y)\,|x = 0,1,\ldots,2^{\frac{n_1+1}{2}} - 1; y = 0,1,\ldots,2^{\frac{n_1-1}{2}} - 1\right\}$$

$P\,(\chi_1) = \frac{1}{2^{n_1}}\left[\frac{3}{2}2^{\frac{3n_1-1}{2}} - 2^{n_1}\right]$.

There are two parts of $\chi_2$

$$\chi_2 = b_1 + b_2$$

Let $r_1 = \left\lfloor 2^{\frac{n_2}{2}} \right\rfloor$, $r_2 = \left\lfloor \sqrt{2^{n_2} + \frac{1}{4}} - \frac{1}{2} \right\rfloor$.

i. $r_1^2 \geq r_2\,(r_2+1)$

$$\begin{aligned}b_1 &= \left\{(x,y)\,|x = i2^{\frac{n_1+1}{2}}; y = 0,1,\ldots,2\,(r_1 - 1 - i)\,2^{\frac{n_1-1}{2}}; i = 0,1,\ldots,r_1 - 1\right\} \\ b_2 &= \left\{(x,y)\,|x = i2^{\frac{n_1+1}{2}}; y = [2\,(r_1 - i) - 1]\,2^{\frac{n_1-1}{2}}; i = 0,1,\ldots,2^{n_2} - r_1^2 - 1\right\}\end{aligned}$$

$P(\chi_2) = \frac{1}{2^{n_2}}\left[(2r_1-1)\,2^{n_2} - \frac{2}{3}r_1^3 - \frac{1}{2}r_1^2 + \frac{1}{6}r_1\right]2^{\frac{n_1-1}{2}}$.

Sum constellation $\mathcal{G}$: $2^R$ points

$$\begin{aligned}
\mathcal{G} &= \mathcal{G}_1 + \mathcal{G}_2 \\
&= \Big\{(x,y)\,|x = i + a2^{\frac{n_1}{2}}; y = j + b2^{\frac{n_1}{2}}; i = 0,1,\ldots,2^{\frac{n_1+1}{2}} - 1; \\
&\quad j = 0,1,\ldots,2^{\frac{n_1-1}{2}} - 1; a = 0,1,\ldots,r_1 - 1; b = 0,1,\ldots,2\,(r_1 - 1 - a)\Big\} \\
&\quad + \Big\{(x,y)\,|x = i + a2^{\frac{n_1+1}{2}}; y = j + [2\,(r_1 - a) - 1]\,2^{\frac{n_1-1}{2}}; \\
&\quad i = 0,1,\ldots,2^{\frac{n_1+1}{2}} - 1; j = 0,1,\ldots,2^{\frac{n_1-1}{2}} - 1; a = 0,1,\ldots,2^{n_2} - r_1^2 - 1\Big\}
\end{aligned}$$

$$\begin{aligned}
P(\mathcal{G}) &= \frac{1}{2^R}\left[2^{n_2}E_1 + 2^{n_1}E_2\right] \\
&= \frac{1}{2^R}\left[\left(\frac{3}{2}2^{\frac{3n_1-1}{2}} - 2^{n_1}\right)2^{n_2} + \left((2m_1-1)\,2^{n_2} - \frac{2}{3}r_1^3 - \frac{1}{2}r_1^2 + \frac{1}{6}r_1\right)2^{\frac{3n_1-1}{2}}\right]
\end{aligned}$$

ii. $r_1^2 < r_2\,(r_2+1)$

$$\begin{aligned}
b_1 &= \left\{(x,y)\,|x = i2^{\frac{n_1+1}{2}}; y = 0,1,\ldots,[2\,(r_2 - i) - 1]\,2^{\frac{n_1-1}{2}}; i = 0,1,\ldots,r_2 - 1\right\} \\
b_2 &= \left\{(x,y)\,|x = i2^{\frac{n_1+1}{2}}; y = 2\,(r_2 - i)\,2^{\frac{n_1-1}{2}}; i = 0,1,\ldots,2^{n_2} - r_2\,(r_2+1) - 1\right\}
\end{aligned}$$

$P(\chi_2) = \frac{1}{2^{n_2}}\left[r_2 2^{n_2+1} - \frac{2}{3}r_1^3 - \frac{3}{2}r_1^2 - \frac{5}{6}r_1\right]2^{\frac{n_1-1}{2}}$.

Sum constellation $\mathcal{G}$: $2^R$ points

$$\begin{aligned}
\mathcal{G} &= \mathcal{G}_1 + \mathcal{G}_2 \\
&= \Big\{ (x,y) \,|x = i + a2^{\frac{n_1}{2}}; y = j + b2^{\frac{n_1}{2}}; i = 0,1,\ldots,2^{\frac{n_1+1}{2}} - 1; \\
&\quad j = 0,1,\ldots,2^{\frac{n_1-1}{2}} - 1; a = 0,1,\ldots,r_2 - 1; b = 0,1,\ldots,[2(r_2 - a) - 1] \Big\} \\
&\quad + \Big\{ (x,y) \,|x = i + a2^{\frac{n_1+1}{2}}; y = j + 2(r_2 - a)\, 2^{\frac{n_1-1}{2}}; i = 0,1,\ldots,2^{\frac{n_1+1}{2}} - 1; \\
&\quad j = 0,1,\ldots,2^{\frac{n_1-1}{2}} - 1; a = 0,1,\ldots,2^{n_2} - r_2(r_2+1) - 1 \Big\}
\end{aligned}$$

$$\begin{aligned}
P(\mathcal{G}) &= \frac{1}{2^R}\left(2^{n_2}E_1 + 2^{n_1}E_2\right) \\
&= \frac{1}{2^R}\left[\left(\frac{3}{2}2^{\frac{3n_1-1}{2}} - 2^{n_1}\right)2^{n_2} + \left(r_2 2^{n_2+1} - \frac{2}{3}r_1^3 - \frac{3}{2}r_1^2 - \frac{5}{6}r_1\right)2^{\frac{3n_1-1}{2}}\right]
\end{aligned}$$

The proof that $\chi_1$, $\chi_2$ can form an AUDCG by decomposing G is shown in Appendix.

## 3.3 Simulation

In this section, we examine the average error performance of SMP and the refined CC we have designed in this paper. The pre-set scenario is described as follows: The room size is 4.0m×4.0m×3.0m. Two transmitted LEDs are located at (0.4, 0, 2.5)m, (0, 0.4, 2.5)m. The two receivers are placed at (0.1, 0, 0.75)m, (0, 0.1, 0.75)m; $A = 1cm^2$; $\theta_{R\frac{1}{2}} = 15°$. $n$ is the additive white Gaussian noise with zero mean and variance $\sigma^2$. The SNR is defined as

$$\text{SNR} = \frac{1}{2\sigma^2}.$$

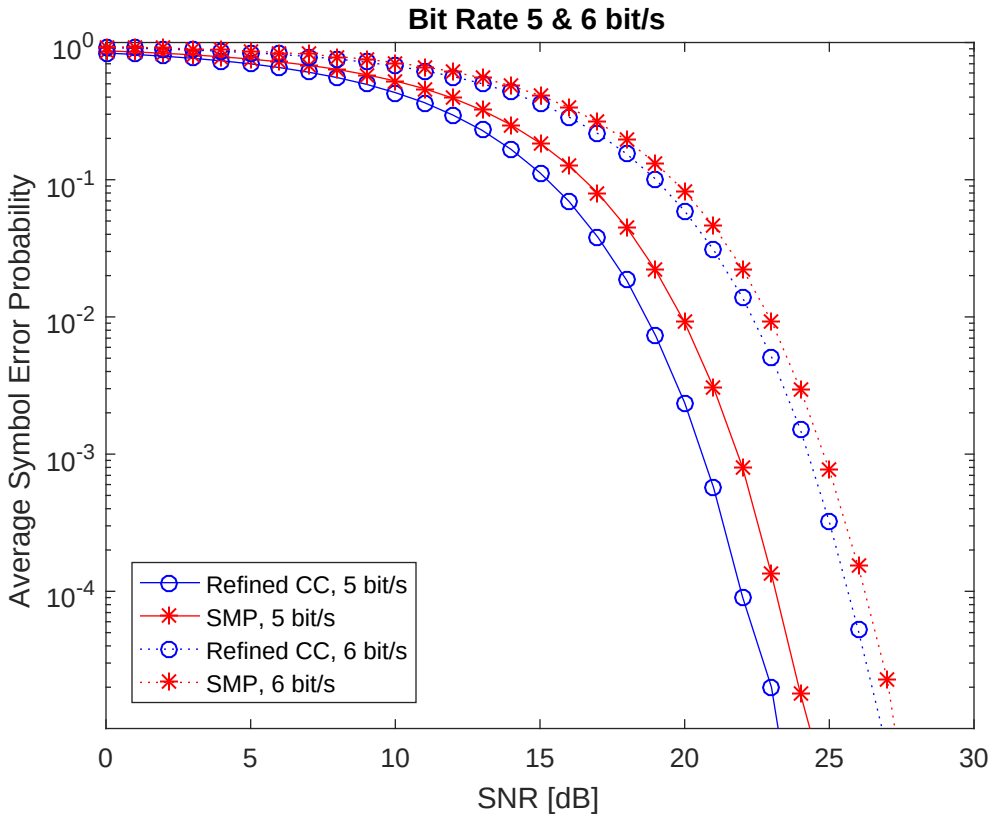


Figure 3.6: The error performance comparison of SMP and refined CC for strategy 1 at R=5, 6 bit/s

SMP and our refined CC are both assumed to use maximum-likelihood (ML) detection with perfect knowledge of the channel at both transmitter side and receiver side. Average symbol error probability will be used as the performance merit. Fig 3.6 and Fig 3.7 show the average error performance of SMP and our refined CC for the purpose to make the $P(\mathcal{G})$ as low as possible (strategy 1). The bit rate is R=5, 6, 7, 8 bit/s, L=32, 64, 128, 256, respectively. From the two figures, we can easily find our refined CC has better performance than SMP. Fig 3.8 and Fig 3.9 show the average error performance of SMP and our refined CC for the purpose to make the bit rate for each user as close as possible (strategy 2). The bit rate is R=5, 6, 7, 8 bit/s, L=32,

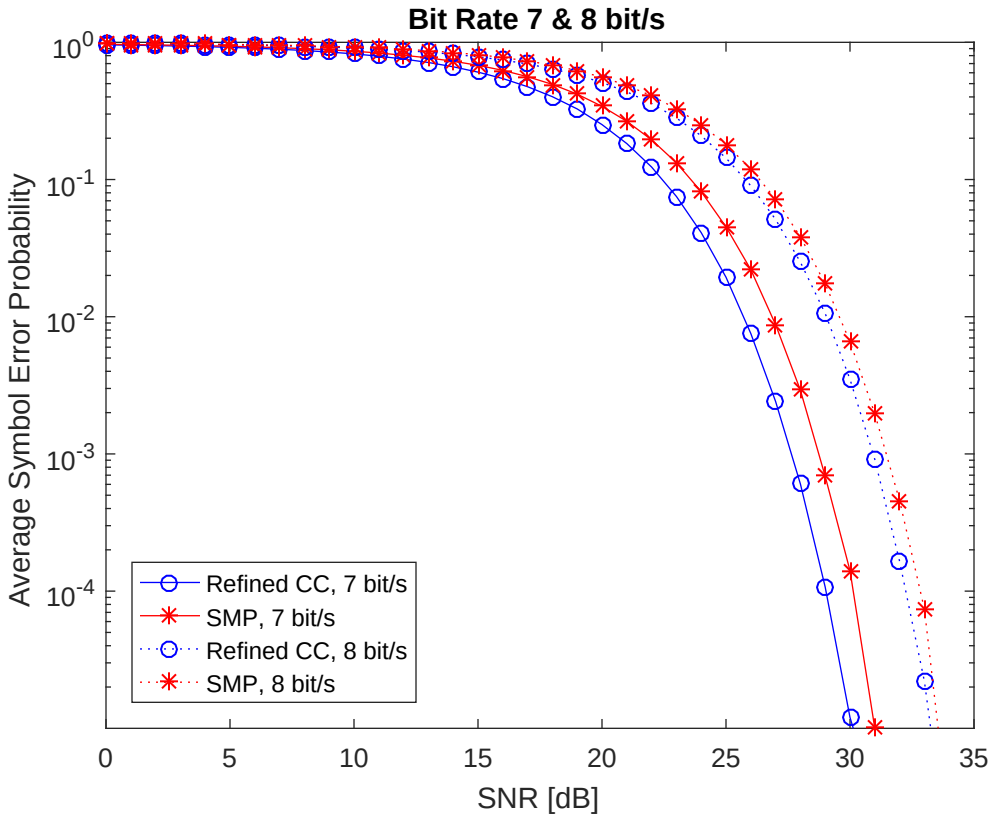


Figure 3.7: The error performance comparison of SMP and refined CC for strategy 1 at R=7, 8 bit/s

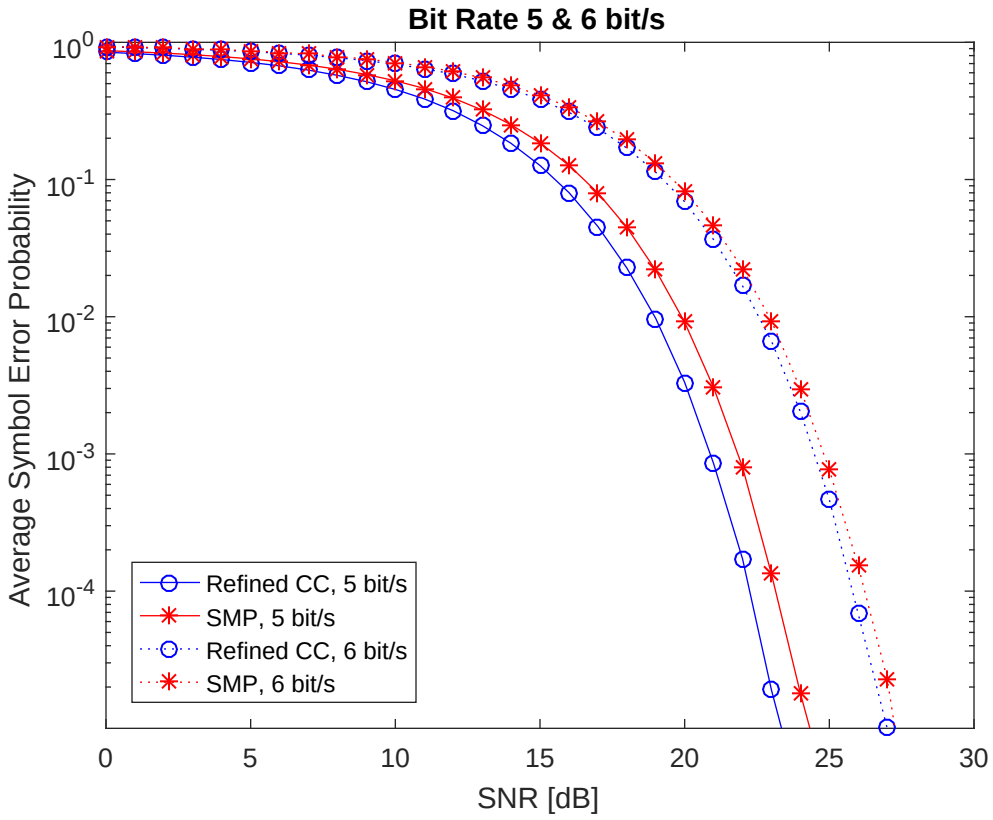


Figure 3.8: The error performance comparison of SMP and refined CC for strategy 2 at R=5, 6 bit/s

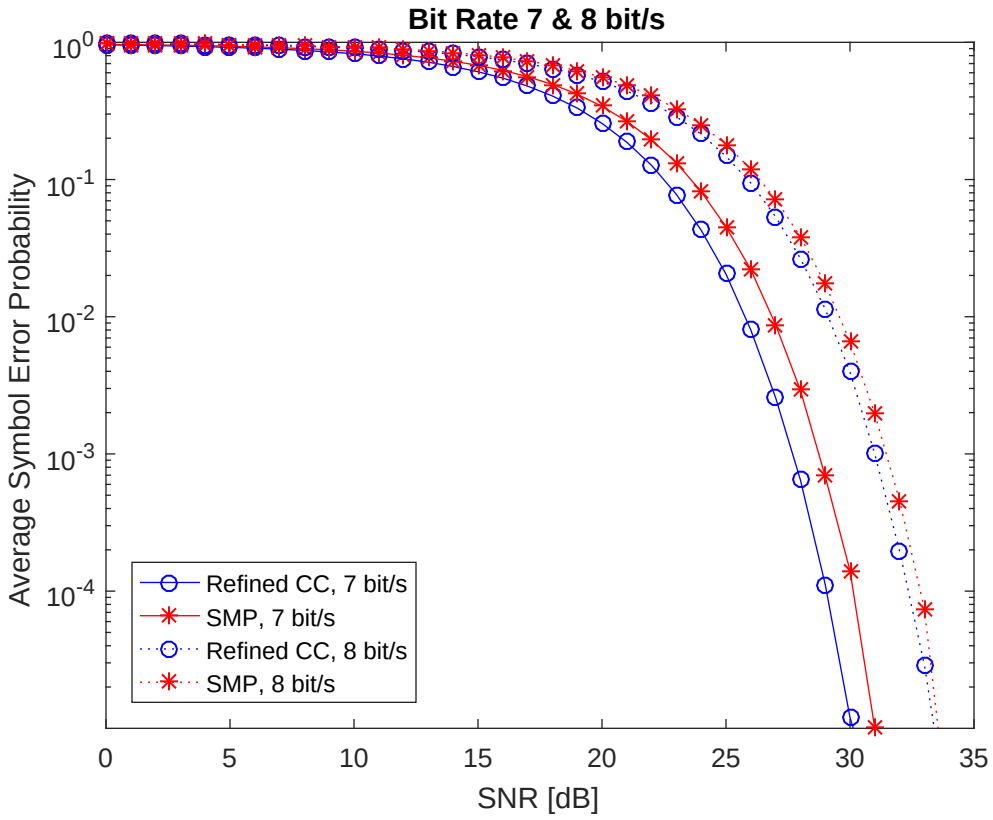


Figure 3.9: The error performance comparison of SMP and refined CC for strategy 2 at R=7, 8 bit/s

64, 128, 256, respectively. From the two figures, we can also see that our designed constellation still has better performance.

With the bit rate becoming higher, the average symbol error probability for both SMP and our refined CC grows high at the same SNR. This is because after power normalization with the same SNR when transmitting, the minimum Euclidian distance will decline significantly if the number of points in a constellation doubles. Thus, the probability to cause an error goes high. Besides, in Methods 2 and 3, we have to move some points to higher energy level. It causes the $P(\mathcal{G})$ to become higher than before. Then, during the transmission, the minimum Euclidian distance would be smaller.

Now, we continue to examine the error performance for sub-constellations. The result is that the average symbol error probability could be even lower than that in sum constellation. For example, in Fig 3.10, we assume that User 1 and User 2 are given (0,1) and (0,6), respectively. Then, the transmitter gives the point (0,7). If the receiver gets (0,7), both users get right information. However, if (1,7) has been obtained, after decomposed into sub-constellations, User 1 will get (1,1) and User 2 will get (0,6), which means User 1 gets wrong information, but User 2 can still get right information, even if the point in sum constellation is wrong. Let's take another look. If (0,5) has been obtained at receiver side, after being decomposed into sub-constellations, user 1 will get (0,1) and user 2 will get (0,4), which means user 1 can still get right information, but user 2 gets wrong information. Therefore, not in all the conditions of received wrong signals could lead to the wrong information for both users.

Fig. 3.11, 3.12, 3.13, 3.14 show the average symbol error probability for each user

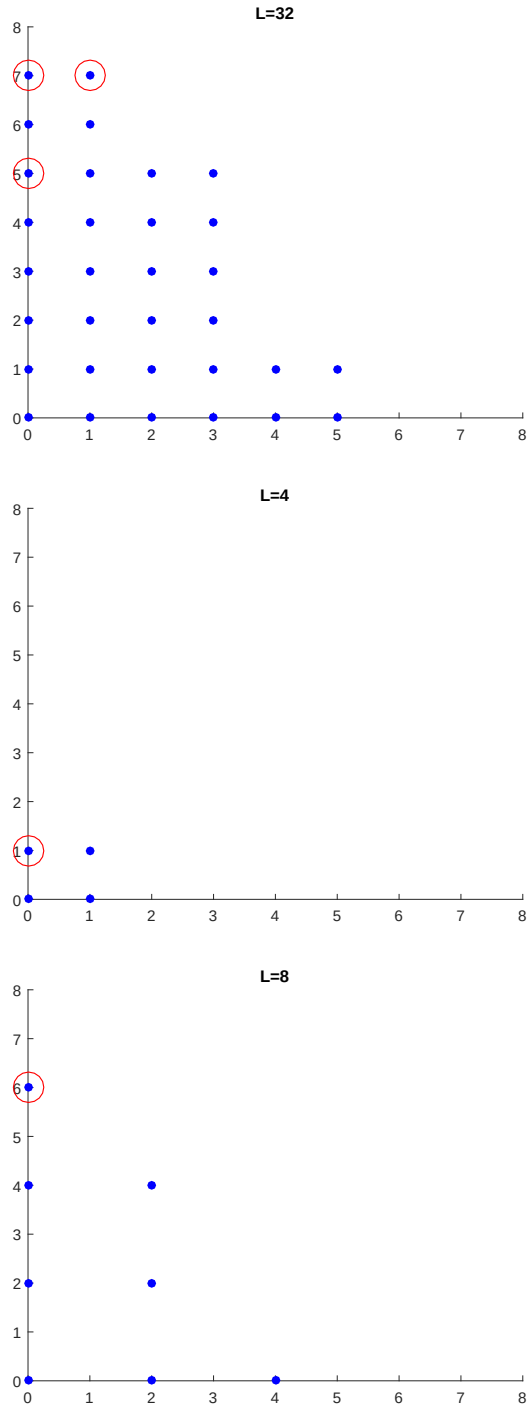


Figure 3.10: Example of the error performance analysis after being decomposed into sub-constellations. The top figure is the sum constellation $\mathcal{G}$, the middle figure is the sub-constellation $\chi_1$, and bottom figure is the sub-constellation $\chi_2$.

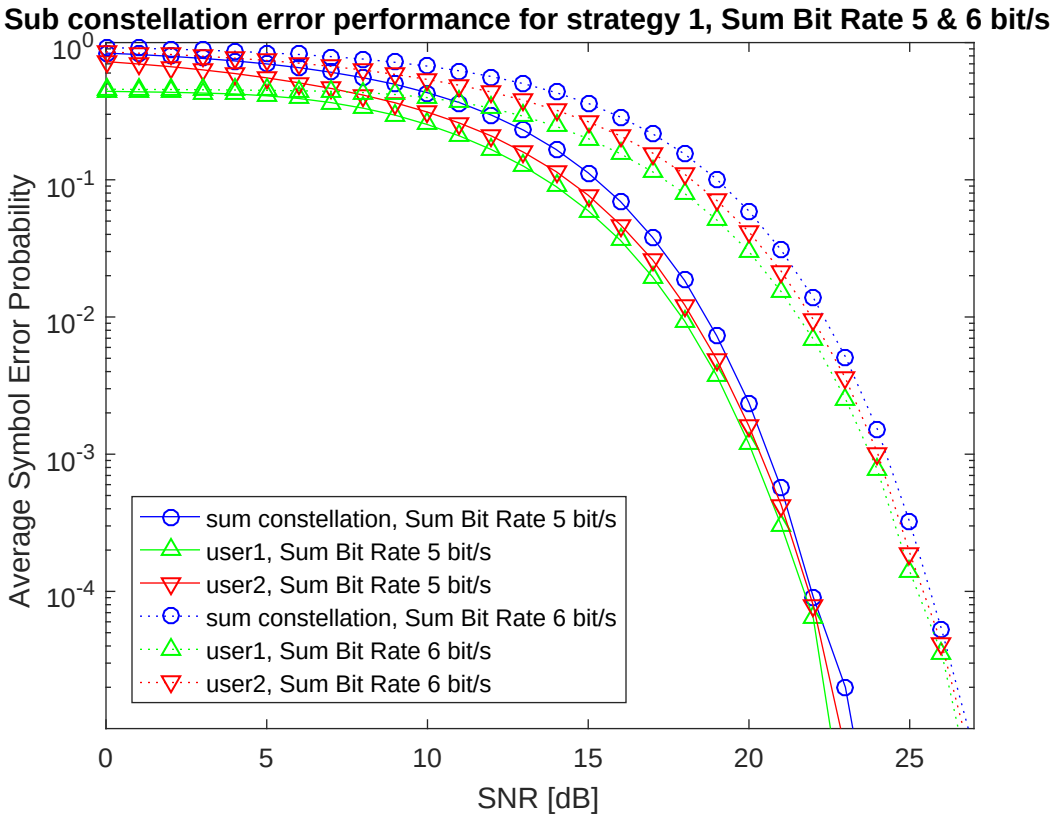


Figure 3.11: sub-constellation error performance for strategy 1 at R=5, 6 bit/s

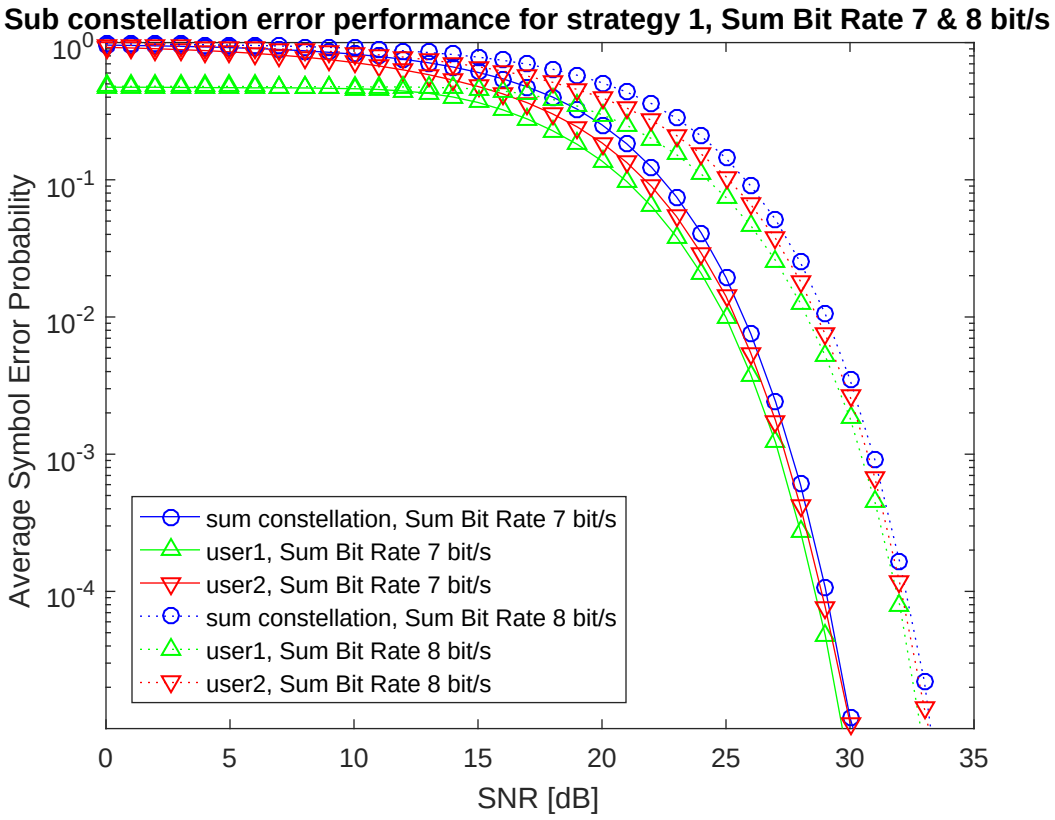


Figure 3.12: sub-constellation error performance for strategy 1 at R=7, 8 bit/s

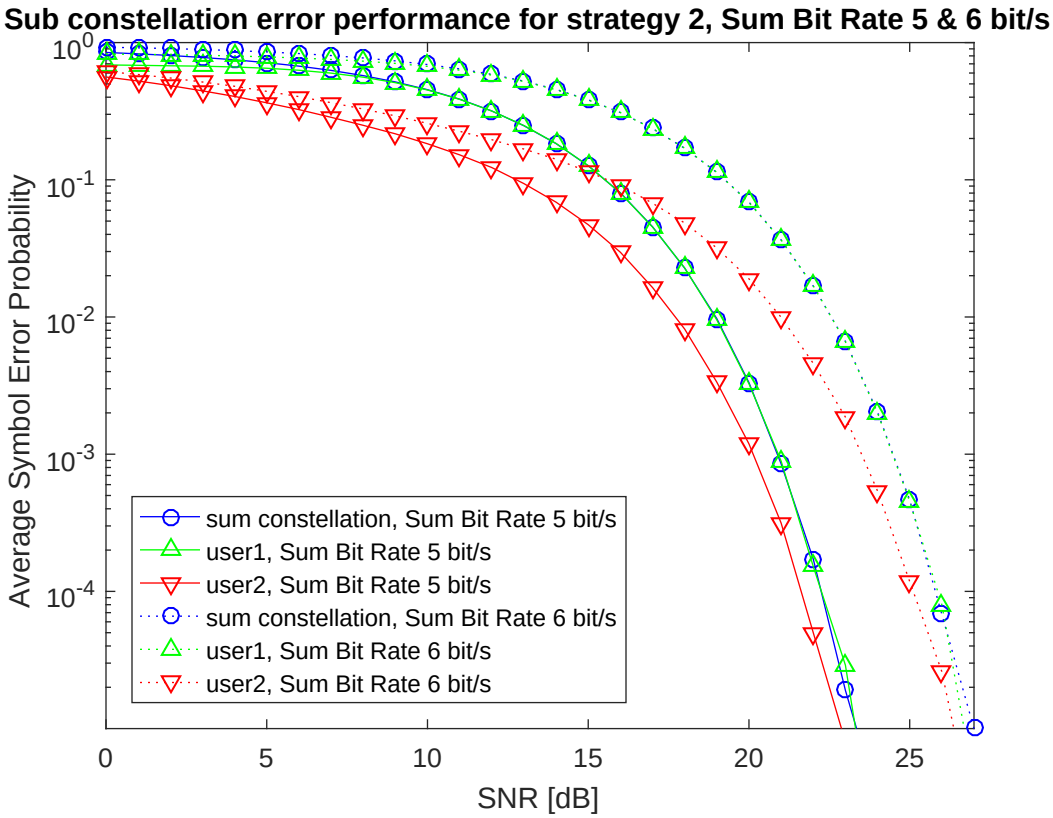


Figure 3.13: sub-constellation error performance for strategy 2 at R=5, 6 bit/s

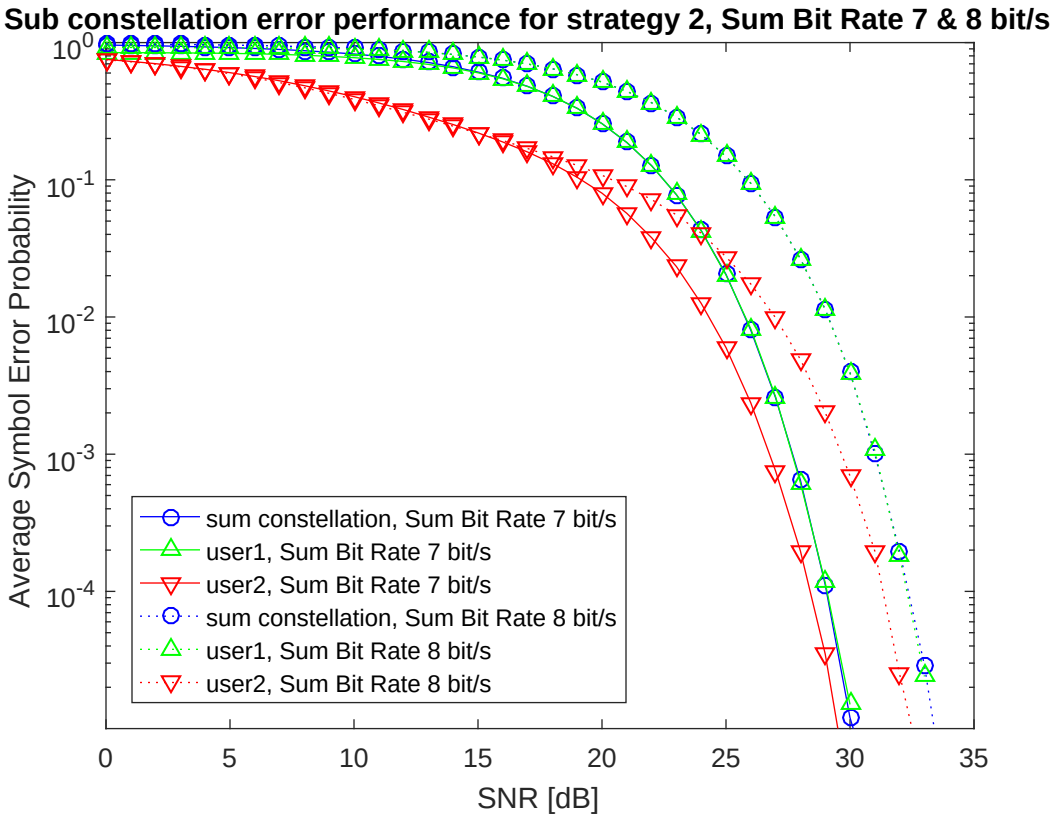


Figure 3.14: sub-constellation error performance for strategy 2 at R=7, 8 bit/s

compared with that of sum constellation. As we can see, in most situations, the error performance for each user is better than sum constellation. On the one hand, in Fig 3.11, 3.12(strategy 1), the user whose bit rate is lower than the other has better error performance, since transmission error for its ordinate does not affect the received information. On the other hand, in Fig 3.13, 3.14(strategy 2), the user whose sub-constellation is like SMP has worse error performance, and the average symbol error probability for this user is nearly the same as sum constellation. This is because just one move to its neighbor points would affect the final received information.

## 3.4 Conclusion

In this chapter, we have introduced three methods to design an AUDCG constellation for multi-user MISO visible light communication system. Our design is based on space-collaborative constellation. We refine it by changing positions of points in the highest energy level or moving points in low energy level to higher one, then make sure it can be decomposed into two sub-constellations which can form an additively uniquely decomposable constellation group. These methods can meet two different stategies in application: (1) Low average optical energy of the sum constellation with large bit rate difference between two users; (2) The same or nearly same bit rate for two users with high average optical energy of the sum constellation. Simulation result shows that, when measured by symbol error probability, our refined CC not only always has better performance than traditional SMP, but also has lower average optical energy. Besides, after being decomposed into sub-constellations, the symbol error probability is even lower than sum constellation.

# Appendix A

# Appendix

## A.1 Proof of Lemma 1

$F(\alpha, \beta, \mu)$ is defined by (2.16). Putting $\begin{cases} \alpha = \theta_U \\ \beta = \theta_L \end{cases}$ into it, we obtain

$$\begin{aligned} F(\theta_U, \theta_L, \mu) &= \mu\Big(\frac{1}{\lambda_2}(\cos\psi - \sin\psi)\sin\theta_U + \frac{1}{\lambda_1}(\cos\psi + \sin\psi)\cos\theta_U\Big) \\ &\quad + \frac{1}{\lambda_2}(\cos\psi - \sin\psi)\sin\theta_L + \frac{1}{\lambda_1}(\cos\psi + \sin\psi)\cos\theta_L \\ &= \Delta\left(\mu\cos(\theta_U - \theta) + \cos(\theta_L - \theta)\right). \end{aligned}$$

Then we have

$$\begin{aligned} a &= \Delta \cos(\theta_U - \theta) \\ &= \frac{1}{\lambda_2}(\cos\psi - \sin\psi)\sin\theta_U + \frac{1}{\lambda_1}(\cos\psi + \sin\psi)\cos\theta_U \\ &= \frac{1}{\sqrt{\lambda_1^2 \sin^2\psi + \lambda_2^2 \cos^2\psi}}, \\ b &= \Delta \cos(\theta_L - \theta) \\ &= \frac{1}{\lambda_2}(\cos\psi - \sin\psi)\sin\theta_L + \frac{1}{\lambda_1}(\cos\psi + \sin\psi)\cos\theta_L \\ &= \frac{1}{\sqrt{\lambda_1^2 \cos^2\psi + \lambda_2^2 \sin^2\psi}}. \end{aligned}$$

□

## A.2 Proof of Theorem 1

Assuming that $\alpha > \beta$.

**Case 1**: **H** is a non-invertible matrix

According to (2.5) and (2.6), if **H** is not invertible, we cannot compute the symbol error probability. So we turn off one of the transmitters. In this situation, the precoding matrix will change to

$$\mathbf{f} = \begin{bmatrix} f_1 \\ f_2 \end{bmatrix}.$$

Let

$$\mathbf{J} = \mathbf{H}^T\mathbf{H} = \begin{bmatrix} j_{11} & j_{12} \\ j_{21} & j_{22} \end{bmatrix},$$

where $j_{12} = j_{21}$. Since $\mathbf{J} \geq 0$, $j_{11}j_{22} - j_{12}^2 \geq 0$.

Let $g^T g = \tilde{\mathbf{H}}^T \tilde{\mathbf{H}} = \mathbf{f}^H \mathbf{H}^T \mathbf{H} \mathbf{f}$. According to the energy constraint (2.14), our problem changes to

$$\max g^T g$$

$$s.t. \quad f_1 + f_2 = \frac{1}{E_s} = e.$$

Since $\mathbf{J} = \mathbf{H}^T \mathbf{H}$, $j_{12} = j_{21}$, then

$$\begin{aligned} g^T g &= j_{11} f_1^2 + j_{22} f_2^2 + 2 j_{12} f_1 f_2 \\ &= j_{11} f_1^2 + j_{22} (e - f_1) + j_{12} f_1 (e - f_1). \end{aligned}$$

Let

$$F(f_1) = (j_{11} + j_{22} - 2j_{12}) f_1^2 - 2e (j_{22} - j_{12}) f_1 + j_{22} e^2,$$

where $f_1 \in [0, e]$.

1. If $j_{11} = 0$, then $j_{12} = 0$,

$$\mathbf{J} = \begin{bmatrix} 0 & 0 \\ 0 & j_{22} \end{bmatrix},$$

$$\begin{aligned} F(f_1) &= j_{22} f_1^2 - 2 j_{22} e f_1 + j_{22} e^2 \\ &= j_{22} (f_1 - e)^2, \end{aligned}$$

where $f_1 = 0$, $F(0)_{max} = j_{22} e^2$.

2. If $j_{22} = 0$, then $j_{12} = 0$,

$$\mathbf{J} = \begin{bmatrix} j_{11} & 0 \\ 0 & 0 \end{bmatrix},$$

$$F(f_1) = j_{11} f_1^2,$$

where $f_1 = e$, $F(e)_{max} = j_{11} e^2$.

3. If $j_{11} \neq 0$, $j_{22} \neq 0$,

   (a) $j_{11} = j_{22} = j_{12}$

$$F(f_1) = j_{22} e^2$$

   Notice that $\forall f_1 \in [0, e]$, $F(f_1) = j_{22} e^2$. Thus, $F(f_1)_{max} = j_{22} e^2$.

   (b) $j_{11} + j_{22} - 2j_{12} > 0$

$$\begin{aligned} \Delta &= [-2e(j_{22} - j_{12})]^2 - 4(j_{11} + j_{22} - 2j_{12}) j_{22} e^2 \\ &= 4b^2 \left(j_{12}^2 - j_{11} j_{22}\right) < 0 \end{aligned}$$

   Then $F(f_1)_{max} = \max\{F(0), F(e)\} = \max\{j_{22} e^2, j_{11} e^2\}$.

   i. If $j_{11} \geq j_{22}$, $F(e)_{max} = j_{11} e^2$.

   ii. If $j_{11} < j_{22}$, $F(0)_{max} = j_{22} e^2$.

We can simplify them into these two conditions below

1. If $j_{11} \geq j_{22}$, $F(e)_{max} = j_{11} e^2$.

$$\mathbf{F}_{\text{opt}} = \begin{pmatrix} e \\ 0 \end{pmatrix}.$$

2. If $j_{11} < j_{22}$, $F(0)_{max} = j_{22}e^2$.

$$\mathbf{F}_{\text{opt}} = \begin{pmatrix} 0 \\ e \end{pmatrix}.$$

In order to guarantee the transmission rate, the constellation size should be improved. Let $q_1 = q^2$. Then,

$$\min \bar{P}_{\text{sep}} = \frac{2\left(q_1 - 1\right)}{q_1} Q\left(\frac{dh \cdot \sqrt{\text{SNR}}}{\sqrt{2}}\right).$$

In practice, the bit error rate (BER) is more widely used. So we can obtain BER through $P_{sep}$. According to (Cho and Yoon, 2002), the average bit error probability of $q$-ary PAM (Grey code mapping) can be written as

$$P_b = \frac{1}{q\log_2 q} \sum_{k=1}^{\log_2 q} \sum_{i=0}^{\left(1-2^{-k}\right)q-1} \left\{ (-1)^{\left\lfloor \frac{i\cdot 2^{k-1}}{q} \right\rfloor} \cdot \left(2^{k-1} - \left\lfloor \frac{i\cdot 2^{k-1}}{q} + \frac{1}{2} \right\rfloor\right) \cdot 2Q\left((2i+1)\frac{d}{\sqrt{N_0}}\right) \right\}.$$

Then, in this condition

$$\min \bar{P}_b = \frac{1}{q_1\log_2 q_1} \sum_{k=1}^{\log_2 q_1} \sum_{i=0}^{\left(1-2^{-k}\right)q_1-1} \left\{ (-1)^{\frac{i\cdot 2^{k-1}}{q_1}} \left(2^{k-1} - \frac{i\cdot 2^{k-1}}{q_1} + \frac{1}{2}\right) \cdot 2Q\left(\frac{(2i+1)\,dh \cdot \sqrt{\text{SNR}}}{\sqrt{2}}\right) \right\}$$

where $h = \sqrt{\left(\mathbf{HF}_{\text{opt}}\right)^T \left(\mathbf{HF}_{\text{opt}}\right)}$.

**Case 2**: **H** is an invertible matrix

Step 1: Fix $\frac{d_1}{d_2} = \mu$, and then optimize the object function by finding the optimal $\alpha$, $\beta$.

Let

$$\begin{aligned} x_1 &= \frac{d\sqrt{\mathrm{SNR}}\,|\sin(\beta-\alpha)|}{\sqrt{2}} d_1 \\ &= \frac{\sqrt{2\cdot\mathrm{SNR}}\mu}{(q-1)\,\Delta} \cdot \frac{\sin(\alpha-\beta)}{\mu\cos(\alpha-\theta)+\cos(\beta-\theta)}, \\ x_2 &= \frac{d\sqrt{\mathrm{SNR}}\,|\sin(\beta-\alpha)|}{\sqrt{2}} d_2 \\ &= \frac{\sqrt{2\cdot\mathrm{SNR}}}{(q-1)\,\Delta} \cdot \frac{\sin(\alpha-\beta)}{\mu\cos(\alpha-\theta)+\cos(\beta-\theta)}. \end{aligned}$$

Then,

$$x_1 = \mu x_2,$$

$$\begin{aligned} & \bar{P}_{\mathrm{sep}}(\alpha,\beta,\mu) \\ = \; & \frac{(q-1)}{q}\left(Q(x_1)+Q(x_2)\right) \\ = \; & \frac{(q-1)}{q}\left(Q\left(\frac{\sqrt{2\cdot\mathrm{SNR}}\mu}{(q-1)\,\Delta}\cdot\frac{\sin(\alpha-\beta)}{\mu\cos(\alpha-\theta)+\cos(\beta-\theta)}\right)\right. \\ & \left. +Q\left(\frac{\sqrt{2\cdot\mathrm{SNR}}}{(q-1)\,\Delta}\cdot\frac{\sin(\alpha-\beta)}{\mu\cos(\alpha-\theta)+\cos(\beta-\theta)}\right)\right). \end{aligned}$$

Let

$$f(\alpha,\beta) = \frac{\sin(\alpha-\beta)}{\mu\cos(\alpha-\theta)+\cos(\beta-\theta)}.$$

Then, taking partial derivative for $\alpha$ and $\beta$ of $\bar{P}_{\mathrm{sep}}$, we obtain

$$\frac{\partial \bar{P}_{\mathrm{sep}}}{\partial\alpha} = -\frac{(q-1)}{q}\cdot\frac{1}{\sqrt{2\pi}}\left(e^{-\frac{x_1^2}{2}}\cdot\frac{\sqrt{2\cdot\mathrm{SNR}}\mu}{(q-1)\,\Delta}+e^{-\frac{x_2^2}{2}}\cdot\frac{\sqrt{2\cdot\mathrm{SNR}}}{(q-1)\,\Delta}\right)\cdot\frac{\cos(\beta-\theta)\left[\mu+\cos(\alpha-\beta)\right]}{\left(\mu\cos(\alpha-\theta)+\cos(\beta-\theta)\right)^2},$$

$$\frac{\partial \bar{P}_{\mathrm{sep}}}{\partial\beta} = \frac{(q-1)}{q}\cdot\frac{1}{\sqrt{2\pi}}\left(e^{-\frac{x_1^2}{2}}\cdot\frac{\sqrt{2\cdot\mathrm{SNR}}\mu}{(q-1)\,\Delta}+e^{-\frac{x_2^2}{2}}\cdot\frac{\sqrt{2\cdot\mathrm{SNR}}}{(q-1)\,\Delta}\right)\cdot\frac{\cos(\alpha-\theta)\left[\mu+\cos(\alpha-\beta)\right]}{\left(\mu\cos(\alpha-\theta)+\cos(\beta-\theta)\right)^2}.$$

As we know, $\cos(\alpha-\theta)>0$, $\cos(\beta-\theta)>0$, $\begin{cases}\theta_L\le\alpha\le\theta_U\\ \theta_L\le\beta\le\theta_U\end{cases}$ and $0\le\theta_U-\theta_L\le\frac{\pi}{2}$, then $\cos(\alpha-\beta)>0$. Thus, $\frac{\partial\bar{P}_{\text{sep}}}{\partial\alpha}<0$ and $\frac{\partial\bar{P}_{\text{sep}}}{\partial\beta}>0$. Therefore, $\bar{P}_{\text{sep}}$ reaches minimum when $\begin{cases}\alpha=\theta_U\\ \beta=\theta_L\end{cases}$.

$$\begin{aligned}&\bar{P}_{\text{sep}}(\theta_U,\theta_L,\mu)\\ =\;&\frac{(q-1)}{q}\left(Q(x_1)+Q(x_2)\right)\\ =\;&\frac{(q-1)}{q}\left(Q\left(\frac{\sqrt{2\cdot\text{SNR}}\mu}{(q-1)\Delta}\cdot\frac{\sin(\theta_U-\theta_L)}{\mu\cos(\theta_U-\theta)+\cos(\theta_L-\theta)}\right)\right.\\ &\left.+Q\left(\frac{\sqrt{2\cdot\text{SNR}}}{(q-1)\Delta}\cdot\frac{\sin(\theta_U-\theta_L)}{\mu\cos(\theta_U-\theta)+\cos(\theta_L-\theta)}\right)\right).\end{aligned}$$

Let

$$x_1 = \frac{\sqrt{2\cdot\text{SNR}}}{q-1}\cdot\frac{\mu}{\mu a+b}\cdot\sin(\theta_U-\theta_L), \tag{A.1}$$

$$x_2 = \frac{\sqrt{2\cdot\text{SNR}}}{q-1}\cdot\frac{1}{\mu a+b}\cdot\sin(\theta_U-\theta_L). \tag{A.2}$$

Step 2: Fix $\alpha$ and $\beta$, and then optimize the object function by finding the optimal $\mu$. Taking derivative for $\mu$ of $\bar{P}_{\text{sep}}$, we obtain

$$\bar{P}'_{sep}(\mu) = \frac{(q-1)}{q}\cdot\frac{1}{\sqrt{2\pi}}\frac{\sqrt{2\cdot\text{SNR}}\sin(\theta_U-\theta_L)}{(q-1)(\mu a+b)^2}\left(e^{-\frac{x_2^2}{2}}a-e^{-\frac{\mu^2x_2^2}{2}}b\right).$$

Let $f(\mu)=e^{-\frac{x_2^2}{2}}a-e^{-\frac{\mu^2x_2^2}{2}}b$. If $\frac{\partial\bar{P}_{\text{sep}}}{\partial\mu}=0$, then $f(\mu)=0$. Let $C_1=\frac{\sqrt{2}\sin(\theta_U-\theta_L)}{q-1}$.

Then $x_2 = \frac{C_1\sqrt{\mathrm{SNR}}}{\mu a+b}$. If we let $f(\mu) \geq 0$, we will obtain

$$e^{-\frac{x_2^2}{2}} a - e^{-\frac{\mu^2 x_2^2}{2}} b \geq 0,$$

$$e^{-\frac{x_2^2}{2}} a \geq e^{-\frac{\mu^2 x_2^2}{2}} b,$$

$$-\frac{x_2^2}{2} + \ln a \geq -\frac{\mu^2 x_2^2}{2} + \ln b,$$

$$\frac{\mu^2 - 1}{(\mu a + b)^2} \cdot \frac{C_1^2 \mathrm{SNR}}{2} \geq \ln \frac{b}{a}.$$

Let $C = \frac{2}{C_1^2} \ln \frac{b}{a}$. Then

$$\mathrm{SNR}\left(\mu^2 - 1\right) \geq \mathrm{C}(\mu \mathrm{a} + \mathrm{b})^2,$$

$$\left(\mathrm{SNR} - \mathrm{Ca}^2\right)\mu^2 - 2abC\mu - \left(Cb^2 + \mathrm{SNR}\right) \geq 0.$$

The discriminant of the quadratic equation $\left(\mathrm{SNR} - \mathrm{Ca}^2\right)\mu^2 - 2abC\mu - (Cb^2 + \mathrm{SNR}) = 0$ is

$$\begin{aligned} \Delta^* &= (-2abC)^2 - 4\left(\mathrm{SNR} - \mathrm{Ca}^2\right)\left[-\left(Cb^2 + \mathrm{SNR}\right)\right] \\ &= 4\mathrm{C} \cdot \mathrm{SNR}\left(b^2 - a^2\right) + 4\mathrm{SNR}^2. \end{aligned}$$

Note that $C$ and $(b^2 - a^2)$ always have the same sign. Hence, $C(b^2 - a^2) \geq 0$. Thus, $\Delta^* > 0$. Then, the roots the quadratic equation are

$$r_{1,2} = \frac{abC \pm \sqrt{\mathrm{C} \cdot \mathrm{SNR}\left(b^2 - a^2\right) + \mathrm{SNR}^2}}{\mathrm{SNR} - \mathrm{Ca}^2}.$$

We can derive the relationship between $r_{1,2}$ and 0. Let $A^* = \mathrm{SNR} - \mathrm{Ca}^2$, $B^* = -2abC$, $D^* = -\left(Cb^2 + \mathrm{SNR}\right)$. Then $r_1 + r_2 = -\frac{B^*}{A^*}$ and $r_1 r_2 = \frac{D^*}{A^*}$.

There are three conditions about the roots of the quadratic equation which rely on the relationship between $a$ and $b$:

Condition 1: $a > b$, that is $C < 0$

$$\begin{aligned} A^* &= \mathrm{SNR} - \mathrm{Ca}^2 > 0 \\ B^* &= -2abC > 0 \end{aligned}$$

1. If $\mathrm{SNR} \leq -\mathrm{Cb}^2$, then $D^* \geq 0$. $r_1 + r_2 = -\frac{B^*}{A^*} < 0$ and $r_1 r_2 = \frac{D^*}{A^*} \geq 0$. Thus, $r_1 < r_2 \leq 0$. Therefore, $f(\mu) > 0$, that is $\bar{P}'_{\mathrm{sep}}(\mu) > 0$ when $\mu \geq 0$. And $\bar{P}_{\mathrm{sep}}$ reaches minimum when $\mu_{\mathrm{opt1}} = 0$.

2. If $\mathrm{SNR} > -\mathrm{Cb}^2$, then $D^* < 0$. $r_1 + r_2 = -\frac{B^*}{A^*} < 0$ and $r_1 r_2 = \frac{D^*}{A^*} < 0$. Thus, $r_1 < 0 < r_2$. Therefore, $f(\mu) < 0$ when $0 < \mu < r_2$, $f(\mu) > 0$ when $\mu > r_2$, which means $\bar{P}_{\mathrm{sep}}$ reaches minimum when $\mu_{\mathrm{opt1}} = r_2$.

Condition 2: $a = b$, that is $C = 0$

$$\begin{aligned} A^* &= \mathrm{SNR} - \mathrm{Ca}^2 = \mathrm{SNR} \\ B^* &= -2abC = 0 \\ D^* &= -\left(Cb^2 + \mathrm{SNR}\right) = -\mathrm{SNR} \end{aligned}$$

In this condition. The roots of the quadratic equation are $\begin{cases} r_1 = -1 \\ r_2 = 1 \end{cases}$. Therefore, $f(\mu) < 0$ when $0 < \mu < 1$, $f(\mu) > 0$ when $\mu > 1$, which means $\bar{P}_{\mathrm{sep}}$ reaches minimum when $\mu_{\mathrm{opt2}} = 1$.

Condition 3: $a < b$, that is $C > 0$

$$\begin{aligned} B^* &= -2abC < 0 \\ D^* &= -\left(Cb^2 + \mathrm{SNR}\right) < 0 \end{aligned}$$

1. If $\mathrm{SNR} > \mathrm{Ca}^2$, then $A^* > 0$. $r_1 + r_2 = -\frac{B^*}{A^*} > 0$ and $r_1 r_2 = \frac{D^*}{A^*} < 0$. Thus, $r_1 < 0 < r_2$. Therefore, $f(\mu) < 0$ when $0 < \mu < r_2$, $f(\mu) > 0$ when $\mu > r_2$, which means $\bar{P}_{\mathrm{sep}}$ reaches minimum when $\mu_{\mathrm{opt3}} = r_2$.

2. If $\mathrm{SNR} = \mathrm{Ca}^2$, then $A^* = 0$. Thus, the only root the equation $r_2 < 0$. Therefore, $f(\mu) < 0$, that is $\bar{P}'_{\mathrm{sep}}(\mu) < 0$ when $\mu \geq 0$. And $\bar{P}_{\mathrm{sep}}$ reaches minimum when $\mu_{\mathrm{opt3}} \to \infty$.

3. If $\mathrm{SNR} < \mathrm{Ca}^2$, then $A^* < 0$. $r_1 + r_2 = -\frac{B^*}{A^*} < 0$ and $r_1 r_2 = \frac{D^*}{A^*} > 0$. Thus, $r_1 < r_2 \leq 0$. Therefore, $f(\mu) < 0$, that is $\bar{P}'_{\mathrm{sep}}(\mu) < 0$ when $\mu \geq 0$. And $\bar{P}_{\mathrm{sep}}$ reaches minimum when $\mu_{\mathrm{opt3}} \to \infty$.

Step 3: Finally, we can get the global minimum value of $\bar{P}_{\mathrm{sep}}$ in this way:

For each three situations of a and b, we can obtain the minimum value of $\bar{P}_{\mathrm{sep}}$ and corresponding $\mathbf{F}_{\mathrm{opt}}$ by using the optimal solution of $\alpha$, $\beta$ and the specific $\mu_{\mathrm{opt}}$ which rely on the relationship of $a$, $b$.

We can get the final optimal solutions based on these three conditions:

1. Condition 1: $0 \leq \psi < \frac{\pi}{4}$

   In this condition, $\tilde{\alpha} = \theta_U$, $\tilde{\beta} = \theta_L$. According to the lemma, we have $a > b$, then

(a) If SNR $\leq -\mathrm{Cb}^2$, then $\tilde{\mu} = 0$ and $\tilde{d}_2 = \frac{1/\mathrm{E_s}}{F(\theta_U,\theta_L,0)} = \frac{2}{bd(q-1)}$. Putting these values into $\mathbf{F}_{\text{opt}}$ and $\bar{P}_{\text{sep}}$, we get

$$\begin{aligned}\mathbf{F}_{\text{opt}} &= \tilde{d}_2\mathbf{V}\begin{pmatrix} \frac{\tilde{\mu}}{\lambda_1}\cos\tilde{\alpha} & \frac{1}{\lambda_1}\cos\tilde{\beta} \\ \frac{\tilde{\mu}}{\lambda_2}\sin\tilde{\alpha} & \frac{1}{\lambda_2}\sin\tilde{\beta} \end{pmatrix} \\ &= \mathbf{V}\begin{pmatrix} 0 & \frac{2}{bd(q-1)\lambda_1}\cos\theta_L \\ 0 & \frac{2}{bd(q-1)\lambda_2}\sin\theta_L \end{pmatrix}.\end{aligned}$$

In this situation, $\mathbf{F}$ is not a full rank matrix, then, $\tilde{\mathbf{H}} = \mathbf{HF}$ is also not a full rank matrix, we cannot compute the symbol error probability in (2.5) and (2.6). Thus, we turn off one of the transmitters and let the other work alone with the same method to deal with non-invertible matrix in case 1. Let $q_1 = q^2$.

i. $j_{11} \geq j_{22}$, $\mathbf{F}_{\text{opt}} = \begin{pmatrix} e \\ 0 \end{pmatrix}$.

ii. $j_{11} < j_{22}$, $\mathbf{F}_{\text{opt}} = \begin{pmatrix} 0 \\ e \end{pmatrix}$.

Then,

$$\min \bar{P}_{\text{sep}} = \frac{2\,(q_1-1)}{q_1} Q\left(\frac{dh\cdot\sqrt{\mathrm{SNR}}}{\sqrt{2}}\right),$$

$$\begin{aligned}\min \bar{P}_b &= \frac{1}{q_1 \log_2 q_1}\sum_{k=1}^{\log_2 q_1}\sum_{i=0}^{\left(1-2^{-k}\right)q_1-1}\left\{(-1)^{\frac{i\cdot 2^{k-1}}{q_1}}\left(2^{k-1}-\frac{i\cdot 2^{k-1}}{q_1}+\frac{1}{2}\right)\right. \\ &\quad \left.\cdot 2Q\left(\frac{(2i+1)\,dh\cdot\sqrt{\mathrm{SNR}}}{\sqrt{2}}\right)\right\},\end{aligned}$$

where $h = \sqrt{(\mathbf{HF}_{\text{opt}})^T (\mathbf{HF}_{\text{opt}})}$.

(b) If SNR $> -\text{Cb}^2$, then $\tilde{\mu} = r_2 = \frac{abC+\sqrt{\text{C}(b^2-a^2)+\text{SNR}^2}}{\text{SNR}-\text{Ca}^2}$, $\tilde{d}_2 = \frac{1/E_s}{F(\theta_U,\theta_L,\tilde{\mu})}$. Putting these values into $\mathbf{F}_{\text{opt}}$ and $\bar{P}_{\text{sep}}$, we get

$$\mathbf{F}_{\text{opt}} = \tilde{d}_2 \mathbf{V} \begin{pmatrix} \frac{\tilde{\mu}}{\lambda_1}\cos\theta_U & \frac{1}{\lambda_1}\cos\theta_L \\ \frac{\tilde{\mu}}{\lambda_2}\sin\theta_U & \frac{1}{\lambda_2}\sin\theta_L \end{pmatrix},$$

$$\min \bar{P}_{\text{sep}} = \frac{(q-1)}{q}\left(Q\left(\frac{d\tilde{\mu}\sqrt{\text{SNR}}}{\sqrt{2}\cdot\sqrt{\left(\tilde{\mathbf{H}}_{\text{opt}}^T\tilde{\mathbf{H}}_{\text{opt}}\right)_{11}^{-1}}}\right) + Q\left(\frac{d\sqrt{\text{SNR}}}{\sqrt{2}\cdot\sqrt{\left(\tilde{\mathbf{H}}_{\text{opt}}^T\tilde{\mathbf{H}}_{\text{opt}}\right)_{22}^{-1}}}\right)\right),$$

$$\begin{aligned}\min \bar{P}_b \;=\; & \frac{1}{q\log_2 q}\sum_{k=1}^{\log_2 q}\sum_{i=0}^{\left(1-2^{-k}\right)q-1}\left\{(-1)^{\frac{i\cdot 2^{k-1}}{q}}\left(2^{k-1}-\frac{i\cdot 2^{k-1}}{q}+\frac{1}{2}\right)\right. \\ & \left.\cdot\left(Q\left(\frac{(2i+1)\,d\tilde{\mu}\sqrt{\text{SNR}}}{\sqrt{2}\cdot\sqrt{\left(\tilde{\mathbf{H}}_{\text{opt}}^T\tilde{\mathbf{H}}_{\text{opt}}\right)_{11}^{-1}}}\right)+Q\left(\frac{(2i+1)\,d\sqrt{\text{SNR}}}{\sqrt{2}\cdot\sqrt{\left(\tilde{\mathbf{H}}_{\text{opt}}^T\tilde{\mathbf{H}}_{\text{opt}}\right)_{22}^{-1}}}\right)\right)\right\},\end{aligned}$$

where $\tilde{\mathbf{H}}_{\text{opt}} = \mathbf{HF}_{\text{opt}}$.

2. Condition 2: $\psi = \frac{\pi}{4}$.

In this condition, $\tilde{\alpha} = \theta_U$, $\tilde{\beta} = \theta_L$. According to the lemma, we have $a = b$. Then no matter how the SNR changes, we have the optimal $\tilde{\mu} = 1$ and $\tilde{d}_2 = \frac{1/E_s}{F(\theta_U,\theta_L,1)} = \frac{2}{(a+b)d(q-1)}$. Thus,

$$\mathbf{F}_{\text{opt}} = \frac{2}{(a+b)\,d\,(q-1)}\mathbf{V}\begin{pmatrix} \frac{1}{\lambda_1}\cos\theta_U & \frac{1}{\lambda_1}\cos\theta_L \\ \frac{\tilde{1}}{\lambda_2}\sin\theta_U & \frac{1}{\lambda_2}\sin\theta_L \end{pmatrix},$$

$$\min \bar{P}_{\text{sep}} = \frac{2\left(q-1\right)}{q} Q\left(\frac{d\sqrt{\text{SNR}}}{\sqrt{2}\cdot\sqrt{\left(\tilde{\mathbf{H}}_{\text{opt}}^{T}\tilde{\mathbf{H}}_{\text{opt}}\right)_{11}^{-1}}}\right),$$

$$\begin{aligned}\min \bar{P}_{b} &= \frac{1}{q\log_2 q}\sum_{k=1}^{\log_2 q}\sum_{i=0}^{\left(1-2^{-k}\right)q-1}\left\{(-1)^{\frac{i\cdot 2^{k-1}}{q}}\left(2^{k-1}-\frac{i\cdot 2^{k-1}}{q}+\frac{1}{2}\right)\right.\\ &\left.\cdot 2Q\left(\frac{\left(2i+1\right)d\sqrt{\text{SNR}}}{\sqrt{2}\cdot\sqrt{\left(\tilde{\mathbf{H}}_{\text{opt}}^{T}\tilde{\mathbf{H}}_{\text{opt}}\right)_{11}^{-1}}}\right)\right\},\end{aligned}$$

where $\tilde{\mathbf{H}}_{\text{opt}} = \mathbf{H}\mathbf{F}_{\text{opt}}$.

3. Condition 3: $\frac{\pi}{4} < \psi \leq \frac{\pi}{2}$

   In this condition, $\tilde{\alpha} = \theta_U$, $\tilde{\beta} = \theta_L$. According to the lemma, we have $a < b$, then

   (a) If $\text{SNR} \leq \text{Ca}^2$, then $\tilde{\mu} \to \infty$ and $\tilde{d}_2 = \lim\limits_{\tilde{\mu}\to\infty} \frac{1/\text{E}_\text{s}}{F(\theta_U,\theta_L,\tilde{\mu})} = \lim\limits_{\tilde{\mu}\to\infty} \frac{2}{(\tilde{\mu}a+b)d(q-1)}$. Putting these values into $\mathbf{F}_{\text{opt}}$ and $\bar{P}_{\text{sep}}$, we get

$$\begin{aligned}\mathbf{F}_{\text{opt}} &= \tilde{d}_2\mathbf{V}\begin{pmatrix}\frac{\tilde{\mu}}{\lambda_1}\cos\tilde{\alpha} & \frac{1}{\lambda_1}\cos\tilde{\beta}\\ \frac{\tilde{\mu}}{\lambda_2}\sin\tilde{\alpha} & \frac{1}{\lambda_2}\sin\tilde{\beta}\end{pmatrix}\\ &= \lim_{\tilde{\mu}\to\infty}\frac{2}{\left(\tilde{\mu}a+b\right)d\left(q-1\right)}\mathbf{V}\begin{pmatrix}\frac{\tilde{\mu}}{\lambda_1}\cos\theta_U & \frac{1}{\lambda_1}\cos\theta_L\\ \frac{\tilde{\mu}}{\lambda_2}\sin\theta_U & \frac{1}{\lambda_2}\sin\theta_L\end{pmatrix}\\ &= \mathbf{V}\begin{pmatrix}\frac{2}{ad(q-1)\lambda_1}\cos\theta_U & 0\\ \frac{2}{ad(q-1)\lambda_2}\sin\theta_U & 0\end{pmatrix}.\end{aligned}$$

   In this situation, $\mathbf{F}$ is not a full rank matrix, then, $\tilde{\mathbf{H}} = \mathbf{H}\mathbf{F}$ is also not a

full rank matrix, we cannot compute the symbol error probability in (2.5) and (2.6). Thus, we turn off one of the transmitters and let the other work alone with the same method to deal with non-invertible matrix in case 1.

Let $q_1 = q^2$.

i. $j_{11} \geq j_{22}$, $\mathbf{F}_{\text{opt}} = \begin{pmatrix} e \\ 0 \end{pmatrix}$.

ii. $j_{11} < j_{22}$, $\mathbf{F}_{\text{opt}} = \begin{pmatrix} 0 \\ e \end{pmatrix}$.

Then,

$$\min \bar{P}_{\text{sep}} = \frac{2\left(q_1 - 1\right)}{q_1} Q\left(\frac{dh \cdot \sqrt{\text{SNR}}}{\sqrt{2}}\right),$$

$$\begin{aligned} \min \bar{P}_b \;=\; & \frac{1}{q_1 \log_2 q_1} \sum_{k=1}^{\log_2 q_1} \sum_{i=0}^{\left(1-2^{-k}\right)q_1 - 1} \left\{ (-1)^{\frac{i \cdot 2^{k-1}}{q_1}} \left(2^{k-1} - \frac{i \cdot 2^{k-1}}{q_1} + \frac{1}{2}\right) \right. \\ & \left. \cdot 2Q\left(\frac{(2i+1)\, dh \cdot \sqrt{\text{SNR}}}{\sqrt{2}}\right) \right\}, \end{aligned}$$

where $h = \sqrt{\left(\mathbf{H}\mathbf{F}_{\text{opt}}\right)^T \left(\mathbf{H}\mathbf{F}_{\text{opt}}\right)}$.

(b) If SNR $>$ Ca$^2$, then $\tilde{\mu} = r_2 = \frac{abC + \sqrt{\text{C}\cdot\text{SNR}(\text{b}^2 - \text{a}^2) + \text{SNR}^2}}{\text{SNR} - \text{Ca}^2}$, $\tilde{d}_2 = \frac{1/E_s}{F(\theta_U, \theta_L, \tilde{\mu})}$.

Putting these values into $\mathbf{F}_{\text{opt}}$ and $\bar{P}_{\text{sep}}$, we get

$$\mathbf{F}_{\text{opt}} = \tilde{d}_2 \mathbf{V} \begin{pmatrix} \frac{\tilde{\mu}}{\lambda_1} \cos\theta_U & \frac{1}{\lambda_1} \cos\theta_L \\ \frac{\tilde{\mu}}{\lambda_2} \sin\theta_U & \frac{1}{\lambda_2} \sin\theta_L \end{pmatrix},$$

$$\min \bar{P}_{\text{sep}} = \frac{(q-1)}{q}\left(Q\left(\frac{d\tilde{\mu}\sqrt{\text{SNR}}}{\sqrt{2}\cdot\sqrt{\left(\tilde{\mathbf{H}}_{\text{opt}}^{T}\tilde{\mathbf{H}}_{\text{opt}}\right)_{11}^{-1}}}\right)+Q\left(\frac{d\sqrt{\text{SNR}}}{\sqrt{2}\cdot\sqrt{\left(\tilde{\mathbf{H}}_{\text{opt}}^{T}\tilde{\mathbf{H}}_{\text{opt}}\right)_{22}^{-1}}}\right)\right),$$

$$\begin{aligned}\min \bar{P}_{b} &= \frac{1}{q\log_2 q}\sum_{k=1}^{\log_2 q}\sum_{i=0}^{\left(1-2^{-k}\right)q-1}\left\{(-1)^{\frac{i\cdot 2^{k-1}}{q}}\left(2^{k-1}-\frac{i\cdot 2^{k-1}}{q}+\frac{1}{2}\right)\right.\\ &\left.\cdot\left(Q\left(\frac{(2i+1)\,d\tilde{\mu}\sqrt{\text{SNR}}}{\sqrt{2}\cdot\sqrt{\left(\tilde{\mathbf{H}}_{\text{opt}}^{T}\tilde{\mathbf{H}}_{\text{opt}}\right)_{11}^{-1}}}\right)+Q\left(\frac{(2i+1)\,d\sqrt{\text{SNR}}}{\sqrt{2}\cdot\sqrt{\left(\tilde{\mathbf{H}}_{\text{opt}}^{T}\tilde{\mathbf{H}}_{\text{opt}}\right)_{22}^{-1}}}\right)\right)\right\},\end{aligned}$$

where $\tilde{\mathbf{H}}_{\text{opt}} = \mathbf{H}\mathbf{F}_{\text{opt}}$.

We will get the same result if $\alpha < \beta$ by using the same method above. Thus, we omit the proof here. □

## A.3 Proof of the fact that the optimal precoding matrix F are off-diagonal

According to (2.26), (2.11), (2.12), we get

$$\begin{aligned}
\mathbf{F}_{\text{opt}}(1,1) &= \frac{\mu}{\lambda_1}\cos\theta_U\cos\psi - \frac{\mu}{\lambda_2}\sin\theta_U\sin\psi \\
&= \frac{\mu}{\lambda_1}\frac{1}{\sqrt{1+\tan^2\theta_U}}\cos\psi - \frac{\mu}{\lambda_2}\frac{1}{\sqrt{1+\cot^2\theta_U}}\sin\psi \\
&= \frac{\mu}{\lambda_1}\frac{1}{\sqrt{1+\left(\frac{\lambda_2}{\lambda_1}\cot\psi\right)^2}}\cos\psi - \frac{\mu}{\lambda_2}\frac{1}{\sqrt{1+\left(\frac{1}{\frac{\lambda_2}{\lambda_1}\cot\psi}\right)^2}}\sin\psi \\
&= \frac{\mu}{\lambda_1}\frac{\lambda_1\sin\psi\cos\psi}{\sqrt{\lambda_1^2\sin^2\psi+\lambda_2^2\cos^2\psi}} - \frac{\mu}{\lambda_2}\frac{\lambda_2\sin\psi\cos\psi}{\sqrt{\lambda_1^2\sin^2\psi+\lambda_2^2\cos^2\psi}} \\
&= 0.
\end{aligned}$$

To prove $\mathbf{F}_{\text{opt}}(2,2)=0$, we can use the same method above. So we omit here.

## A.4 The proof that $\chi_1$, $\chi_2$ can form an AUDCG by decomposing G

$\chi_1$, $\chi_2$, $\mathcal{G}$ are defined by (3.1) (3.2) (3.3), respectively. $|\chi_1|=2$, $|\chi_2|=2^{2n}$, $|\mathcal{G}|=2^{2n+1}$.

$$\because \mathcal{G}=\chi_1+\chi_2, |\mathcal{G}|=|\chi_1|\cdot|\chi_2|$$

$$\therefore \mathcal{G}=\chi_1 \biguplus \chi_2$$

which means that the sum constellation $\mathcal{G}$ can be additively uniquely decomposed to two finite-size constellations.

# Bibliography

(Sep. 2011). IEEE standard for local and metropolitan area networks-Part 15.7: short-range wireless optical communication using visible light. *IEEE Std*, **802.15.7-2011**, 1309.

Barry, J. R. (2012). *Wireless infrared communications*, volume 280. Springer Science & Business Media.

Bouchet, O., Faulkner, G., Grobe, L., Gueutier, E., Langer, K., *et al.* (2011). Deliverable d4. 2b physical layer design and specification. *7th Framework Programme Information & Communication Technologies*.

Chen, Y.-A., Chang, Y.-T., Tseng, Y.-C., and Chen, W.-T. (August 2015). A framework for simultaneous message broadcasting using cdma-based visible light communications. *IEEE Sensors J.*, **15**(12), 6819–6827.

Cho, K. and Yoon, D. (November 2002). On the general ber expression of one-and two-dimensional amplitude modulations. *IEEE Trans. Commun.*, **50**(7), 1074–1080.

Elgala, H., Mesleh, R., and Haas, H. (2009). Indoor broadcasting via white leds and ofdm. *IEEE Trans. Consum. Electron.*, **55**(3), 1127–1134.

Fath, T. and Haas, H. (December 2013). Performance comparison of mimo techniques for optical wireless communications in indoor environments. *IEEE Trans. Commun.*, **61**(2), 733–742.

Jha, M. K., Addanki, A., Lakshmi, Y., and Kumar, N. (2015). Channel coding performance of optical mimo indoor visible light communication. In *2015 International Conference on Advances in Computing, Communications and Informatics (ICACCI)*, pages 97–102.

Jia, L., Wang, J.-B., Wang, J.-y., and Chen, M. (April 2015). Comparison of different space time coding for transmit diversity in vlc systems with csk modulation. In *2015 IEEE International Broadband and Photonics Conference (IBP)*, pages 40–48.

Kahn, J. M. and Barry, J. R. (1997). Wireless infrared communications. *Proc. IEEE*, **85**(2), 265–298.

Karp, S., Gagliardi, R. M., Moran, S. E., and Stotts, L. B. (2013). *Optical channels: fibers, clouds, water, and the atmosphere*. Springer Science & Business Media.

Kumar, N., Lourenço, N., Terra, D., Alves, L. N., and Aguiar, R. L. (2012). Visible light communications in intelligent transportation systems. In *Intelligent Vehicles Symposium (IV), 2012 IEEE*, pages 748–753.

Lee, E. J. and Chan, V. W. (November 2004). Part 1: Optical communication over the clear turbulent atmospheric channel using diversity. *IEEE J. Sel. Areas Commun.*, **22**(9), 1896–1906.

Li, Y., Wang, L., Ning, J., Pelechrinis, K., Krishnamurthy, S. V., and Xu, Z. (2012). Vico: A framework for configuring indoor visible light communication networks. In

*Mobile Adhoc and Sensor Systems (MASS), 2012 IEEE 9th International Conference on*, pages 136–144.

Marcuse, D. (August 1991). Calculation of bit-error probability for a lightwave system with optical amplifiers and post-detection gaussian noise. *J. Lightw. Technol.*, **9**(4), 505–513.

O'Brien, D. C., Faulkner, G., Le Minh, H., Bouchet, O., Tabach, M., *et al.* (December 2008a). Home access networks using optical wireless transmission. In *Personal, Indoor and Mobile Radio Communications, 2008. PIMRC 2008. IEEE 19th International Symposium on*, pages 1–5.

O'Brien, D. C., Zeng, L., Le-Minh, H., Faulkner, G., Walewski, J. W., and Randel, S. (Sept. 2008b). Visible light communications: Challenges and possibilities. In *Personal, Indoor and Mobile Radio Communications, 2008. PIMRC 2008. IEEE 19th International Symposium on*, pages 1–5.

Selvan, V., Iqbal, M. S., and Al-Raweshidy, H. (Aug. 2014). Performance analysis of linear precoding schemes for very large multi-user mimo downlink system. In *2014 Fourth International Conference on Innovative Computing Technology (INTECH)*, pages 219–224. IEEE.

Shoreh, M. H., Fallahpour, A., and Salehi, J. A. (2015). Design concepts and performance analysis of multicarrier cdma for indoor visible light communications. *IEEE J. Opt. Commun. Netw.*, **7**(6), 554–562.

Tiwari, S. V., Sewaiwar, A., and Chung, Y.-H. (Jan. 2015). Smart home technologies

using visible light communication. In *Consumer Electronics (ICCE), 2015 IEEE International Conference on*, pages 379–380.

Yamazato, T., Takai, I., Okada, H., Fujii, T., Yendo, T., *et al.* (July 2014). Image-sensor-based visible light communication for automotive applications. *IEEE Commun. Mag.*, **52**(7), 88–97.

Yendo, T., Tehrani, M. P., Yamazato, T., Okada, H., Fujii, T., *et al.* (2010). High-speed-camera image processing based led traffic light detection for road-to-vehicle visible light communication. In *2010 IEEE Intelligent Vehicles Symposium (IV)*, pages 793–798.

Yu, Z., Baxley, R. J., and Zhou, G. T. (2013). Multi-user miso broadcasting for indoor visible light communication. In *Acoustics, Speech and Signal Processing (ICASSP), 2013 IEEE International Conference on*, pages 4849–4853. IEEE.

Zhu, X. and Kahn, J. M. (August 2002). Free-space optical communication through atmospheric turbulence channels. *IEEE Trans. Commun.*, **50**(8), 1293–1300.

Zhu, Y.-J., Liang, W.-F., Zhang, J.-K., and Zhang, Y.-Y. (2015). Space-collaborative constellation designs for mimo indoor visible light communications. *Photonics Technology Letters, IEEE*, **27**(15), 1667–1670.